

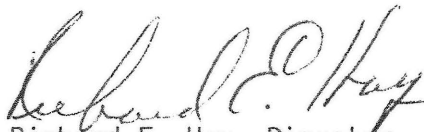
This document is available to the U.S. public through the National Technical Information Service, Springfield, Virginia 22161

## FOREWORD

This report documents the results of an experimental study to examine the feasibility of using adhesive bonds on bridges for tensile splices, beam flange splices and end-bolted cover plates.

The results of the research indicate that the idea of replacing welded connections with adhesive bonds has promise within reasonable limitations. Follow-up work to specify adhesive properties, specific bridge details, and suitable environments is now underway.

Sufficient copies of the report are being distributed to provide a minimum of two copies to each regional office, one copy to each division office and two copies to each State highway agency. Direct distribution is being made to the division offices.



Richard E. Hay, Director  
Office of Engineering  
and Highway Operations  
Research and Development  
Federal Highway Administration

## NOTICE

This document is disseminated under the sponsorship of the Department of Transportation in the interest of information exchange. The United States Government assumes no liability for its contents or use thereof. The contents of this report reflect the views of the contractor, who is responsible for the accuracy of the data presented herein. The contents do not necessarily reflect the official policy of the Department of Transportation. This report does not constitute a standard, specification, or regulation.

The United States Government does not endorse products or manufacturers. Trade or manufacturers' names appear herein only because they are considered essential to the object of this document.



|   |  |   |           |
|---|--|---|-----------|
| 1. Report No.<br>FHWA/RD-84/037   | 2. Government Accession No.                          | 3. Recipient's Catalog No.  |           |
| 4. Title and Subtitle<br>Application of Adhesives to Steel Bridges  |  | 5. Report Date<br>November 1984   |           |
|   |  | 6. Performing Organization Code   |           |
| 7. Author(s)<br>P. Albrecht, A. Sahli, D. Crute, Ph. Albrecht,<br>and B. Evans  |  | 8. Performing Organization Report No.   |           |
| 9. Performing Organization Name and Address<br>Blunt and Evans Consulting Engineers<br>9700-D George Palmer Highway<br>Lanham, Maryland 20706   |  | 10. Work Unit No.<br>35K1-142   |           |
|   |  | 11. Contract or Grant No.<br>DTFH 61-81-C-00098   |           |
|   |  | 13. Type of Report and Period Covered<br>Final Report 9/81-9/83   |           |
| 12. Sponsoring Agency Name and Address<br>Offices of Research, Development and Technology<br>Federal Highway Administration<br>6300 Georgetown Pike<br>McLean, VA. 22101  |  | 14. Sponsoring Agency Code  |           |
| 15. Supplementary Notes<br>Contract Manager Thomas Krylowski (HNR-10)   |  |   |           |
| 16. Abstract<br><br>This study examined the feasibility of adhesive bonding and bolting tensile splices, beam flange splices and cover plates with ends bolted. The specimens were subjected to fatigue and static loading. The results showed that bonding the contact surfaces significantly increased the fatigue life of high-strength bolted splices. Bonding cover plates increased the fatigue life by a factor of 20 over that of conventionally welded cover plates. While bonding greatly increased the slip resistance of bolted joints, it had no effect on the ultimate strength of the joint. In an additional series of tests it was found that the creep strength of the adhesive bond decreases with time, particularly in outdoor environments when the ambient temperatures are high. Successful application of bonding technology requires careful adhesive selection for the intended service environment, characterization of adhesive properties, and detail design that limits cleavage and peel stresses in the bond line. |  |   |           |
| 17. Key Words<br>Adhesive, bolted connections, creep, fatigue, static, slip resistance, bearing, friction, steel, bridges   |  | 18. Distribution Statement<br>No restrictions. This document is available to the public through the National Technical Information Service, Springfield, Virginia 22161 |           |
| 19. Security Classif. (of this report)<br>Unclassified  | 20. Security Classif. (of this page)<br>Unclassified | 21. No. of Pages  | 22. Price |

## TABLE OF CONTENTS

|   | <u>Page</u> |
|---|-------------|
| LIST OF TABLES . . . . .                                    | iv          |
| LIST OF FIGURES. . . . .                                    | vi          |
| 1. INTRODUCTION . . . . .                                   | 1           |
| 1.1 Application of Adhesives . . . . .                      | 1           |
| 1.2 Objectives . . . . .                                    | 2           |
| 1.3 Adhesive Selection . . . . .                            | 3           |
| 2. TEST SPECIMENS AND PROCEDURES. . . . .                   | 5           |
| 2.1 Specimens. . . . .                                      | 5           |
| 2.2 Bolts-To-Member Strength Ratio . . . . .                | 7           |
| 2.3 Fabrication. . . . .                                    | 11          |
| 2.4 Adhesives. . . . .                                      | 12          |
| 2.5 Assembly . . . . .                                      | 13          |
| 2.6 Testing. . . . .  | 15          |
| 2.7 Fatigue Crack Measurement. . . . .                      | 19          |
| 2.8 AASHTO Category B Rhomboid . . . . .                    | 20          |
| 3. FATIGUE STRENGTH OF SERIES A TENSILE SPLICES . . . . .   | 35          |
| 3.1 Experiment Design. . . . .                              | 35          |
| 3.2 Crack Initiation and Propagation . . . . .              | 35          |
| 3.3 Fatigue Test Data. . . . .                              | 38          |
| 3.4 Comparison With Previous Work. . . . .                  | 43          |
| 4. FATIGUE STRENGTH OF SERIES B BEAM SPLICES. . . . .       | 66          |
| 4.1 Experiment Design. . . . .                              | 66          |
| 4.2 Crack Initiation and Propagation . . . . .              | 67          |
| 4.3 Fatigue Test Data. . . . .                              | 68          |
| 4.4 Comparison With Previous Work. . . . .                  | 71          |
| 5. FATIGUE STRENGTH OF SERIES B BEAM COVER PLATES . . . . . | 90          |
| 5.1 Experiment Design. . . . .                              | 90          |
| 5.2 Crack Initiation and Propagation . . . . .              | 90          |
| 5.3 Fatigue Test Data. . . . .                              | 91          |
| 5.4 Comparison With Previous Work. . . . .                  | 92          |

## TABLE OF CONTENTS (continued)

|  | <u>Page</u> |
|--|-------------|
| 6. STATIC STRENGTH OF SERIES C TENSILE SPLICES . . . . .                 | 106         |
| 6.1 Experiment Design . . . . .  | 106         |
| 6.2 Definition of Slip Coefficient and Slip Load. . . . .                | 106         |
| 6.3 Static Test Data. . . . .  | 107         |
| 6.4 Comparison with AASHTO Specifications and<br>Previous Work . . . . . | 110         |
| 7. STATIC STRENGTH OF SERIES D BEAM SPLICES. . . . .                     | 134         |
| 7.1 Experiment Design . . . . .  | 134         |
| 7.2 Definition of Slip Coefficient. . . . .                              | 134         |
| 7.3 Static Test Data. . . . .  | 134         |
| 7.4 Comparison With Previous Work . . . . .                              | 137         |
| 8. CREEP STRENGTH OF SERIES E TENSILE SPECIMENS                          | 148         |
| 8.1 Experiment Design . . . . .  | 148         |
| 8.2 Creep Measurements. . . . .  | 148         |
| 8.3 Creep Test Data . . . . .  | 149         |
| 8.4 Comparison With Previous Work . . . . .                              | 153         |
| 9. FINDINGS AND CONCLUSIONS. . . . .                                     | 170         |
| REFERENCES. . . . .  | 173         |

## LIST OF TABLES

| <u>Table</u>   | <u>Page</u> |
|--|-------------|
| 1 Mechanical Properties of A588 Grade B Steel for<br>Tensile and Beam Specimens. . . . . | 21          |
| 2 Chemical Composition of A588 Grade B Steel for<br>Tensile and Beam Specimens. . . . .  | 22          |
| 3 Typical Properties of Adhesive and Accelerators . . . . .                              | 23          |
| 4 Fatigue Test Matrix for Series A Tensile Specimens. . . . .                            | 47          |
| 5 Dimensions of Cracks in Series A Tensile Specimens;<br>Two-Bolt Splices. . . . .       | 48          |
| 6 Dimensions of Cracks in Series A Tensile Specimens;<br>One-Bolt Splices. . . . .       | 50          |
| 7 Fatigue Test Data for Series A Tensile Specimens;<br>Two-Bolt Splices. . . . .         | 52          |
| 8 Fatigue Test Data for Series A Tensile Specimens;<br>One-Bolt Splices. . . . .         | 54          |
| 9 Summary of Stress Ranges in Series A Tensile Specimens. . . . .                        | 56          |
| 10 Fatigue Test Matrix for Series B Beam Splices . . . . .                               | 73          |
| 11 Dimensions of Cracks in Series B Beams with Six-Bolt<br>Splices . . . . .             | 74          |
| 12 Dimensions of Cracks in Series B Beams with Four-<br>Bolt Splices. . . . .            | 77          |
| 13 Summary of Types of Cracks at Beam Splices. . . . .                                   | 78          |
| 14 Fatigue Test Data for Series B Beams with Six-Bolt<br>Splices . . . . .               | 79          |
| 15 Fatigue Test Data for Series B Beams with Four-Bolt<br>Splices . . . . .              | 81          |
| 16 Fatigue Test Matrix for Series B Bonded Cover Plates. . . . .                         | 95          |
| 17 Dimensions of Cracks at Bonded Cover Plates on Series<br>B Beams . . . . .            | 96          |
| 18 Fatigue Test Data for Series B Cover Plates . . . . .                                 | 99          |

# LIST OF TABLES (continued)

| <u>Table</u> |  | <u>Page</u> |
|--------------|--|-------------|
| 19           | Comparison of Previous and Present Fatigue Data<br>for Cover-Plate Ends . . . . .  | 100         |
| 20           | Static Test Matrix for Series C Tensile Specimens. . . . .   | 116         |
| 21           | Static Test Data for Series C Tensile Specimens;<br>Two-Bolt Splices . . . . .   | 117         |
| 22           | Mean Slip Data for Series C Tensile Specimens and<br>Allowable Shear Stresses for Friction-Type Joints. . . . .            | 118         |
| 23           | Static Test Data for Series C Tensile Specimens;<br>One Bolt Splices . . . . .   | 119         |
| 24           | Slip Coefficients and Allowable Shear Stresses for<br>Friction-Type Bolted Joints With Blast Cleaned<br>Surfaces . . . . . | 120         |
| 25           | Static Test Matrix for Series D Beam Splices . . . . .   | 139         |
| 26           | Static Test Data for Series B Beam Splices . . . . .   | 140         |
| 27           | Creep Test Matrix for Series D Double Strap Specimens. . . . .   | 157         |
| 28           | Results of Indoor Creep Tests. . . . .   | 158         |
| 29           | Results of Outdoor Creep Tests . . . . .   | 161         |

## LIST OF FIGURES

| <u>Figure</u>  | <u>Page</u> |
|--|-------------|
| 1 Series A and C Tensile Splices. . . . .  | 24          |
| 2 Series B and D Beams. . . . .  | 25          |
| 3 Series E Double Strap Specimens . . . . .  | 26          |
| 4 Jig to Hold Tensile Specimens in Place Upon Bonding . .  | 27          |
| 5 Adhesively Bonded Beams with C-Clamps Applied to<br>Cover Plates. . . . .  | 28          |
| 6 Jig to Hold Creep Specimens in Place Upon Gluing. . . .  | 29          |
| 7 Contact Surface Appearance of Tensile Specimens<br>After Test Ended. . . . .   | 30          |
| 8 Spring-Loaded Frames Used in Task E . . . . .  | 31          |
| 9 (a) Definition of Crack Measurement Procedure;<br>(b) Typical Cracked Section at Failure . . . . .                                     | 32          |
| 10 Definition of Type of Crack, Crack Angle, Distance of<br>Crack Initiation from Hole Center Line, and Zone of<br>Crack Growth. . . . . | 33          |
| 11 Definition of AASHTO Category B Rhomboid. . . . .   | 34          |
| 12 Typical Fatigue Crack Surfaces; Specimen A8 (Top) and<br>A27 (Bottom). . . . .  | 57          |
| 13 Fretting Fatigue Cracks . . . . .   | 58          |
| 14 Fatigue Test Data for Series A Tensile Specimens; Two-<br>Bolt Splices. . . . .   | 59          |
| 15 Fatigue Test Data for Series A Tensile Specimens; One-<br>Bolt Splices. . . . .   | 60          |
| 16 Summary of Fatigue Test Data for Series A Tensile<br>Specimens . . . . .  | 61          |
| 17 Fatigue Strength of Bearing-Type Joints in Terms of<br>Gross Area Stress Range (Ref. 15) . . . . .                                    | 62          |
| 18 Effect of Yield Point on Fatigue Strength of Bolted<br>Joints (Ref. 21). . . . .  | 63          |

# LIST OF FIGURES (continued)

| <u>Figure</u> |  | <u>Page</u> |
|---------------|--|-------------|
| 19            | Effect of Number of Bolt Rows on Fatigue Strength of Bolted Joints (Ref. 22) . . . . .   | 64          |
| 20            | Effect of Bolting Some but not all Cross Sectional Elements on Fatigue Strength of Bolted Joints (Ref. 20)   | 65          |
| 21            | Typical Crack Initiation and Propagation at First Bolt Row (Splice B7-1) . . . . .   | 82          |
| 22            | Fatigue Crack in Splice Plate at Second Bolt Row (Splice B14-2). . . . .   | 83          |
| 23            | Typical Fretting Fatigue Crack Ahead of First Bolt Row. Crack Tip was stopped by Drilling a Hole (Splice B15-1). . . . .                           | 84          |
| 24            | Typical Crack Initiation and Propagation at Bolt Hole .  | 85          |
| 25            | Fatigue Test Data for Series D Beam Specimens with Six-Bolt Splices. . . . .   | 86          |
| 26            | Fatigue Test Data for Series B Beam Specimens with Four-Bolt Splices . . . . .   | 87          |
| 27            | Comparison of Fatigue Test Data for Series A and B Splices . . . . .   | 88          |
| 28            | Comparison of Previous and Present Fatigue Test Data for Nonbonded Beam Splices. . . . .   | 89          |
| 29            | C-Scan of Cover Plate End B2-1. Bonded Areas are Clear, Debonded Areas are Dark . . . . .  | 102         |
| 30            | Typical Bolt Hole Cracks at Cover Plate Ends B5-1 (Top) and B9-1 (Bottom). Hole and Bolt at Crack Tip in Web are Part of Temporary Repair. . . . . | 103         |
| 31            | Fatigue Test Data for Series B Beam Cover Plates. . . . .  | 104         |
| 32            | Comparison of Mean Fatigue Strength of All Data Sets with Mean of Category A Through E' Data. See Table 19. . . . .                                | 105         |
| 33            | Load-Elongation Curves of Nonbonded Two-Bolt Splices C1-C4 . . . . .   | 121         |
| 34            | Load-Elongation Curves of Nonbonded Two-Bolt Splices C17-C19 . . . . .   | 122         |
| 35            | Typical Series C Two-Bolt Splices at Failure; Specimen C4 (Top) and C6 (Bottom). . . . .   | 123         |

# LIST OF FIGURES (continued)

| <u>Figure</u> |   | <u>Page</u> |
|---------------|---|-------------|
| 36            | Load-Elongation Curves of Bonded Two-Bolt Splices<br>C5-C8 . . . . .  | 124         |
| 37            | Load-Elongation Curves of Bonded Two-Bolt Splices<br>C20-C22 . . . . .  | 125         |
| 38            | Load-Elongation Curves of Nonbonded One-Bolt Splices<br>C9-C12. . . . .   | 126         |
| 39            | Load-Elongation Curves of Bonded One-Bolt Splices<br>C13-C16 . . . . .  | 127         |
| 40            | Typical Series C One-Bolt Splices at Failure;<br>Specimen C12 (Top) and C16 (Bottom) . . . . .                            | 128         |
| 41            | Slip Coefficients and Allowable Shear Stresses for<br>Friction-Type Bolted Joints With Blast Cleaned<br>Surfaces. . . . . | 129         |
| 42            | Load-Elongation Curves for Shear Tests (Ref. 3) . . . .   | 130         |
| 43            | Load-Elongation Curves for Shear Tests With Bolt and<br>Epoxy Formation 991-67 (Ref. 3) . . . . .                         | 131         |
| 44            | Load-Slip Curves for Bearing-Type Specimens (Ref. 3). .   | 132         |
| 45            | Load-Slip Curves for Friction-Type Specimens (Ref. 3) .   | 133         |
| 46            | Load-Slip Curves of Nonbonded Beam Splices. . . . .   | 141         |
| 47            | Load-Slip Curves of Bonded Beam Splices . . . . .   | 142         |
| 48            | Load-Deflection Curves of Two-Bolt Beam Splices . . . .   | 143         |
| 49            | Load-Deflection Curves of Four-Bolt Beam Splices. . . .   | 144         |
| 50            | Load-Deflection Curves of Six-Bolt Beam Splices . . . .   | 145         |
| 51            | Four-Bolt Beam Splices at End of Test;<br>Splice D3 (Top) and D4 (Bottom) . . . . .                                       | 146         |
| 52            | Tension Flange Contact Surfaces of Beam Splices<br>D3 (Top) and D4 (Bottom). . . . .                                      | 147         |
| 53            | Specimens Showing Various Modes of Failure. . . . .   | 163         |
| 54            | Creep Strength of Double Strap Specimens. . . . .   | 164         |
| 55            | Creep Displacements of Indoor Specimens at 50% Stress<br>Level . . . . .  | 165         |



## LIST OF FIGURES (continued)

| <u>Figure</u> |   | <u>Page</u> |
|---------------|---|-------------|
| 56            | Creep Displacements of Indoor Specimens at 40% Stress Level . . . . .                     | 166         |
| 57            | Creep Displacements of Outdoor Specimens at 40% Stress Level. . . . .                     | 167         |
| 58            | Creep Displacements of Outdoor Specimens at 30% Stress Level. . . . .                     | 168         |
| 59            | Stress Distribution in a Double Lap Adhesive Joint. Adapted from Fig. 6, Ref. 41. . . . . | 169         |



## CHAPTER 1: INTRODUCTION

### 1.1 Application of Adhesives

The application of adhesives to metal fabrication, like many other technological innovations, was pioneered by the aircraft industry. One of the first aircraft to be constructed in part with epoxy resins was the B-52, some 25 years ago. Since then the aerospace industry developed technology to the point where today epoxy resins are used to bond critical parts in commercial and military aircraft and spacecraft, including the Atlas rocket, Minuteman missile, Cruise missile, and the Space Shuttle. (36)

The most ambitious adhesive bonding effort to date has been at Wright-Patterson AFB, the \$18-million PABST (Primary Adhesively Bonded Structure Technology) program, which ran from 1976 through 1981. The PABST project led to the construction of a totally adhesive bonded 42-foot-long circumferential fuselage section of a McDonnell Douglas YC-15 military aircraft. The section successfully withstood the equivalent of four aircraft lifetimes of testing. In addition, researchers deliberately made cracks in the fuselage skin to see what would happen to them under simulated flight conditions. These cracks did not grow to catastrophic proportions, as they might have in riveted structures. (42)

Behind the drive in the aerospace industry to replace mechanical fasteners with adhesives is the desire to prolong aircraft life and reduce costly maintenance. Rivet holes, for example, are points of weakness in airplane skins where fatigue cracks can form, requiring repair or reducing the lifetime of the structure. Metallic fasteners can corrode or loosen. In addition, adhesives are well-suited for

bonding light-weight composites to underlying structures, an important feature in aircraft since composites weigh much less than metals.<sup>(43)</sup>

Although epoxy resins were introduced to the construction industry at about the same time as to the aerospace industry, the development of adhesive technology has not fared as well, mainly for two reasons. First, a lack of research funding has limited the development. Second, the general conservative nature of the construction industry slows the introduction of new technology.

Adhesives have been applied to bridge construction and rehabilitation in the following areas: (1) epoxy/aggregate mortar; (2) coating and surfacing; (3) nonstructural bonding; and (4) structural bonding. Wider applications can be expected in the future, as the potential of adhesive technology is fully developed.

## 1.2 Objectives

The results of a recently completed study showed that attaching a cover plate to the tension flange of a steel beam with longitudinal welds along the central region, and with friction-type high-strength bolted connections at the nonwelded ends, increased the fatigue life by a factor of 16 over that of conventionally end-welded cover plates.<sup>(5,7)</sup> Accordingly, end-bolted cover plates have Category B fatigue strength, whereas long welded attachments have Category E strength.<sup>(1)</sup> The large increase in life is possible because friction-type bolted connections can transfer force from one plate to another with much less stress concentration than would occur in rigid welded connections.

Similarly, one would expect an increase in the fatigue strength of structural details when adhesives help to distribute and to transfer the load over a larger area, thus reducing stress concentrations. Two

main applications come to mind. One deals with load-carrying bolted joints, such as splices, and consists of reinforcing the joint with adhesives applied on the plate contact surfaces. In doing so, the force is transmitted over the full contact surface rather than only at the clamped regions surrounding the bolts. This could increase both the fatigue and static strength of the joints.

The other main application deals with the fatigue strength of attachments that are presently welded. The severity of the stress concentration and, hence, the fatigue strength depend on the length of the attachment. For example, the mean fatigue life of a Category B welded plate girder without attachments drops by a factor of 2.5 for Category C 2-in (50 mm) attachments, by a factor of 7 for Category D 4-in (100 mm) attachments, and by a factor of 16 for Category E 8-in (200 mm) and longer attachments. Since end-bolting cover plates raised the fatigue strength from Category E to Category B, one may expect similar improvements when attachments are adhesively bonded.

The objective of this experimental study is to explore ways of increasing the fatigue and static strength of structural details by using adhesives.

### 1.3 Adhesive Selection

The selection of the acrylic structural adhesive, Versilok 201, for use in the present study was largely based on a previous evaluation of adhesives.<sup>(4)</sup> In that study, 39 manufacturers had submitted information on various adhesives. The researchers chose 11 adhesives for testing. After preliminary shear and tensile tests, they selected 3 adhesives - Lord Versilok 204, Dexter Hysol EA934, and Dexter Hysol EA9309. The Versilok adhesives were chosen for their high shear and

tensile strength, rapid cure at room temperature, and minimal requirements for surface preparation. They chose Versilok 204 over Versilok 201 for high viscosity, not considered an important factor in our testing. The Dexter Hysol products were selected as the best among the epoxy-based adhesives tested. In the shear strength tests, conducted at three different temperatures, Versilok 201 had the highest average strength. In the tensile test, it fell only slightly below Versilok 204. The Versilok curing times were far quicker than any others, and they had much greater tolerance for oils left on the metal surface. The epoxy adhesive EA9309 had higher creep strength than Versilok 204.

In a series of pilot tests performed in the present study, 28 3 in x 5/16 in x 12 in (76 mm x 8 mm x 300 mm) long attachments were bonded to the tension flange of W14 x 30 beams, 12 with epoxy adhesive EA9309 and 16 with acrylic adhesive Versilok 201. All attachments gradually debonded from both ends under cyclic loading. Since those bonded with Versilok 201 had longer fatigue lives, the adhesive Versilok 201 was selected for use in the present study.

## CHAPTER 2: TEST SPECIMENS AND PROCEDURES

The feasibility of using adhesive to bond structural details on highway bridges was experimentally examined in this study with the following six series of tests:

- Fatigue strength of Series A tensile splices
- Fatigue strength of Series B beam splices
- Fatigue strength of Series B beam cover plates
- Static strength of Series C tensile splices
- Static strength of Series D beam splices
- Creep strength of Series E double strap specimens.

### 2.1 Specimens

Tensile Specimens: The Series A and C specimens are shown in Fig. 1. The specimens with two-bolt splices consisted of two 2-1/2 in x 5/8 in x 12 in long (64 mm x 16 mm x 305 mm) main plates and two 2-1/2 in x 5/16 in x 10 in long (64 mm x 8 mm x 254 mm) splice plates. They were connected with two bolts in double shear on either side of the splice center line. The specimens with one-bolt splices consisted of two 2-1/2 in x 5/8 in x 9-1/2 in long (64 mm x 16 mm x 241 mm) main plates and two 2-1/2 in x 5/16 in x 5 in long (64 mm x 8 mm x 127 mm) splice plates connected with one bolt on both sides of the splice center line.

All plates were fabricated from steel that satisfied the tensile and chemical requirements of ASTM A588 Standard Specification for High-Strength Low-Alloy Structural Steel with 50,000 psi (345 MPa)

Minimum Yield Point. The mechanical properties and chemical compositions are summarized in Tables 1 and 2, respectively.

All bolts for the tensile specimens were 5/8-in (16 mm) diameter ASTM A325 Type 3 high-strength bolts. The washers and nuts were ASTM F436 Grade 3 hardened steel washers and ASTM A563 Grade C/3 structural hex nuts.

The tensile specimens were assembled and tested without or with adhesive applied on the contact surfaces of the bolted splices. They are hereafter referred to as the nonbonded and bonded specimens.

Beam Specimens: The Series B and D specimens consisted of 15 ft-6 in (4724 mm) long W14 x 30 beams tested on a 15-ft (4572 mm) span. The flanges of the Series B fatigue test beams were connected at midspan with six-bolt or four-bolt splices, as shown in Fig. 2.

The flange splice plates were 6-3/4 in x 1/2 in x 1 ft-3 1/4 in (171 mm x 13 mm x 387 mm) long and 6-3/4 in x 1/2 in x 10-1/4 in (171 mm x 13 mm x 260 mm) long, respectively. They were connected with six or four bolts in single shear on both sides of midspan. The flanges of the Series D static test beams were connected at midspan with six-bolt, four-bolt, and two-bolt splices, as shown in Fig. 2. The former two were identical to the flange splices on the fatigue test beams. The latter consisted of 6-3/4 in x 1/2 in x 5-1/4 in (171 mm x 13 mm x 133 mm) long splice plates connected with two bolts on both sides of midspan.

All beam webs were connected with two 5-1/4 in x 3/16 in x 6 in (146 mm x 5 mm x 152 mm) long splice plates that were attached with two bolts in double shear on both sides of midspan.



In addition to the previously described splice details, the Series B beams had two 6-3/4 in x 1/2 in x 3 ft-9 in (171 mm x 13 mm x 1143 mm) cover plates adhesive bonded to the tension flange. All cover plate ends facing the midspan were clamped to the flanges with two bolts.

The beams, splice plates, and cover plates were fabricated from ASTM A588 steel. The tensile properties and chemical composition are given in Tables 1 and 2, respectively.

The bolts used in all beam splices were 3/4-in (19 mm) diameter A325 high-strength bolts.

The beam specimens were assembled and tested with the contact surfaces of the bolted splices either nonbonded or bonded.

Creep specimens: The double strap tensile specimens used in the Series D creep tests, shown in Fig. 3, consisted of two 1 in x 1/2 in x 4-1/2 in (25 mm x 13 mm x 108 mm) long main adherends. The straps were 1 in x 1/4 in x 1-1/8 in (25 mm x 6 mm x 29 mm) or 1 in x 1/4 in x 2-1/16 in (1 mm x 6 mm x 53 mm) long and overlapped each adherend by 1/2 in or 1 in (13 mm or 25 mm), respectively. All contact surfaces were adhesive bonded.

## 2.2 Bolts-to-Member Strength Ratio:

The two-bolt tensile specimens and the six-bolt beam specimens were designed so that the bolts and the member would fail at about the same ultimate load. The number of bolts in the other specimens were reduced to determine experimentally to what degree bolts can be replaced by adhesives without lowering the static and fatigue strength of the member.

The AASHTO allowable bolts-to-member strength ratio allows one to compare the relative joint strength of the specimens tested in the present study against that of bridge members.

Since Art. 1.7.15 of the AASHTO specifications requires that a splice shall be designed for at least 75% of the member's strength, and assuming that the bolts are not oversized, the bolts-to-member strength ratio of splices used in bridges fall in the range  $0.75 \leq (P_b/P_m)$  or  $(M_b/M_m) \leq 1.0$ .

Tensile Specimens: The AASHTO allowable bolts-to-member strength ratio of the Series A and C tensile specimens is given by:

$$\frac{P_b}{P_m} = \frac{m n F_v A_b}{F_t A}$$

in which:

$P_b$  = AASHTO allowable load carried by bolts

$P_m$  = AASHTO allowable load carried by tensile specimen

$m$  = number of shearing planes

$n$  = number of bolts

$F_v$  = allowable shear stress in bolt

$A_b$  = bolt gross area

$F_t$  = allowable tensile stress in plate

$A$  = Cross sectional area of member

This ratio is calculated below for the two-bolt splice, assuming friction-type connection with blast cleaned contact surfaces. Allowable load for two 5/8-in (16 mm) diameter A325 bolts in double shear:

$$\begin{aligned} P_b &= m n F_v A_b \\ &= 2 \times 2 \times 25 \times 0.307 = 30.7 \text{ kips} \quad (137 \text{ kN}) \end{aligned}$$

Allowable load for A588 steel member with minimum specified tensile properties:

- Gross area:

$$A = 2.5 \times 0.625 = 1.56 \text{ in}^2 \quad (1,006 \text{ mm}^2)$$

- Net area:

$$15\% A = 0.15 \times 1.56 = 0.23 \text{ in}^2 \quad (148 \text{ mm}^2)$$

$$t(d_h + 1/16) = 5/8 (11/16 + 1/16) = 0.47 \text{ in}^2 \quad (303 \text{ mm}^2)$$

$$\begin{aligned} A_n &= A - [t(d_h + 1/16) - 0.15A] \\ &= 1.56 - [0.47 - 0.23] = 1.32 \text{ in}^2 \quad (852 \text{ mm}^2) \end{aligned}$$

$$P_m = 0.55 F_y A_g = 0.55 \times 50 \times 1.56 = 42.9 \text{ kips} \quad (191 \text{ kN})$$

$$P_m = 0.46 F_u A_n = 0.46 \times 70 \times 1.32 = 42.5 \text{ kips governs} (189 \text{ kN})$$

- Allowable bolts-to-member strength ratio:

$$\frac{P_b}{P_m} = \frac{30.7}{42.5} = 0.72$$

The corresponding ratio for the one-bolt splice is,  $P_b/P_m = 0.36$ .

Beam Specimens: The AASHTO allowable bolts-to-member strength ratio of the Series B and D beam specimens is given by:

$$\frac{M_b}{M_m} = \frac{m n F_v A_b d}{(S_n F_b) \text{ or } (F_b A_n d)}$$

in which:

$M_b$  = AASHTO allowable moment carried by bolts

$M_m$  = AASHTO allowable moment carried by beam

$m$  = number of shearing planes

$n$  = number of bolts

$F_v$  = allowable shear stress in bolt

$A_b$  = bolt gross area

$d$  = beam depth

$S_n$  = net section modulus

$F_b$  = allowable bending stress in beam or splice plate

$A_n$  = net area of splice plate

This ratio is calculated below for the six-bolt splice, assuming friction-type connection with blast cleaned contact surfaces. Allowable moment for six 3/4-in (19 mm) diameter A325 bolts per flange, in single shear:

$$F_v = 25 \text{ ksi} \quad (172 \text{ MPa})$$

$$\begin{aligned} M_b &= m n F_v A_b d \\ &= 1 \times 6 \times 25 \times 0.442 \times 13.86 = 918.5 \text{ kip in} \quad (103.7 \text{ kN m}) \end{aligned}$$

Allowable moment for W14 x 30 beam of A588 steel

- Cross Sectional Properties of W14 x 30 beam:

$$d = 13.86 \text{ in}, b_f = 6.73 \text{ in}, t_f = 0.38$$

$$t_w = 0.27 \text{ in}, I = 290 \text{ in}^4, S = 41.9 \text{ in}^3$$

$$A_f = b_f t_f = 6.73 \times 0.38 = 2.59 \text{ in}^2 \quad (1,672 \text{ mm}^2)$$

$$15\% A_f = 0.15 \times 2.59 = 0.39 \text{ in}^2 \quad (251 \text{ mm}^2)$$

$$2t_f (d_h + 1/16) = 2 \times 0.38 (13/16 + 1/16) = 0.67 \text{ in}^2 \quad (429 \text{ mm}^2)$$

$$\Delta A = 2t_f (d_h + 1/16) - 0.15A_f = 0.28 \text{ in}^2 \quad (181 \text{ mm}^2)$$

$$I_n = I - 2\Delta A (d/2 - t_f/2)^2$$

$$= 290 - 2 \times 0.28 (13.86/2 - 0.38/2)^2$$

$$I_n = 264.6 \text{ in}^4 \quad (110 \times 10^6 \text{ mm}^4)$$

$$S_n = \frac{I_n}{d/2} = \frac{264.6}{13.86/2} = 38.2 \text{ in}^3 \quad (626 \times 10^3 \text{ mm}^3)$$

- Allowable bending moment for W14 x 30 beam:

$$F_b = 0.55 F_y = 0.55 \times 50 = 27.5 \text{ ksi} \quad (190 \text{ MPa})$$

$$M = S_n F_b = 38.2 \times 27.5 = 1050.5 \text{ kip in (governs)} \quad (119 \text{ kN m})$$

- Splice plate:

$$A = 6.73 \times 0.50 = 3.37 \text{ in}^2 \quad (2,172 \text{ mm}^2)$$

$$15\% A = 0.15 \times 3.37 = 0.50 \text{ in}^2 \quad (326 \text{ mm}^2)$$

$$2t(d_h + 1/16) = 2 \times 1/2 (13/16 + 1/16) = 0.88 \text{ in}^2 \quad (565 \text{ mm}^2)$$

$$\Delta A = 2t(d_h + 1/16) - 0.15 A = 0.38 \text{ in}^2 \quad (242 \text{ mm}^2)$$

$$A_n = A - \Delta A = 3 \text{ in}^2 \quad (1,935 \text{ mm}^2)$$

- Allowable bending moment for splice plates:

$$F_b = 0.55 F_y = 0.55 \times 50 = 27.5 \text{ ksi} \quad (190 \text{ MPa})$$

$$M = F_b A_n d = 27.5 \times 3 \times 13.86 = 1143 \text{ kip in} \quad (130 \text{ kN m})$$

- Allowable bolts-to-member strength ratio:

$$\frac{M_b}{M_m} = \frac{918.5}{1050.5} = 0.87$$

The corresponding ratio for the four-bolt and the two-bolt splices are

$$M_b/M_m = 0.58 \text{ and } M_b/M_m = 0.29.$$

### 2.3 Fabrication

All beams and plates were rolled at Bethlehem Steel's Sparrows Point, Maryland plant. The test specimens were fabricated by High Steel Structures, Lancaster, Pennsylvania. The fabricator was instructed to use the same fabrication techniques, workmanship, and inspection procedures that are typical of steel bridge construction. All plates were shot blasted (wheelabrased), using No. 330 cast steel shot, to a near white surface condition. The specimens were then assembled for shipment with bolts hand-tightened.

As the Series C specimens were being tested it became apparent that the nonbonded specimens with two-bolt splices were slipping into bearing at lower loads than others. An examination of the contact surfaces showed that the fabricator had ground these specimens along the

edges and around the holes, after blast cleaning and drilling, to remove burrs. The ground areas were shiny and smooth. The Series C specimens with one-bolt splices had not been ground. To ensure all uniform surface condition, six additional two-bolt specimens, No. C17-C22, were ordered with the instruction to blast clean the specimens after drilling and grinding.

The same thing was happening with the Series D specimens. Since the beams with two-bolt splices had already been tested, it was decided, for reasons of economy, not to fabricate new ones. The beams with four-bolt and six-bolt splices had not yet been tested. They were sand blasted around the holes and edges to restore the full surface area to blast cleaned condition.

Some Series A and B specimens had been ground, but only around the holes. This should not have affected the results, because there is no significant difference in fatigue life of friction-type and bearing-type joints even when the data for both are plotted against the gross area stress range.<sup>(6)</sup>

## 2.4 Adhesives

The specimens were bonded with Versilok 201, an acrylic structural adhesive for bonding metals, composites, and engineering thermoplastics that is manufactured by Hughson Chemicals. The selection of the adhesive was largely based on research done previously at Case Institute of Technology, as summarized in Section 1.3.<sup>(4)</sup> In preliminary tests performed in the present study, Versilok 201 was found to be more resistant to impact and cleavage stresses than the epoxy adhesive Dexter Hysol EA9309 that had also been recommended in Ref. 4.

Versilok 201 adhesive is available as a no-mix system or a mix-in system. In the first case, Accelerator No. 4 is applied on the surface of one or both plates. The adhesive is applied on the other plate as soon as the accelerator dries, in one to three minutes at 75<sup>0</sup>F (24<sup>0</sup>C), or up to several weeks thereafter.

In the mix-in system four to six parts of Accelerator No. 5 by weight are added to 100 parts of Versilok 201. The short five-minute pot life of the mix-in system requires that the parts be joined immediately after the adhesive is applied.

For mix-in and no-mix systems, the adhesive begins to cure on contact with the accelerator. The bond becomes handleable after 8-16 minutes at 75<sup>0</sup>F (24<sup>0</sup>C) and develops full properties after 24 hours. Optimum bond line thickness is 5-10 mils (0.13 - 0.26 mm). Table 3 summarizes the typical properties of the adhesive and accelerators reported by the manufacturer.

The Series A to D specimens were bonded with the no-mix system, because the time needed to assemble and tighten the bolted joints exceeded the pot life of the mix-in system. The Series E creep specimens were bonded with the mix-in system.

## 2.5 Assembly

Series A to D Specimens: All tensile and beam specimens were assembled in the Laboratory prior to testing. The nonbonded specimens were bolted in the as-received condition. The bonded and bolted specimens were spliced as follows:

1. Clean all steel contact surfaces with a cloth.
2. Apply Accelerator No. 4 on all contact surfaces (both sides).

3. Apply Versilok 201 adhesive on one side of contact surfaces after the accelerator has dried.
4. Sprinkle 0.010-in (0.25 mm) diameter glass beads with a salt shaker on the contact surfaces to control the bond line thickness.
5. Place all plates and bolts in assembly jig.
6. Install nuts, and tension bolts to the specified values.
7. Cure specimens in laboratory air.

All tensile specimens were assembled in a jig, shown in Fig. 4, that was designed to hold the parts in place for bolting. Jigs were not needed for the beam specimens. In this case, the web splice kept the beam halves aligned. The web splices were not bonded.

In addition to the midspan splices, all Series B fatigue beams had two cover plates bonded and bolted to the tension flange, as was previously described for the splices. Four steel blocks held against the cover plates with firmly hand tightened C-clamps maintained pressure on the bond line during curing (Fig. 5).

All specimens were air cured at room temperature for at least 48 hours and not longer than two weeks.

Bolt Tensioning: The 5/8-in and 3/4-in (16 mm and 19 mm) diameter bolts were tensioned to 19 and 28 kips (84.5 and 124.5 kN), that is 70% of the specified minimum tensile strength of the bolts, rounded off to the nearest kip. The bolts were tensioned with a torque wrench that was calibrated with a Skidmore-Wilhelm device every time a group of specimens was assembled.

Series E Specimens: The creep specimens were assembled as follows:

1. Clean all steel contact surfaces with a cloth. When needed,



remove oil and crayon marks with trichloroethylene, a solvent recommended by the adhesive manufacturer.

2. Mix Versilok 201 adhesive and Accelerator No. 5.
3. Apply glue on strap plates.
4. Sprinkle 0.010-in (0.25 mm) diameter glass beads on contact surfaces.
5. Place parts in jig. (Fig. 6)
6. Clamp parts with a 3 in (75 mm) hand tightened clamp.
7. Remove excess adhesive between ends of main adherends.

Two batches of specimens were cured for 31 hours, all others for at least 46 hours. See Tables 28 and 29.

Bond Line Thickness: The method of ensuring that the bond line would have the desired thickness was recommended by the vendor for bonded surfaces alone. It was also applied in this study to specimens that were bonded and bolted. When the specimens were taken apart, and the contact surfaces examined under a microscope, it was found that the bolt-clamping force had squeezed the adhesive and the glass beads out of the area surrounding the bolt holes and towards the plate edges, as shown in Fig. 7.

## 2.6 Testing

Series A: Thirty-five of the 39 tensile fatigue specimens were tested at the University of Maryland and four specimens (A24, A27, A32, and A33) at the Turner Fairbank Highway Research Center (T-FHRC) of the Federal Highway Administration (FHWA), McLean, Virginia. The testing equipment at both laboratories consisted of a load-controlled MTS closed loop system of 100 kips (445 kN) dynamic capacity, driven by a 40 gallon/

min. (151 l/min) hydraulic power supply. The specimens were held with hydraulically actuated self-aligning flat plate friction grips that ensured central loading.

The cyclic load wave was sinusoidal, of constant amplitude, and applied at frequencies of 4, 6, 8, and 10 cycles per second at the 30, 23, 21, and 18 ksi (207, 159, 145, and 124 MPa) stress ranges, respectively. The applied load was monitored with an oscilloscope which displayed the voltage signal output from the load cell.

The test was stopped when the fatigue crack had severed the specimen into two parts.

Series B: All beam fatigue specimens were tested at the University of Maryland. The tests were carried out with a load-controlled MTS closed-loop system of 50 kips (223 kN) maximum dynamic capacity. The load was applied with a single jack and distributed with a spreader beam to the two loading points. The cyclic load waves were sinusoidal, of constant amplitude, and applied at frequencies of 3 and 4 cycles per second at 30 and 23 ksi (207 and 159 MPa) stress ranges, respectively.

The beams were carefully aligned in the test frame before loading, and all dimensions were checked. Two electrical-resistance, temperature compensated strain gages were bonded to the inside of the tension flange to verify the alignment and to double check the load.

A detail was said to have failed when a crack had emerged from under the bolt head or nut, and when a fretting crack had grown through the thickness of the flange or splice plate to a length of about 2 in (50 mm). Previous experience with testing bolted beam specimens had shown that the so-determined fatigue life was at least 98% of the number of cycles to beam failure.<sup>(7, 8)</sup> The end of a test was controlled

automatically by limiting the increment of midspan displacement caused by cracking to 0.015 in (0.4 mm).

Fatigue cracks were repaired with splice plates and high-strength C-clamps. Testing was then continued. In this manner, up to four data points were obtained per beam, two each for splice and cover plate ends. Testing of some details was discontinued when: (1) crack extension at the previously failed details could no longer be controlled, or (2) a large number of load cycles produced no visible cracking.

Series C: All static strength testing of tensile specimens were performed at the T-FHRC. Specimen C1 was tested in a Universal machine of 200-kip (890 kN) capacity that was equipped with flat wedge grips. Specimens C2 to C22 were tested with the same system used in Series A. The applied load versus total specimen elongation was automatically recorded with an X-Y plotter.

To determine the effect of type of loading on slip behavior, half of the specimens were tested under load control, mostly at a rate of 30 kips/min (133 kN/min), and the other half under stroke control, at a rate of 0.12 in/min (3 mm/min). The loading rate of each specimen is given in Tables 21 and 23.

Series D: The static strength beam specimens B1 and B2 with two-bolt splices, were tested at the University of Maryland, with the same equipment used for the Series B tests. Specimens B3 to B6, with four and six-bolt splices, were tested at the T-FHRC using a hand-operated hydraulic jack of 150 kip (667 kN) maximum load capacity. The two-point loading of all beams was applied with a single jack over a spreader beam. The beams were laterally braced at the load points.

The midspan deflection and the slip of the splice plate relative to the tension flange of each half beam were measured with dial gages. The load was applied in increments, and the gage readings were recorded when the load had stabilized.

Series E: The 100% and 80% stress level tests, each lasting at most ten minutes, were performed on a Tinius-Olsen tension-compression testing machine. The load was applied at a rate of 1,200 psi/min (8.3 MPa/min), according to ASTM Specification D648.<sup>(9)</sup> Temperatures in the testing laboratory ranged from 73-88°F (23-31°C).

In the 100% tests, the load was increased at the specified rate until failure. The failure loads were averaged for each lap length, and the loads for all succeeding nominal stress level tests were fractions of these averages. In the 80% tests, the load was increased to 80% of these average values, and then sustained until failure. The duration of sustained loading was recorded as the time to failure.

The 60% to 20% tests were performed in twelve spring-loaded frames, as shown in Fig. 8. The 2.5 in (64 mm) long extra heavy duty compression springs had 2 in (51 mm) outside and 1 in (25 mm) inside diameters. The rated capacity was 2.4 kips (10.7 kN) at 5/8-in (15.9 mm) displacement.

The specimens were gripped at each end by means of a tool hardened steel pin and a clevis, to ensure central loading of the specimen and bond line. A threaded rod extended from the top clevis through a hole in the cross bar over the two springs. A load applied with the testing machine on the cross bar placed the springs and the frame under compression, but not the specimen. Once the desired load was reached, the nut on the threaded rod was tightened against the cross bar. Upon

release of the load on the testing machine, the spring compression was balanced by an equal tension force in the specimen. The spring length was measured before and after the force transfer. The value of the load applied with the testing machine was then adjusted for changes in spring length, generally 4% or less, due to specimen elongation and bending of the cross bar.

The recorded time to failure began when the compression load was lifted from the cross bar, putting the specimen in tension.

## 2.7 Fatigue Crack Measurements

The following fatigue crack dimensions, illustrated in Figs. 9 and 10, were recorded at the end of each test:

$a$  = crack length projected on a plane normal to the nominal tensile stress.

$d$  = offset between the crack initiation point and the normal plane through the center of the bolt hole.

$\alpha_i$  = angle between the crack plane and the normal plane, at the crack initiation point.

$\alpha_f$  = crack plane angle at the final crack size.

Positive offsets and angles face the specimen ends; negative values face the specimen midlength. Cracks initiating at the holes are identified by the row number; fretting cracks by the letter F.

All fatigue crack dimensions are summarized in Tables 5 and 6 for the Series A tensile specimens, Tables 11 and 12 for the Series B beam splices, and in Table 17 for Series B beam cover plates.

## 2.8 AASHTO Category B Rhomboid

High-strength bolted joints are designed for fatigue to the allowable stress ranges of Category B. The calculated stress ranges are those in the base metal at the gross section of slip resistant friction-type joints, and at the net section of bearing-type joints.

The fatigue test data of this study are compared against the AASHTO Category B rhomboid. It is defined as the space containing 95.5% of the data points for plain welded beams from which the Category B allowable S-N line was derived.<sup>(1, 10)</sup> The rhomboid, shown in Fig. 11, is delineated by the following four lines:

1. Lower confidence limit, equal to the AASHTO allowable S-N line for Category B details:

$$\log N_d = (b - 2s) - m \log F_{sr}$$

with intercept  $b = 10.870$ , slope  $m = 3.372$ , standard deviation  $s = 0.147$ , and:

$N_d$  = number of design cycles

$F_{sr}$  = allowable stress range corresponding to the AASHTO design load

2. Upper confidence limit:

$$\log N = (b + 2s) - m \log f_r$$

3. Lower cut-off equal to the AASHTO fatigue limit of 16 ksi (110 MPa) for over 2,000,000 cycles of loading.
4. Upper cut-off equal to the highest stress range tested in Ref. 10,  $f_r = 42$  ksi (290 MPa).

Table 1: Mechanical properties of A588 Grade B steel for tensile and beam specimens

| Component                | Specimen No. | Heat No. | No. of Tests | Yield Point (ksi) | Tensile Strength (ksi) | Elongation 8 in Gage | CVN Energy (ft·lbs)                  |
|--------------------------|--------------|----------|--------------|-------------------|------------------------|----------------------|--------------------------------------|
| <u>Tensile specimens</u> |              |          |              |                   |                        |                      |                                      |
| Main plate               | C1-C16       | 92473-68 | 3            | 65.6              | 87.9                   | 21.2                 | 122 @ 25 <sup>0</sup> F              |
|                          | C17-C22      | 83098-6C | 3            | 73.3              | 98.1                   | 21.0                 | ...                                  |
| Splice plate             | C1-C16       | 401P5931 | 3            | 61.0              | 79.6                   | 19.0                 | 50 <sup>a</sup> @ 40 <sup>0</sup> F  |
|                          | C17-C22      | 930606D  | 3            | 77.9              | 106.0                  | 20.0                 | ...                                  |
| <u>Beam specimens</u>    |              |          |              |                   |                        |                      |                                      |
| W14 x 30 beam            | A11          | 181J544  | ..           | 56.6              | 77.6                   | 23.2                 | 106 <sup>a</sup> @ 25 <sup>0</sup> F |
| Splice and Cover plate   | A11          | 92473-68 | 3            | 67.0              | 89.2                   | 20.0                 | 78 @ 25 <sup>0</sup> F               |

Conversion Factors: 1 in = 25.4 mm, 1 ksi = 6.895 MPa

Note: a. Charpy size 10 mm x 7.5 mm

Table 2: Chemical composition of A588 Grade B steel for  
tensile and beam specimens

| Component                | Specimen No. | Composition, in Percent |      |       |       |      |      |      |      |       |      |
|--------------------------|--------------|-------------------------|------|-------|-------|------|------|------|------|-------|------|
|                          |              | C                       | Mn   | P     | S     | Si   | Cu   | Ni   | Cr   | V     | Al   |
| <u>Tensile specimens</u> |              |                         |      |       |       |      |      |      |      |       |      |
| Main Plate               | C1-C16       | 0.12                    | 1.05 | 0.019 | 0.011 | 0.25 | 0.28 | 0.25 | 0.47 | 0.06  | ...  |
|                          | C17-C22      | 0.11                    | 1.25 | 0.012 | 0.018 | 0.28 | 0.31 | 0.35 | 0.58 | 0.07  | ...  |
| Splice Plate             | C1-C16       | 0.12                    | 0.11 | 0.008 | 0.017 | 0.23 | 0.27 | 0.27 | 0.49 | 0.032 | ...  |
|                          | C17-C22      | 0.10                    | 0.17 | 0.010 | 0.020 | 0.42 | 0.29 | 0.32 | 0.50 | 0.06  | ...  |
| <u>Beam specimens</u>    |              |                         |      |       |       |      |      |      |      |       |      |
| W14 x 30                 | A11          | 0.16                    | 0.94 | 0.009 | 0.020 | 0.23 | 0.30 | 0.29 | 0.54 | 0.27  | 0.02 |
| Splice and Cover plate   | A11          | 0.12                    | 1.05 | 0.019 | 0.011 | 0.25 | 0.28 | 0.25 | 0.47 | 0.06  | ...  |



Table 3: Typical properties of adhesive and accelerators

| Characteristics                                    | Versilok 201                           | Accelerator<br>No. 4                                      | Accelerator<br>No. 5   |
|--|--|---|------------------------|
| Appearance   | Off-white liquid                       | Slightly hazy<br>to clear<br>amber liquid                 | Creamy white<br>liquid |
| Solvents   | None- 100<br>percent reactive          | Methylene<br>chloride/<br>MIBK/<br>Trichloroethy-<br>lene | None                   |
| Pot life mix system <sup>a</sup><br>at 75°F (24°C) | 5 minutes <sup>b</sup>                 | N/A <sup>c</sup>  | N/A                    |
| Handleable bonds at<br>75°F (24°C)                 | 8-16 minutes                           | N/A   | N/A                    |
| Full properties                                    | 24 hours <sup>d</sup>                  | N/A   | N/A                    |
| Weight mix ratio<br>(Versilok 201/acc.)            | N/A                                    | N/A   | 20:1                   |
| Cure   | 15 minutes at<br>room tempera-<br>ture | N/A   | N/A                    |
| Required clamping<br>pressure                      | 0                                      | 0   | 0                      |
| Shelf life   | 6 months                               | 6 months  | 6 months               |

Notes: a. Depends upon mass of the mixed adhesive  
b. When using accelerator No. 5  
c. N/A = not applicable  
d. When using accelerator No. 4 or 5

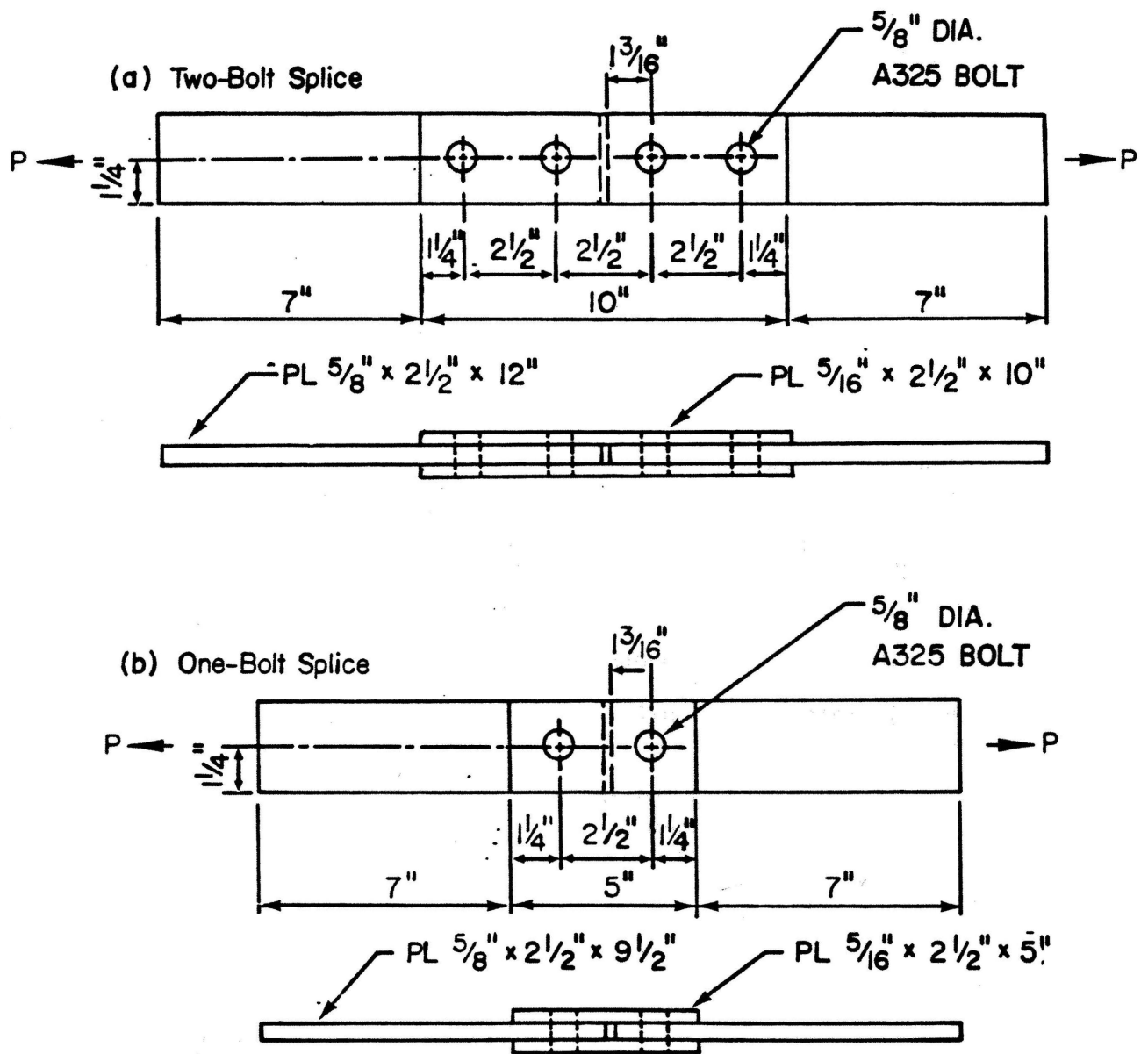


Figure 1: Series A and C tensile splices

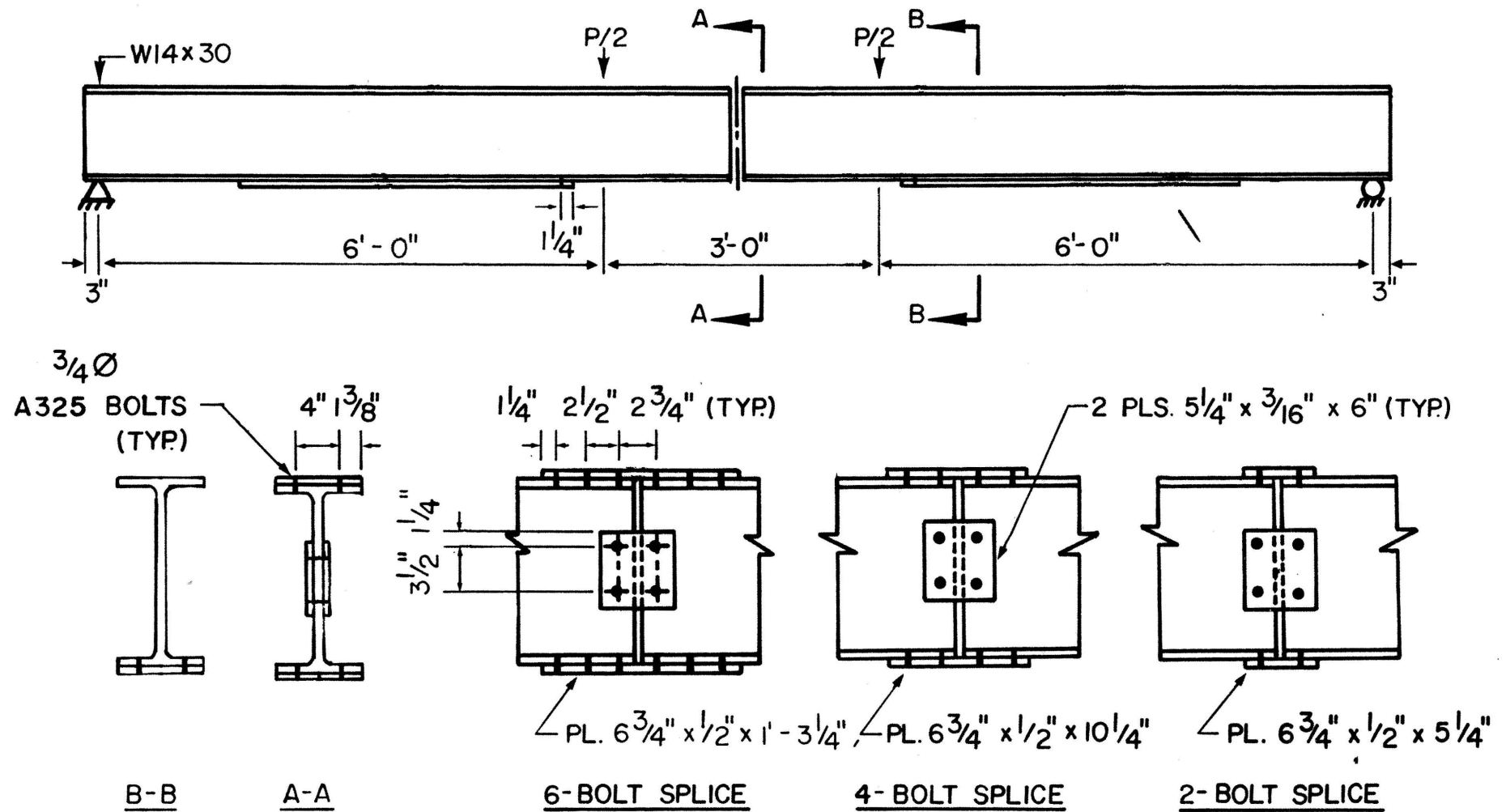


Figure 2: Series B and D beams

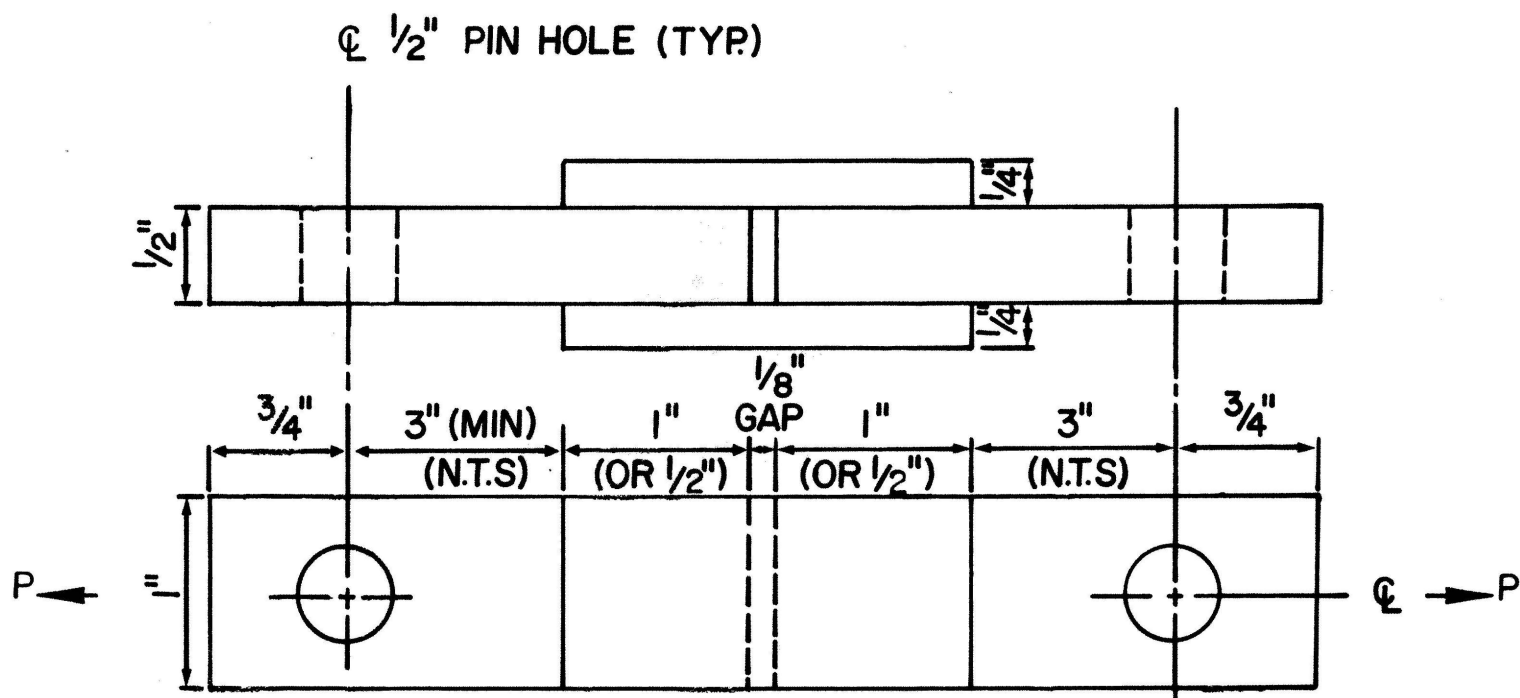
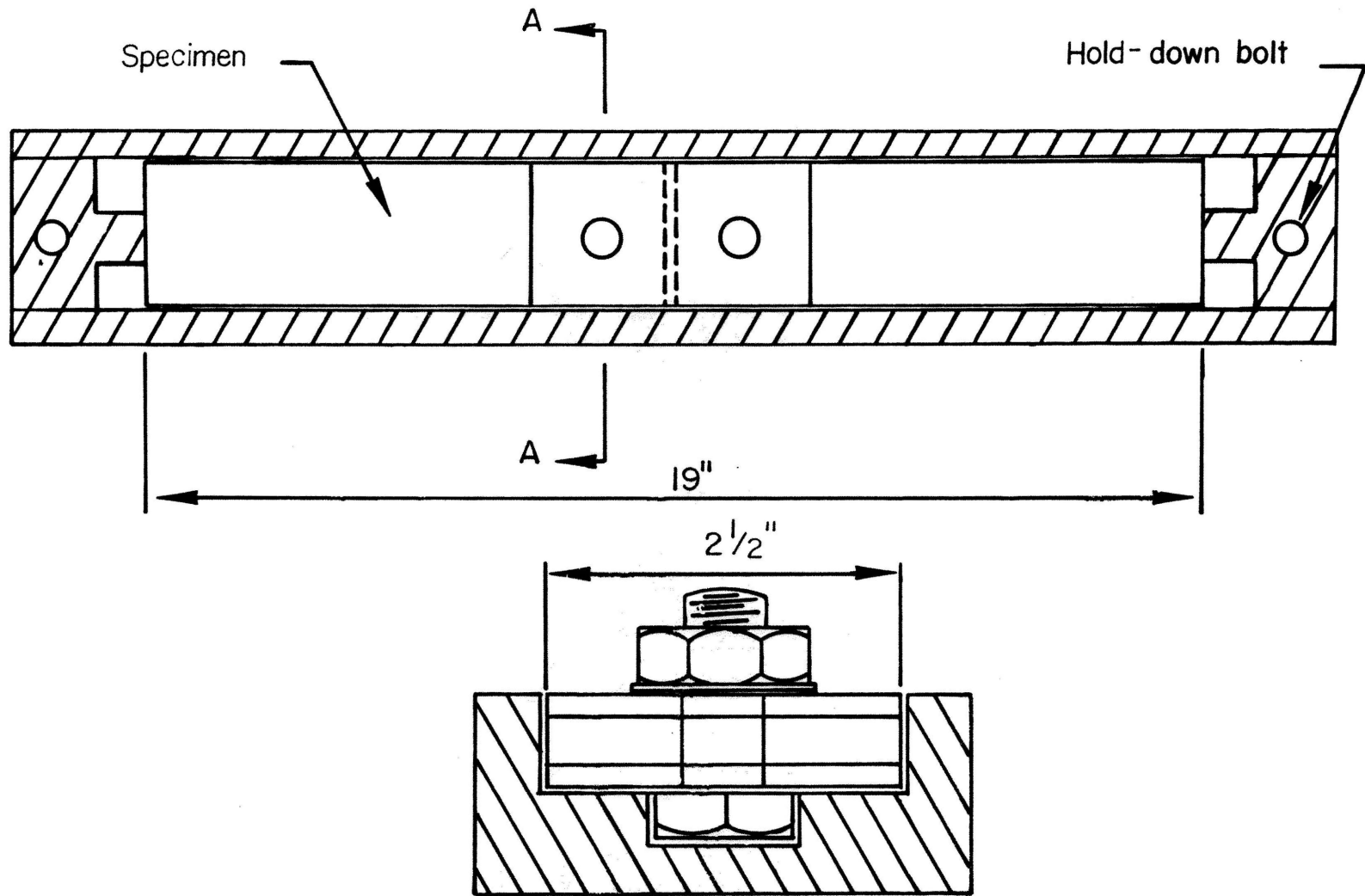


Figure 3: Series E double strap specimens



Section A-A

Figure 4: Jig to hold tensile specimens in place upon bonding

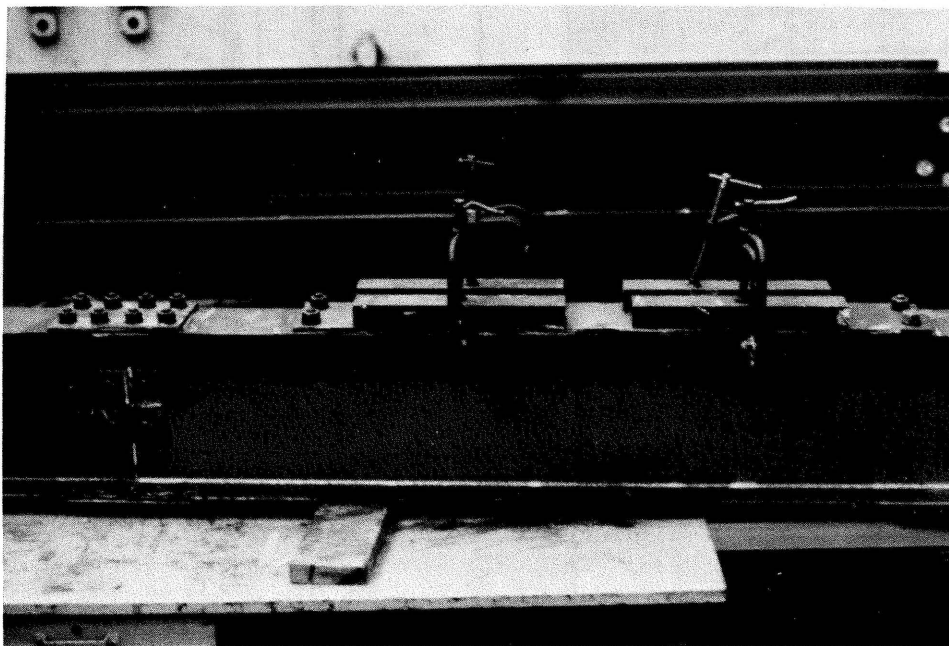


Figure 5: Adhesively bonded beams with C-clamps applied to cover plates

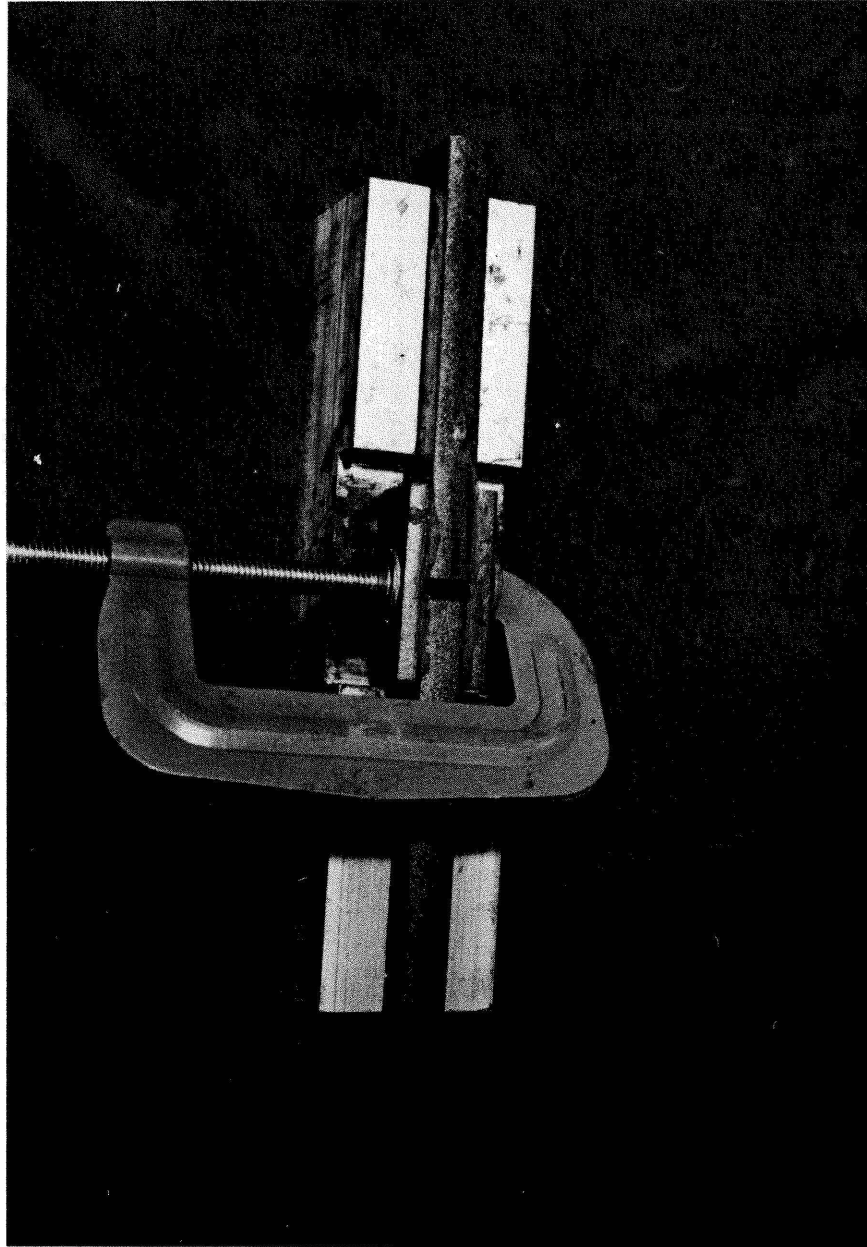


Figure 6: Jig to hold creep specimens in place upon glueing

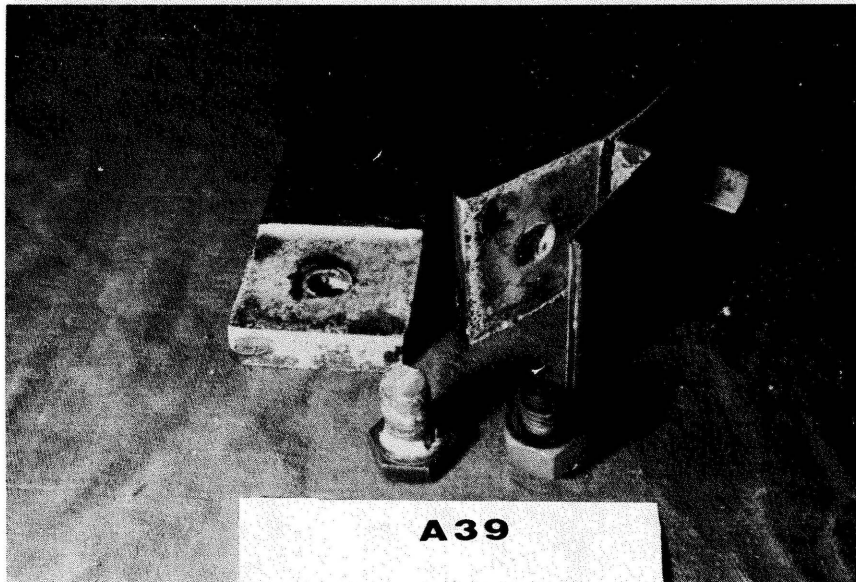


Figure 7: Contact surface appearance of tensile specimens after test ended



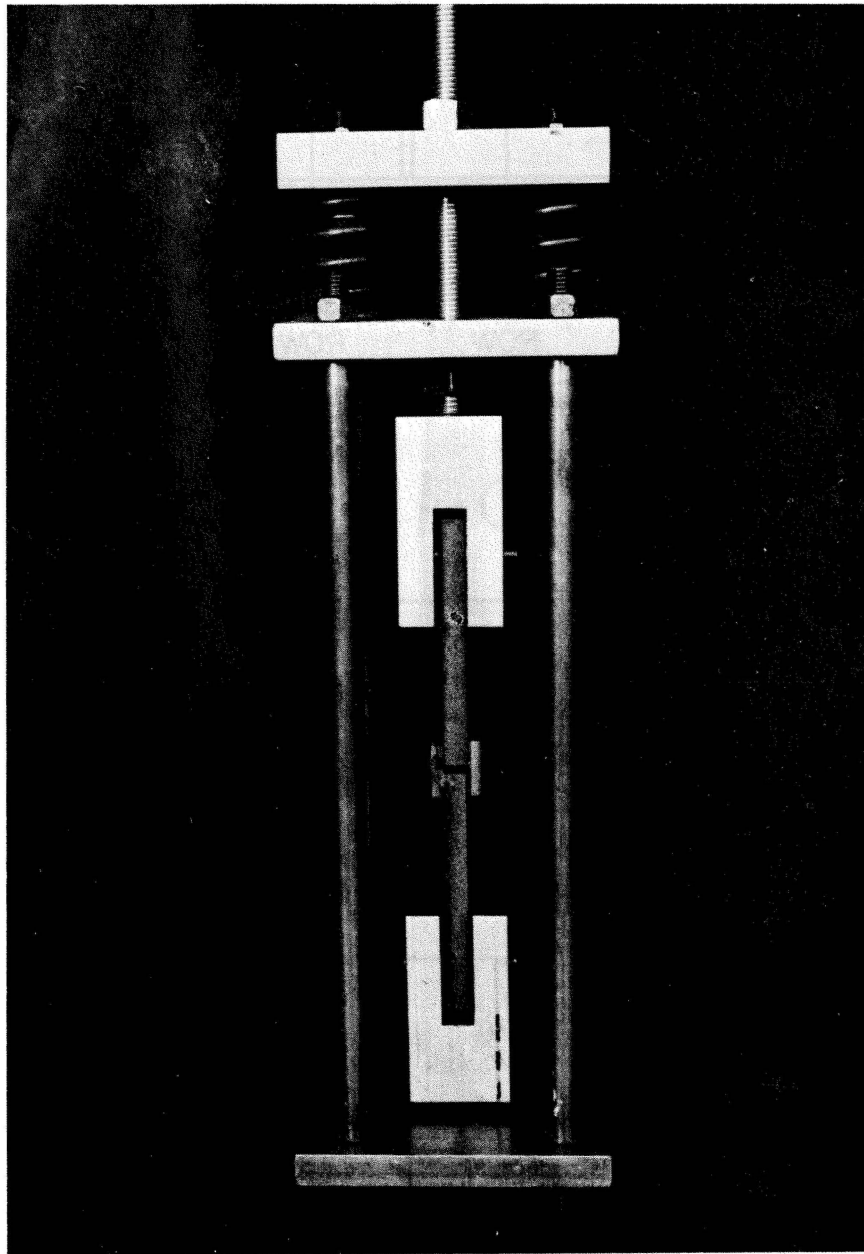
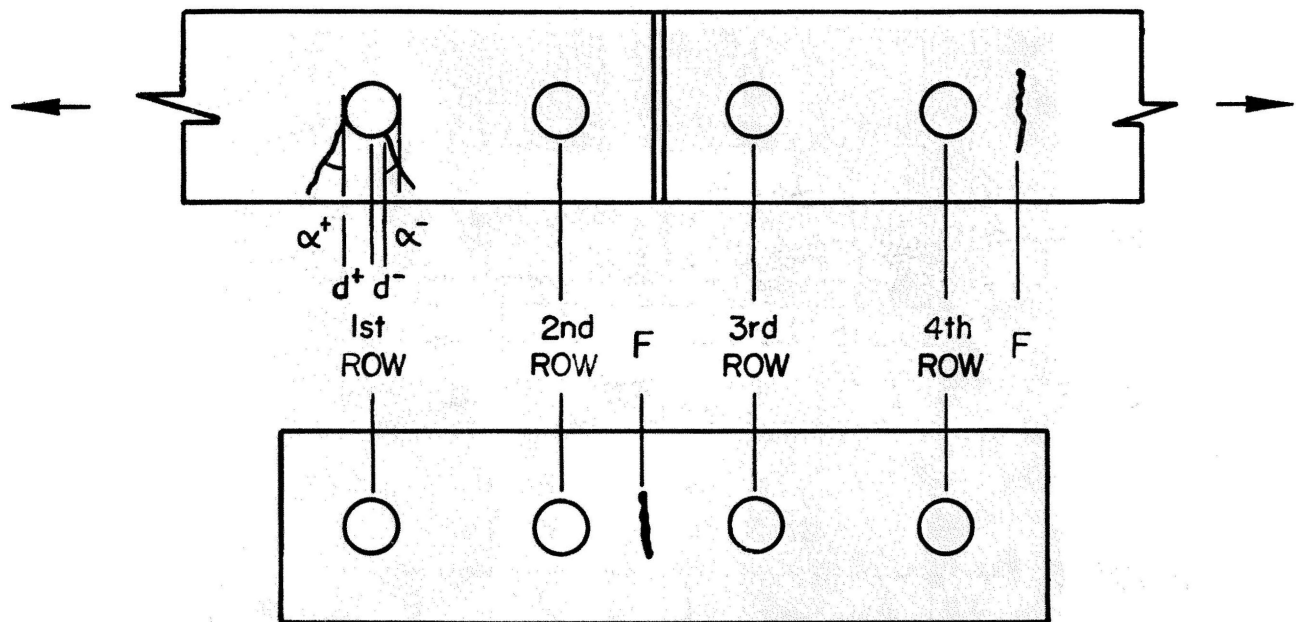
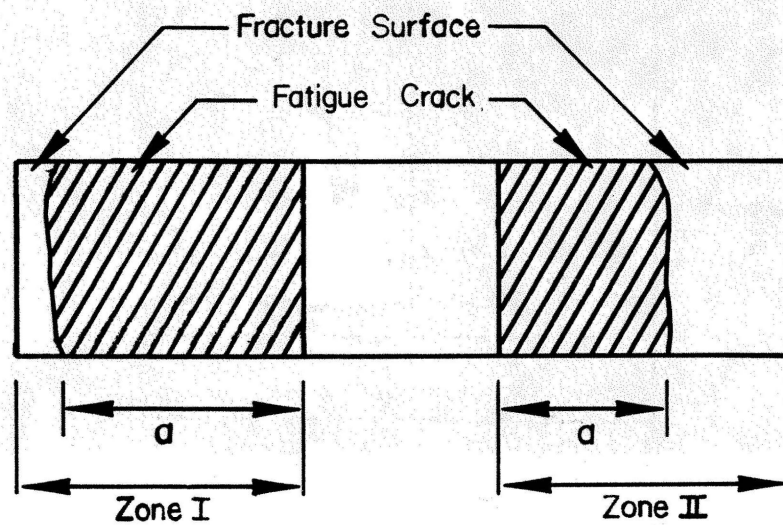


Figure 8: Spring-loaded frames used in Task E



(a)



(b)

Figure 9: (a) Definition of crack measurement procedure  
(b) Typical cracked section at failure

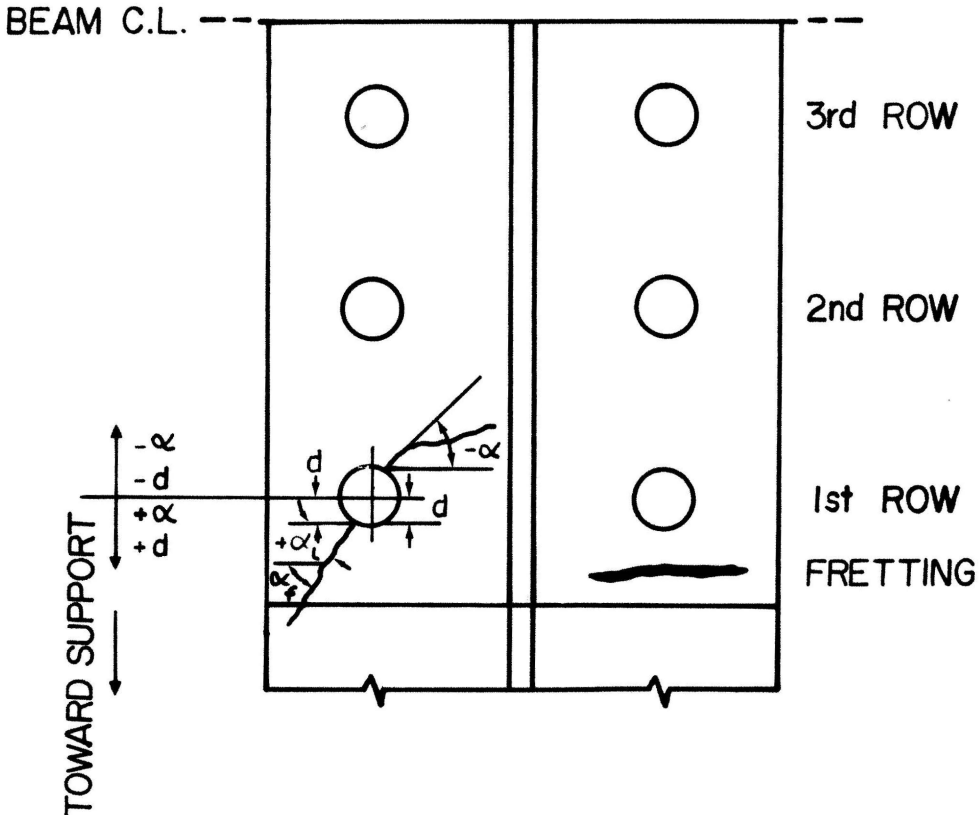


Figure 10: Definition of type of crack, crack angle, distance of crack initiation from hole center line, and zone of crack growth

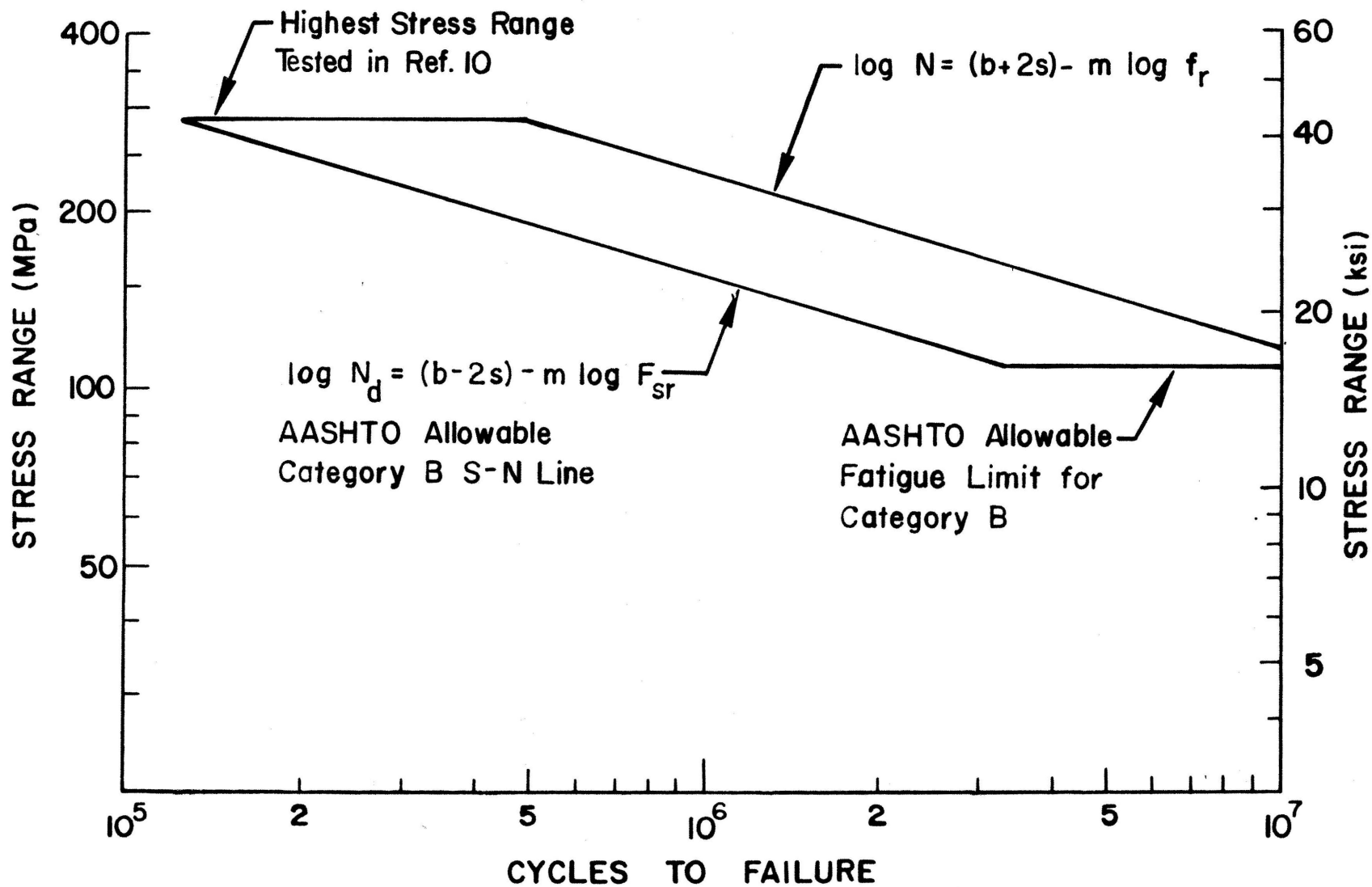


Figure 11: Definition of AASHTO Category B rhomboid

## CHAPTER 3: FATIGUE STRENGTH OF SERIES A TENSILE SPLICES

### 3.1 Experiment Design

The fatigue test matrix for the Series A tensile specimens, shown in Table 4, consisted of 39 specimens arranged in a three-way factorial with four levels of stress range, two-bolt and one-bolt splices, nonbonded or bonded contact surfaces, and two to four replicate tests per cell.

The specimens are shown in Fig. 1. The bolts-to-member strength ratio, calculated in Section 2.2, were  $P_b/P_m = 0.72$  and  $0.36$  for two-bolt and one-bolt splices, respectively.

The specimens were cycled at the four gross area stress ranges of 18, 21, 23 and 30 ksi (124, 145, 159 and 207 MPa). The minimum stress was 1 ksi (7 MPa) in all tests. It was decided not to test any bonded two-bolt splices in the two empty cells at 18 and 21-ksi (124 and 145 MPa) stress range, when the data for their nonbonded counterparts indicated that they would not fail. One-bolt specimens were not tested at 30-ksi (207 MPa) stress range, because the bolts would have been stressed to 80 ksi (545 MPa), a value close to the ultimate shear strength of A325 bolts.

The two levels of bolting and bonding in the test matrix were chosen to determine experimentally if: (1) bonding in addition to bolting increases the fatigue strength; and (2) to what degree bolts can be replaced by adhesives without lowering the fatigue strength.

### 3.2 Crack Initiation and Propagation

Figure 9 illustrates the types and dimensions of the fatigue

cracks in the Series A tensile specimens. Tables 5 and 6 summarize the recorded crack dimensions at the two-bolt and one-bolt splices, respectively.

Two-Bolt Splices: Of the 12 nonbonded two-bolt splices of specimens A1-A12, six failed from cracks that initiated at the first bolt hole in the main plate, one from fretting in the main plate ahead of the first bolt hole, and one at the second bolt hole in the splice plate. The remaining four specimens, A1-A4, did not fail.

Of the eight bonded two-bolt splices of specimens A13-A20, six failed from cracks that initiated at the first bolt hole in the main plate, and one at the second bolt hole in the splice plate. Specimen A15 did not fail.

The bolt hole cracks initiated along the bore or at the intersection of the bore with the specimen surface. They propagated at first as part-through or corner cracks, shown in Fig. 12, until their length along the bore was equal to the plate thickness. Thereafter, they propagated as through cracks across the plate until the net ligament ruptured in a ductile mode at stresses near the ultimate tensile strength of the plates. No brittle failures were observed. The bolt hole cracks initiated close to the intersection points of the normal plane with the edge of the hole. The offset,  $d$  (Fig. 9) varied from +0.08 in (2 mm) to -0.12 in (-3 mm) for nonbonded and bonded specimens alike. The crack angle at initiation,  $\alpha_i$ , varied from +7 degrees to -6 degrees. There was no correlation between the offset and the angle.

The fretting cracks were initiated by rubbing of the plates against each other. Figure 13 shows a fretting fatigue crack.

The nonbonded and bonded two-bolt splices failed in equal

numbers at the first bolt hole in the main plate (six), and at the second bolt hole in the splice plate (one). Only one nonbonded splice failed from a fretting crack. Evidently, bonding did not alter the mode of failure. The cracking behaviors were similar even though most nonbonded specimens slipped into bearing whereas all bonded specimens remained in friction (Table 7).

One-Bolt Splices: Of the nine nonbonded one-bolt splices of specimens A21-A29, four failed from cracks that initiated at the bolt hole in the main plate, three at the bolt hole in the splice plate, one from fretting in the splice plate ahead of the bolt hole, and one in the bolt. Of the ten bonded splices of specimens A30-A39, three failed from cracks that initiated at the bolt hole in the main plate, six in the bolt, and one (A30) did not fail.

The bolt hole cracks initiated and propagated in the same manner as those in the two-bolt splices. But the location of their initiation points varied more about the normal plane. The offsets ranged from +0.28 in (7.1 mm) to -0.14 in (3.6 mm), and the angles at initiation from +49 degrees to -22 degrees.

The two shearing planes were located at 5/16 in (7.9 mm) and 15/16 in (23.8 mm) from the bolt head. The first shearing plane was located in the body of the bolt (threads excluded) and was never the site of a fatigue crack. The second shearing plane was located at the runout of the last thread. Fractographic examination indicated that it was the site of fatigue cracks when the angular orientation caused the edge of a plate to bear on the bolt at the end of the last thread.

The bolts did not fatigue crack in the two-bolt splice because, for equal loads, the shearing stress was only one-half of that in the one-bolt splice.

### 3.3 Fatigue Test Data

Two-Bolt Splices: The fatigue test data for the nonbonded and bonded two-bolt splices are summarized in Table 7. The table lists for each splice the tensile stress range on the gross and net areas of the plates, the fatigue life, and whether the splice remained in friction or slipped into bearing.

The data points were plotted in Fig. 14 on the basis of gross area stress range with open and solid triangles, respectively, for the nonbonded and bonded splices. All runouts were identified with an arrow. Splice No. A7, labeled F in Fig. 14, failed from a fretting crack. It had a relatively long life.

One-half of the nonbonded splices slipped into bearing and the other half remained in friction. The data points for the former were labeled "b" in Fig. 14. All bonded splices behaved as friction-type joints. Bonding, in addition to bolting, increased the fatigue life, on average, by a factor of 1.73, from 1,899,000 to 3,264,000 cycles at 23-ksi (159 MPa) stress range, and from 446,000 to 775,000 cycles at 30-ksi (207 MPa) stress range.

The mean regression line, standard deviation, and coefficient of correlation were calculated for the splices tested at 23 and 30-ksi (159 and 207 MPa) stress range. The results for the eight non-bonded splices No. A5-A12 are:

$$\log N = 13.7076 - 5.456 \log f_r \quad (3.1)$$

$$s = 0.3273$$

$$r = 0.74$$

and for the eight bonded splices No. A13-A20:



$$\log N = 13.8804 - 5.410 \log f_r \quad (3.2)$$

$$s = 0.2445$$

$$r = 0.83$$

The intercepts of Eqs. 3.1 and 3.2, for stress range in units of MPa, are 18.2821 and 18.4165, respectively. The two mean regression lines were plotted in Fig. 14. The distance between them corresponds to the factor of 1.73 increase in life due to bonding.

Figure 14 also compares the data with the AASHTO Category B rhomboid, defined in Section 2.8. Most data points fell inside the rhomboid. The data points for four splices that did not fail (A2-A4, A15) and for the splice with a fretting crack (A7) fell above the rhomboid. Only two data points (A5 and A10) fell below the rhomboid.

Table 7 compares the log-mean life of each group of replicate tests with the mean life of Category B welded beams at the corresponding gross and net area stress ranges in the splices. The latter values were calculated from:  $\log N = 10.870 - 3.372 \log f_r^{(10)}$ . The following is concluded:

1. The mean lives of the nonbonded friction-type splices were much longer than the corresponding Category B mean lives for gross area stress range.
2. The mean lives of the nonbonded bearing-type splices were, on average, a factor of 1.5 longer than the Category B mean lives for net area stress range, but only one-half of those for gross area stress range.
3. The mean lives of the bonded specimens were equal to or greater than the Category B mean life for gross area stress range.

From the limited number of tests it cannot be determined to what degree the increase in life due to bonding was achieved by: (1) changing the splice behavior from bearing-type to friction-type; or (2) increasing the area of force transfer by friction from the ring around the bolt hole to the 2-1/2 in x 2-1/2 in (64 mm x 64 mm) bonded area per bolt.

One-Bolt Splices: The fatigue test data for the nonbonded and bonded one-bolt splices are summarized in Table 8. The data points were plotted in Fig. 15 on the basis of gross area stress range with open and solid triangles, respectively, for the nonbonded and bonded splices. The points for the four splices (A29, A33, A38 and A39) that failed by shearing of the bolt at very short lives fell outside of the plot and are not shown. The other three splices (A32, A36 and A37) with premature bolt failures were labeled "B".

Bonding changed the behavior of all splices from bearing-type to friction-type. Excluding the splices with bolt failures, bonding in addition to bolting increased the fatigue life by a factor of 3.81 at 21-ksi (145 MPa) stress range and by a factor greater than 1.22 at 18-ksi (124 MPa) stress range. The sample sizes for one-bolt splices were too small for regression analysis.

Only the data points for four splices (A22, A23, A24 and A30) tested at 18-ksi (124 MPa) stress range fell inside or above the Category B rhomboid, as shown in Fig. 15. All others fell below the rhomboid. The comparison of the log-mean life for each group of replicate tests with the corresponding mean life of Category B welded beams (Table 8) suggests the following conclusions:

1. The mean lives of the nonbonded and bonded splices were shorter than the Category B mean lives for gross area stress range.
2. Excluding the splices with bolt failures, the mean fatigue lives of the nonbonded and bonded specimens were a factor of 1.9 and 2.3, respectively, longer than the Category B mean lives for net area stress range.

The bolts had been underdesigned on purpose to determine the fatigue strength of a splice in which bolts and adhesive share in the load transfer. The one-bolt splices had a bolt-to-member strength ratio of 0.36, one-half of the 0.72 ratio for two-bolt splices. The AASHTO allowable stresses for A588 steel and A325 bolts are 27 ksi (186 MPa) for member axial tension, 25 ksi (172 MPa) for bolt shear, and 60 ksi (414 MPa) for bolt bearing. The ratio of these allowable stresses is 1/0.93/2.22. The corresponding ratio of stresses for the one-bolt splices was much higher, 1/2.55/4.00. Relative to the member axial stress, the bolts were overstressed by a factor of 2.74 on shear and a factor of 1.80 on bearing.

Table 9 summarizes the stress ranges for member axial tension, bolt shear, bolt bearing, and adhesive shear in all two-bolt and one-bolt splices. The bolt shear stresses are given for threads excluded and threads not excluded from a shear plane, because the 15/16 in (23.8 mm) distance from the bolt head to the second shear plane was, by chance, equal to the body length of the bolt to the runout of the last thread. The 2-1/4 in (57.2 mm) long bolts had a 1-in (25.4 mm) grip length and a 1-1/4 in (31.8 mm) full thread length. The bolt shear stresses were calculated assuming that the adhesive would

not transfer shear. The adhesive shear stresses were calculated for a 2.5 in x 2.5 in (64 mm x 64 mm) tributary area minus the bolt hole area, and assuming that the bolts would not transfer shear. The bolt and adhesive shear stresses are upper limits on the actual values because both elements shared in the load transfer.

The high shear stress range was the reason for the bolt failures in the nonbonded one-bolt splices. These failures always occurred in the second shear plane. Fractographic examination showed that this type of failure was induced when the angular orientation of the bolt caused the crack to initiate at the runout of the last thread. Bolts rotated 90 degrees from this orientation had the bearing point of the shearing plane shifted from the thread runout to the body of the bolt; they did not fail.

The high cyclic shear deformations failed the adhesive of several bonded one-bolt splices during the fatigue test. This changed their behavior from friction-type to bearing-type. Indeed, the ten bonded splices behaved initially as friction-type joints, but six of them (Table 8) eventually failed by shearing of the bolt when the thread runout was located in the second shearing plane.

The high rate of shear deformations generated heat in the one-bolt bonded splices and contributed to eventual adhesive failure. As is shown in Chapter 8, the strength of the adhesive used in this study was heat sensitive. In contrast, the two-bolt splices were fatigue tested at the same rate of loading but at one-half the rate of shear deformations, because the number of bolts and the bonded area were twice those of the one-bolt splices. None of the two-bolt splices exhibited bolt failures, adhesive failures during the fatigue test, or heat build-up.

Summary: Figure 16 summarizes the fatigue test data for the Series A tensile specimens. Each point represents the log-mean fatigue life for a group of two-bolt and one-bolt splices, either nonbonded or bonded. The data points for specimens that failed by bolt shearing were neglected. Also shown for purposes of comparison are the Category B mean and allowable lines. The results suggest the following conclusions:

1. Adhesive bonding, in addition to bolting, consistently increased the fatigue life.
2. Reducing the bolt-to-member strength ratio from 0.72 for two-bolt splices to 0.36 for one-bolt splices shortened the fatigue life to a degree that could not be recovered by bonding.
3. Bonded specimens should be cycled at slower frequencies more representative of bridge loading.

### 3.4 Comparison with Previous Work

Nonbonded Splices: The results of 377 fatigue tests of bolted splices that were reported in five domestic<sup>(12, 13, 14, 15, 16)</sup> and six foreign studies<sup>(17, 18, 19, 20, 21, 22)</sup> were collected and analyzed in a separate report.<sup>(6)</sup> To permit a meaningful comparison of the previous data with those for nonbonded splices tested in this study, the following types of specimens were excluded: (1) non-symmetrical specimens deforming out-of-plane under axial loading; (2) coated or weathered specimens; and (3) specimens subjected to negative stress ratios,  $R < 0$ . The following conclusions were taken from Ref. 6. They are illustrated with the S-N plots shown in Figs. 17-20.

1. Most data points for specimens with friction-type and bearing-type connections fell inside the AASHTO Category B rhomboid when both types were plotted on the basis of gross area stress range.<sup>(12, 13, 15, 21)</sup> This conclusion holds for specimens with wide variations of bolts-to-member strength ratio, acting in friction as well as in bearing. Birkemoe had also concluded that the fatigue life for steel plates in bolted connections was a function of gross section rather than net section stress.<sup>(15)</sup> See for example Fig. 17.
2. The few data points for flat plate specimens that fell along the lower bound or below the rhomboid came from specimens with:
  - 4, 7 and 11 bolt rows.
  - Edge distances smaller than the AASHTO minimum values.
  - Ratio of maximum stress to yield strength greater than 0.85 on the gross section and greater than 1.0 on the net section.
3. The fatigue life increased as the yield strength increased.<sup>(12, 21)</sup> See Fig. 18.
4. The fatigue life decreased as the number of bolt rows increased to four or more.<sup>(22)</sup> See Fig. 19.
5. Axially loaded tension members, in which the load was transmitted by bolts through some but not all of the cross sectional elements of the member, had Category C fatigue strength.<sup>(20)</sup> See Fig. 20.
6. Other variables influenced the fatigue life, but their effects were not sufficiently significant to merit consideration for design purposes.

7. The fatigue lives of the few beam specimens that were tested correlated well with the fatigue lives of the tensile specimens.<sup>(20)</sup>

Given the limitations on maximum stress, edge distance, bolt spacing, etc., imposed by the AASHTO specifications, there appears to be no need to design bearing-type joints for fatigue on the basis of the net section stress range. All bolted joints, whether friction-type or bearing-type, could be designed to Category B on the basis of gross area stress range. While long bolted joints have shorter lives, it may not be necessary to reduce the allowable stress range because their design is not normally governed by fatigue. The fatigue strength of members that transfer load through some but not all cross sectional elements should be lowered from Category B to Category C.

In comparison, all but two nonbonded two-bolt splices also exhibited Category B strength, when the data points were plotted against the gross area stress range. The one-bolt splices had lower fatigue strength, but their bolt-to-member strength ratio,  $P_b/P_m = 0.36$ , did not conform, by choice, with AASHTO Art. 1.7.15, requiring that splices shall not be designed to less than 75 percent of the strength of the member.

Bonded Splices: Chesson performed some exploratory tests on bolted and bonded shear block specimens similar to those sometimes used in tests of slip resistance of bolted joints.<sup>(3)</sup> The specimens consisted of sand blasted quenched and tempered steel plates, SAE Grade 5 bolts of strength comparable to that of A325 bolts, and epoxies with AREA formulations.

The results were reported to be disappointing. From the failures it was seen that the resin did not bond well the sand blasted surfaces of the shear blocks. After unsuccessful attempts to solve this problem, by using increasingly elaborate degreasing techniques and surface preparations, this series of explorations was discontinued.

Since the specimen dimensions, method of loading, applied stresses, and fatigue lives were not reported in Ref. 3, it is not possible to assess if other factors have contributed to debonding.



Table 4: Fatigue test matrix for Series A  
tensile specimens

| Stress Range<br>ksi (MPa) | Two-Bolt Splices |        | One-Bolt Splices |        |
|---------------------------|------------------|--------|------------------|--------|
|                           | Nonbonded        | Bonded | Nonbonded        | Bonded |
| 18<br>(124)               | A1               | ...    | A21              | A30    |
|                           | A2               | ...    | A22              | A31    |
|                           | ..               | ...    | A23              | A32    |
|                           | ..               | ...    | A24              | A33    |
| 21<br>(145)               | A3               | ...    | A25              | A34    |
|                           | A4               | ...    | A26              | A35    |
|                           | ..               | ...    | A27              | A36    |
|                           | ..               | ...    | ...              | A37    |
| 23<br>(159)               | A5               | A13    | A28              | A38    |
|                           | A6               | A14    | A29              | A39    |
|                           | A7               | A15    | ...              | ...    |
|                           | A8               | A16    | ...              | ...    |
| 30<br>(207)               | A9               | A17    | ...              | ...    |
|                           | A10              | A18    | ...              | ...    |
|                           | A11              | A19    | ...              | ...    |
|                           | A12              | A20    | ...              | ...    |

Table 5: Dimensions of cracks in Series A tensile specimens;  
Two-bolt splices

| Specimen No.             | Cracked Element | Type of Crack | Zone of Crack Growth | Offset from Hole Center Line d (in.) | Crack Angle at               |                           | Crack Length at Failure a(in.) |
|--------------------------|-----------------|---------------|----------------------|--------------------------------------|------------------------------|---------------------------|--------------------------------|
|                          |                 |               |                      |                                      | Initiation $\alpha_i$ (deg.) | Failure $\alpha_f$ (deg.) |                                |
| <u>Nonbonded Splices</u> |                 |               |                      |                                      |                              |                           |                                |
| A1                       | ..              | ..            | ..                   | ..                                   | ..                           | ..                        | ..                             |
| A2                       | ..              | ..            | ..                   | ..                                   | ..                           | ..                        | ..                             |
| A3                       | ..              | ..            | ..                   | ..                                   | ..                           | ..                        | ..                             |
| A4                       | ..              | ..            | ..                   | ..                                   | ..                           | ..                        | ..                             |
| A5                       | Splice plate    | 2nd           | I                    | 0.01                                 | 7                            | 9                         | 0.87                           |
|                          |                 |               | II                   | -0.12                                | 0                            | 0                         | 0.47                           |
| A6                       | Main plate      | 1st           | I                    | 0.08                                 | 4                            | -11                       | 0.87                           |
|                          |                 |               | II                   | -0.02                                | 0                            | 0                         | 0.55                           |
| A7                       | Main plate      | F             | ..                   | ..                                   | ..                           | ..                        | 0.94                           |
| A8                       | Main plate      | 1st           | ..                   | 0.06                                 | 9                            | -14                       | 0.85                           |
| A9                       | Main plate      | 1st           | ..                   | 0.08                                 | 7                            | -20                       | 0.83                           |
| A10                      | Main plate      | 1st           | ..                   | 0.08                                 | 7                            | -13                       | 0.87                           |

Table 5: Dimensions of cracks in Series A tensile specimens;  
Two-bolt splices (continued)

| Specimen No.          | Cracked Element | Type of Crack | Zone of Crack Growth | Offset from Hole Center Line d (in.) | Crack Angle at               |                           | Crack Length at Failure a (in.) |
|-----------------------|-----------------|---------------|----------------------|--------------------------------------|------------------------------|---------------------------|---------------------------------|
|                       |                 |               |                      |                                      | Initiation $\alpha_i$ (deg.) | Failure $\alpha_f$ (deg.) |                                 |
| A11                   | Main plate      | 1st           | ..                   | -0.04                                | 0                            | -12                       | 0.87                            |
| A12                   | Main plate      | 1st           | I                    | 0.01                                 | 0                            | -12                       | 0.67                            |
|                       |                 |               | II                   | 0.04                                 | -3                           | -14                       | 0.59                            |
| <u>Bonded Splices</u> |                 |               |                      |                                      |                              |                           |                                 |
| A13                   | Main plate      | 1st           | ..                   | -0.01                                | 5                            | -4                        | 0.87                            |
| A14                   | Main plate      | 1st           | ..                   | 0.08                                 | 0                            | -5                        | 0.91                            |
| A15                   | ...             | ..            | ..                   | ..                                   | ..                           | ..                        | ..                              |
| A16                   | Main plate      | 1st           | ..                   | 0.02                                 | -6                           | 0                         | 0.89                            |
| A17                   | Main plate      | 1st           | ..                   | 0.04                                 | 3                            | 23                        | 0.78                            |
| A18                   | Splice plate    | 2nd           | ..                   | 0.04                                 | -3                           | 10                        | 0.75                            |
| A19                   | Main plate      | 1st           | I                    | -0.12                                | 0                            | 8                         | 0.59                            |
|                       |                 |               | II                   | -0.08                                | 0                            | 8                         | 0.47                            |
| A20                   | Main plate      | 1st           | ..                   | -0.04                                | 0                            | 3                         | 0.69                            |

Note: See Fig. 9 for definition of crack types and dimensions.

Table 6: Dimensions of cracks in Series A tensile specimens;  
One-bolt splices

| Specimen No.             | Cracked Element | Type of Crack | Zone of Crack Growth | Offset from Hole Center Line d (in.) | Crack Angle                  |                           | Crack Length at Failure a (in.) |
|--------------------------|-----------------|---------------|----------------------|--------------------------------------|------------------------------|---------------------------|---------------------------------|
|                          |                 |               |                      |                                      | Initiation $\alpha_i$ (deg.) | Failure $\alpha_f$ (deg.) |                                 |
| <u>Nonbonded Splices</u> |                 |               |                      |                                      |                              |                           |                                 |
| A21                      | Main plate      | 1st           | ..                   | -0.14                                | -14                          | -28                       | 0.89                            |
| A22                      | Splice plate    | 1st           | ..                   | -0.12                                | 0                            | 20                        | -2.36                           |
| A23                      | Main plate      | 1st           | ..                   | 0.08                                 | 4                            | -5                        | 0.87                            |
| A24                      | Splice plate    | 1st           | I                    | 0.20                                 | 20                           | 6                         | 1.0                             |
|                          |                 |               | II                   | 0.14                                 | -3                           | 13                        | 0.81                            |
| A25                      | Main plate      | 1st           | I                    | 0.28                                 | 49                           | 49                        | 0.94                            |
|                          |                 |               | II                   | -0.10                                | -4                           | -14                       | 0.47                            |
| A26                      | Splice plate    | 1st           | ..                   | -0.07                                | 0                            | -8                        | 0.32                            |
| A27                      | Main plate      | 1st           | I                    | 0.02                                 | 0                            | -34                       | 0.69                            |
|                          |                 |               | II                   | -0.14                                | 31                           | -10                       | 0.39                            |
| A28                      | Splice plate    | F             | ..                   | -0.42                                | ..                           | ..                        | 2.25                            |
| A29                      | Bolt            | ..            | ..                   | ..                                   | ..                           | ..                        | ..                              |

Table 6: Dimensions of cracks in Series A tensile specimens;  
One-bolt splices (continued)

| Specimen No.          | Cracked Element | Type of Crack | Zone of Crack Growth | Offset from Hole Center Line d (in.) | Crack Angle                  |                           | Crack Length at Failure a (in.) |
|-----------------------|-----------------|---------------|----------------------|--------------------------------------|------------------------------|---------------------------|---------------------------------|
|                       |                 |               |                      |                                      | Initiation $\alpha_i$ (deg.) | Failure $\alpha_f$ (deg.) |                                 |
| <u>Bonded Splices</u> |                 |               |                      |                                      |                              |                           |                                 |
| A30                   | ..              | ..            | ..                   | ..                                   | ..                           | ..                        | ..                              |
| A31                   | Main plate      | 1st           | I                    | -0.10                                | -11                          | -11                       | 0.79                            |
|                       |                 |               | II                   | -0.10                                | -16                          | -16                       | 2.55                            |
| A32                   | Bolt            | ..            | ..                   | ..                                   | ..                           | ..                        | ..                              |
| A33                   | Bolt            | ..            | ..                   | ..                                   | ..                           | ..                        | ..                              |
| A34                   | Main plate      | 1st           | I                    | -0.20                                | 0                            | -5                        | 0.87                            |
|                       |                 |               | II                   | -0.02                                | -7                           | 5                         | 0.65                            |
| A35                   | Main plate      | 1st           | I                    | -0.08                                | -14                          | -6                        | 0.67                            |
|                       |                 |               | II                   | -0.18                                | -22                          | -2                        | 0.63                            |
| A36                   | Bolt            | 1st           | ..                   | ..                                   | ..                           | ..                        | ..                              |
| A37                   | Bolt            | 1st           | ..                   | ..                                   | ..                           | ..                        | ..                              |
| A38                   | Bolt            | 1st           | ..                   | ..                                   | ..                           | ..                        | ..                              |
| A39                   | Bolt            | 1st           | ..                   | ..                                   | ..                           | ..                        | ..                              |

Note: See Fig. 9 for definition of crack types and dimensions.

Table 7: Fatigue test data for Series A tensile specimens;  
Two-bolt splices

| Spec.<br>No.             | Stress Range                             |   | Type of<br>Joint at<br>Start of Test | Fatigue <sup>a</sup><br>Life<br>N<br>(x10 <sup>3</sup> ) | Log-Mean<br>Life<br>(x10 <sup>3</sup> ) | Category B Mean Life for                          |   |
|--------------------------|--|---|--------------------------------------|--|---|---|---|
|                          | Gross<br>Area<br>f <sub>r</sub><br>(ksi) | Net<br>Area<br>f <sub>rn</sub><br>(ksi) |                                      |  |   | Gross Area<br>Stress Range<br>(x10 <sup>3</sup> ) | Net Area<br>Stress Range<br>(x10 <sup>3</sup> ) |
|                          |  |   |                                      |  |   |   |   |
| <u>Nonbonded Splices</u> |  |   |                                      |  |   |   |   |
| A1                       | 18                                       | 24.8                                    | Friction                             | 2,678-R  | > 5,020                                 | 4,337   | 1,472   |
| A2                       | 18                                       | 24.8                                    | Friction                             | 9,412-R  |   |   |   |
| A3                       | 21                                       | 28.9                                    | Friction                             | 10,050-R   | > 10,037                                | 2,580   | 879   |
| A4                       | 21                                       | 28.9                                    | Friction                             | 10,024-R   |   |   |   |
| A5                       | 23                                       | 31.7                                    | Bearing                              | 678  | 4,050 <sup>b</sup><br>891 <sup>c</sup>  | 1,898   | 643   |
| A6                       | 23                                       | 31.7                                    | Friction                             | 2,509  |   |   |   |
| A7                       | 23                                       | 31.7                                    | Friction                             | 6,538  |   |   |   |
| A8                       | 23                                       | 31.7                                    | Bearing                              | 1,170  |   |   |   |
| A9                       | 30                                       | 41.3                                    | Bearing                              | 612  | 446                                     | 775   | 264   |
| A10                      | 30                                       | 41.3                                    | Bearing                              | 244  |   |   |   |
| A11                      | 30                                       | 41.3                                    | Bearing                              | 494  |   |   |   |
| A12                      | 30                                       | 41.3                                    | Bearing                              | 535  |   |   |   |
| <u>Bonded Splices</u>    |  |   |                                      |  |   |   |   |
| A13                      | 23                                       | 31.7                                    | Friction                             | 2,001  | > 3,264                                 | 1,898   | 643   |
| A14                      | 23                                       | 31.7                                    | Friction                             | 1,790  |   |   |   |
| A15                      | 23                                       | 31.7                                    | Friction                             | 10,003-R   |   |   |   |
| A16                      | 23                                       | 31.7                                    | Friction                             | 3,170  |   |   |   |

Table 7: Fatigue test data for Series A tensile specimens;  
Two-bolt splices (continued)

| Spec.<br>No. | Stress Range                    |                                  | Type of<br>Joint at<br>Start of Test | Fatigue <sup>a</sup><br>Life<br>N<br>( $\times 10^3$ ) | Log-Mean<br>Life<br>( $\times 10^3$ ) | Category B Mean Life for                        |   |
|--------------|---------------------------------|----------------------------------|--------------------------------------|--|---------------------------------------|---|---|
|              | Gross<br>Area<br>$f_r$<br>(ksi) | Net<br>Area<br>$f_{rn}$<br>(ksi) |                                      |  |                                       | Gross Area<br>Stress Range<br>( $\times 10^3$ ) | Net Area<br>Stress Range<br>( $\times 10^3$ ) |
| A17          | 30                              | 41.3                             | Friction                             | 683  |                                       |   |   |
| A18          | 30                              | 41.3                             | Friction                             | 733  |                                       |   |   |
| A19          | 30                              | 41.3                             | Friction                             | 793  | 775                                   | 775   | 264   |
| A20          | 30                              | 41.3                             | Friction                             | 911  |                                       |   |   |

Conversion factor: 1 ksi = 6.895 MPa

- Note:
- a. The symbol R designates a runout test.
  - b. Log-mean life of friction-type splices A6 and A7
  - c. Log-mean life of bearing-type splices A5 and A8.

Table 8: Fatigue test data for Series A tensile specimens;  
One-bolt splices

| Spec.<br>No.             | Stress Range                             |   | Type of<br>Joint at<br>Start of Test | Fatigue <sup>a</sup><br>Life<br>N<br>(x10 <sup>3</sup> ) | Log-Mean<br>Life<br>(x10 <sup>3</sup> ) | Category B Mean Life for                          |   |
|--------------------------|--|---|--------------------------------------|--|---|---|---|
|                          | Gross<br>Area<br>f <sub>r</sub><br>(ksi) | Net<br>Area<br>f <sub>rn</sub><br>(ksi) |                                      |  |   | Gross Area<br>Stress Range<br>(x10 <sup>3</sup> ) | Net Area<br>Stress Range<br>(x10 <sup>3</sup> ) |
| <u>Nonbonded Splices</u> |  |   |                                      |  |   |   |   |
| A21                      | 18                                       | 24.8                                    | Bearing                              | 755  | 2,824                                   | 4,337   | 1,472   |
| A22                      | 18                                       | 24.8                                    | Bearing                              | 2,678  |   |   |   |
| A23                      | 18                                       | 24.8                                    | Bearing                              | 9,412  |   |   |   |
| A24                      | 18                                       | 24.8                                    | Bearing                              | 3,343  |   |   |   |
| A25                      | 21                                       | 28.9                                    | Bearing                              | 128  | 162                                     | 2,580   | 879   |
| A26                      | 21                                       | 28.9                                    | Bearing                              | 425  |   |   |   |
| A27                      | 21                                       | 28.9                                    | Bearing                              | 79   |   |   |   |
| A28                      | 23                                       | 31.7                                    | Bearing                              | 85 <sup>b</sup>  | 1,898                                   |   | 643   |
| A29                      | 23                                       | 31.7                                    | Bearing                              | 6 <sup>b</sup>   |   |   |   |
| <u>Bonded Splices</u>    |  |   |                                      |  |   |   |   |
| A30                      | 18                                       | 24.8                                    | Friction                             | 10,000-R   | > 3,432 <sup>c</sup>                    | 4,337   | 1,472   |
| A31                      | 18                                       | 24.8                                    | Friction                             | 1,178 <sup>b</sup>                                       |   |   |   |
| A32                      | 18                                       | 24.8                                    | Friction                             | 1,168 <sup>b</sup>                                       |   |   |   |
| A33                      | 18                                       | 24.8                                    | Friction                             | 44 <sup>b</sup>  |   |   |   |



Table 8: Fatigue test data for Series A tensile specimens;  
One-bolt splices (continued)

| Spec.<br>No. | Stress Range                             |   | Type of<br>Joint at<br>Start of Test | Fatigue <sup>a</sup><br>Life<br>N<br>(x10 <sup>3</sup> ) | Log-Mean<br>Life<br>(x10 <sup>3</sup> ) | Category B Mean Life for                          |   |
|--------------|--|---|--------------------------------------|--|---|---|---|
|              | Gross<br>Area<br>f <sub>r</sub><br>(ksi) | Net<br>Area<br>f <sub>rn</sub><br>(ksi) |                                      |  |   | Gross Area<br>Stress Range<br>(x10 <sup>3</sup> ) | Net Area<br>Stress Range<br>(x10 <sup>3</sup> ) |
| A34          | 21                                       | 28.9                                    | Friction                             | 590  | 617 <sup>c</sup>                        | 2,580   | 879   |
| A35          | 21                                       | 28.9                                    | Friction                             | 645 <sup>b</sup>   |   |   |   |
| A36          | 21                                       | 28.9                                    | Friction                             | 100 <sup>b</sup>   |   |   |   |
| A37          | 21                                       | 28.9                                    | Friction                             | 109 <sup>b</sup>   |   |   |   |
| A38          | 23                                       | 31.7                                    | Friction                             | 10 <sup>b</sup>  | 1,898                                   | 1,898   | 643   |
| A39          | 23                                       | 31.7                                    | Friction                             | 13 <sup>b</sup>  |   |   |   |

Conversion factor: 1 ksi = 6.895 MPa

Notes: a. The symbol R designates a runout test.  
b. Splice failed by shearing of bolt.  
c. Log-mean life excluding splices with bolt failures.

Table 9: Summary of stress ranges in Series A tensile specimens

| Applied Load Range (kip) | Member Axial Tension |                | Bolt Shear <sup>a</sup> |                         | Bolt Bearing (ksi) | Adhesive Shear <sup>b</sup> (ksi) |
|--------------------------|----------------------|----------------|-------------------------|-------------------------|--------------------|-----------------------------------|
|                          | Gross Area (ksi)     | Net Area (ksi) | Threads Excluded (ksi)  | Threads Not Excl. (ksi) |                    |                                   |
| <u>Two-Bolt Splices</u>  |                      |                |                         |                         |                    |                                   |
| 28.1                     | 18                   | 24.8           | 22.9                    | 31.1                    | 36.0               | 1.19                              |
| 32.8                     | 21                   | 28.9           | 26.7                    | 36.3                    | 42.0               | 1.39                              |
| 35.9                     | 23                   | 31.7           | 29.3                    | 39.8                    | 46.0               | 1.53                              |
| 46.9                     | 30                   | 41.3           | 38.2                    | 51.9                    | 60.0               | 1.99                              |
| <u>One-Bolt Splices</u>  |                      |                |                         |                         |                    |                                   |
| 28.1                     | 18                   | 24.8           | 45.9                    | 62.3                    | 72.0               | 2.38                              |
| 32.8                     | 21                   | 28.9           | 53.5                    | 72.6                    | 84.0               | 2.78                              |
| 35.9                     | 23                   | 31.7           | 58.6                    | 79.5                    | 92.0               | 3.08                              |

Notes: a. Neglecting force transfer by adhesive shear.  
b. Neglecting force transfer by bolt shear.

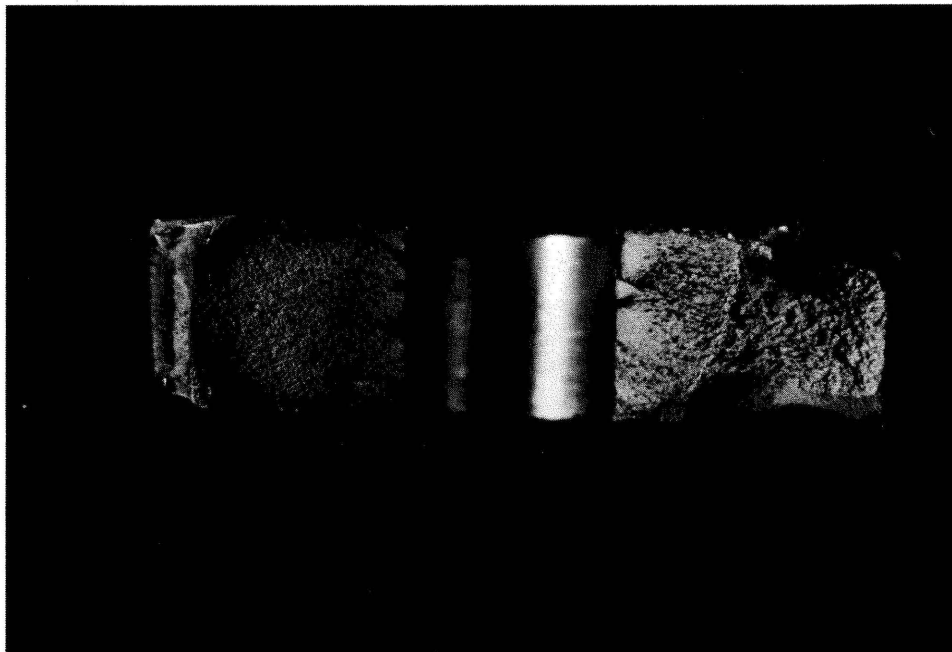
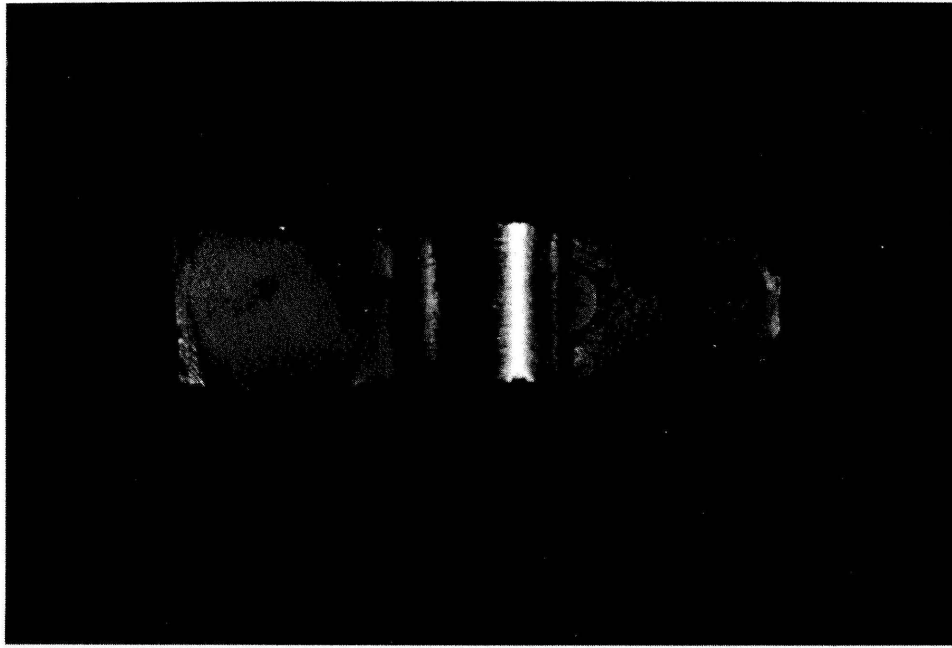


Figure 12: Typical fatigue crack surfaces;  
Specimen A8 (top) and A27 (bottom)

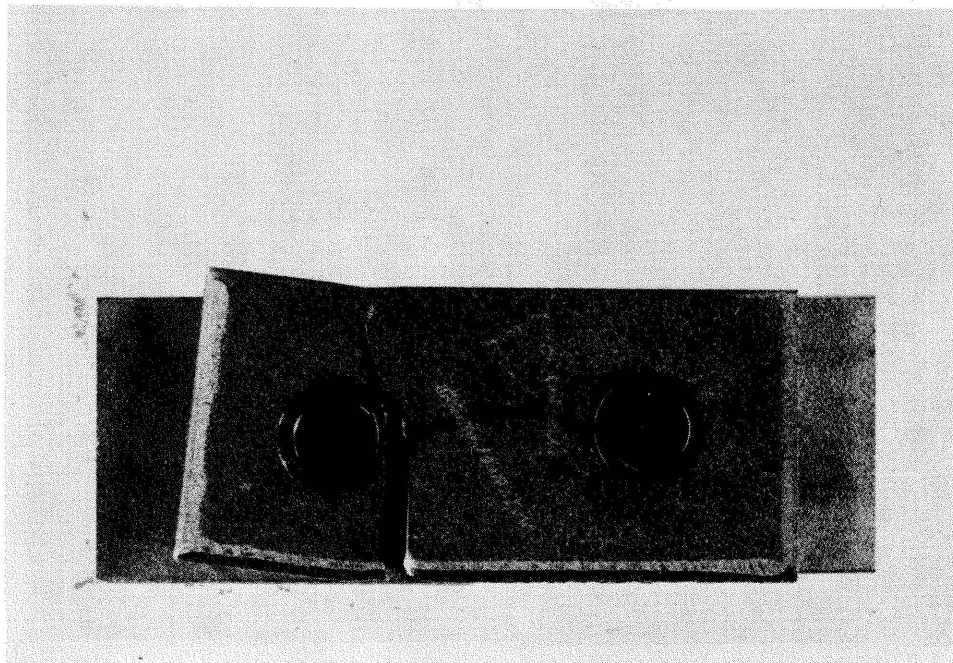


Figure 13: Fretting Fatigue Cracks

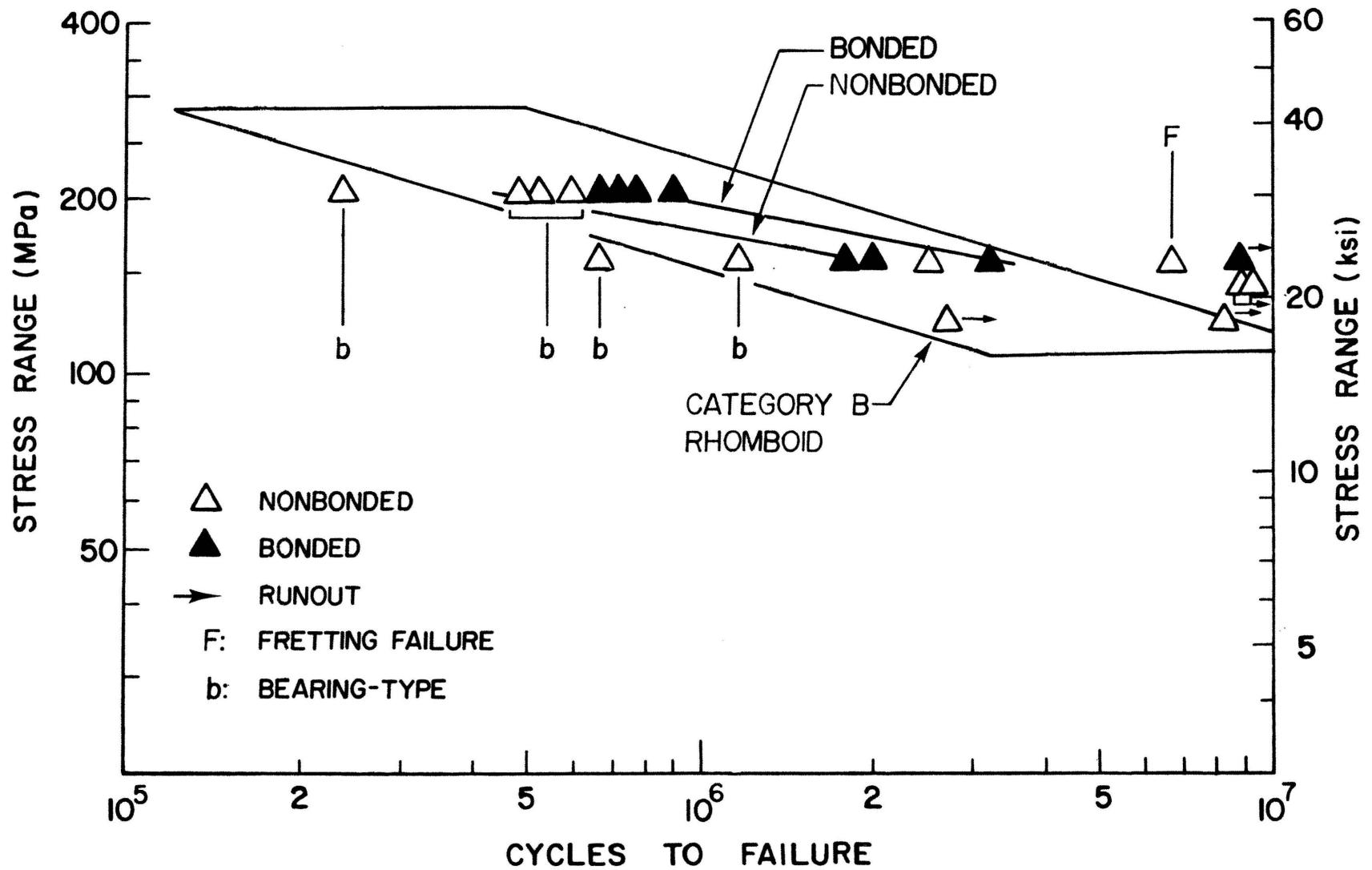


Figure 14: Fatigue test data for Series A tensile specimens;  
Two-bolt splices.

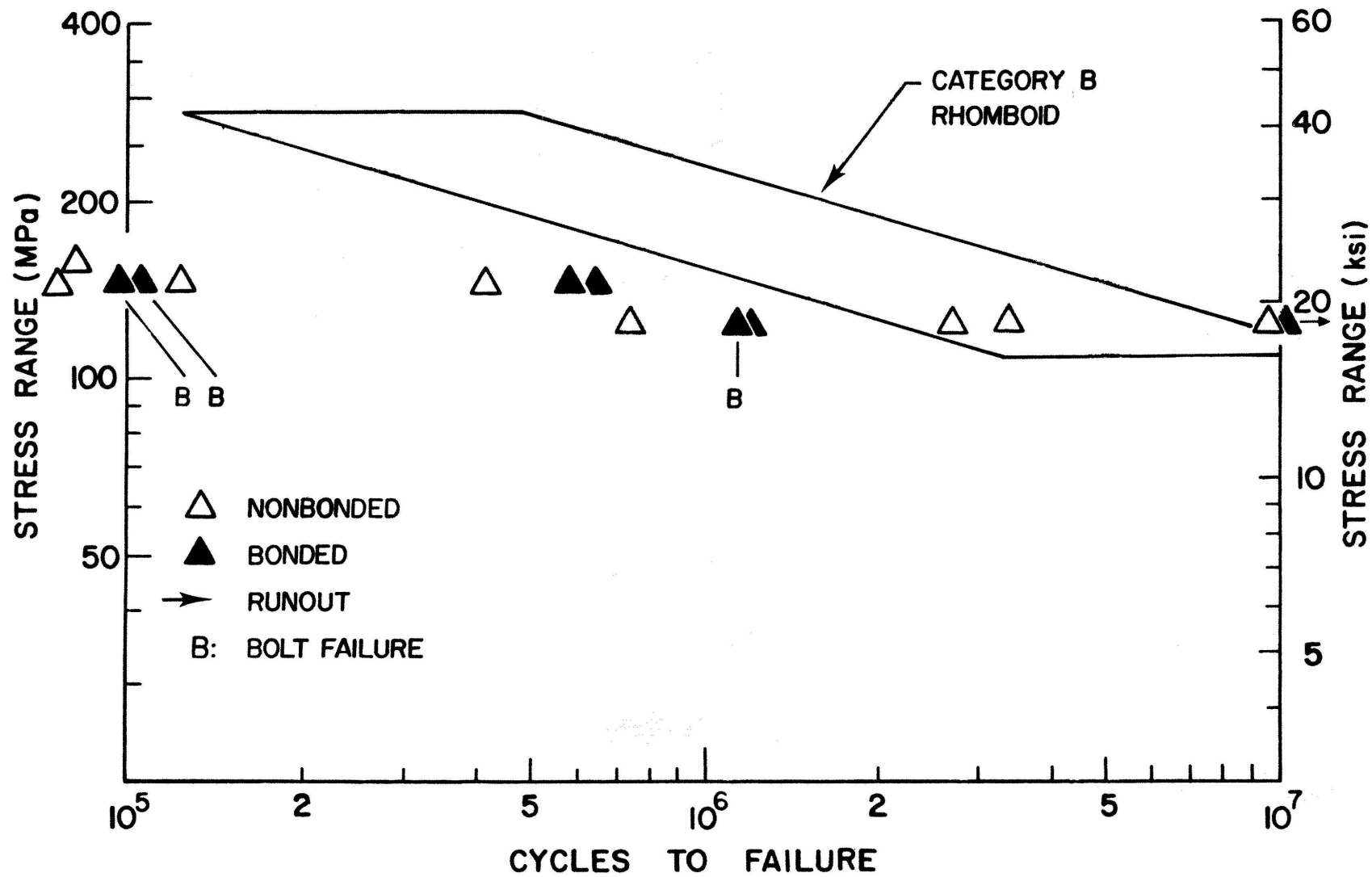


Figure 15: Fatigue test data for Series A tensile specimens; One-bolt splices.



Figure 16: Summary of fatigue test data for Series A tensile specimens

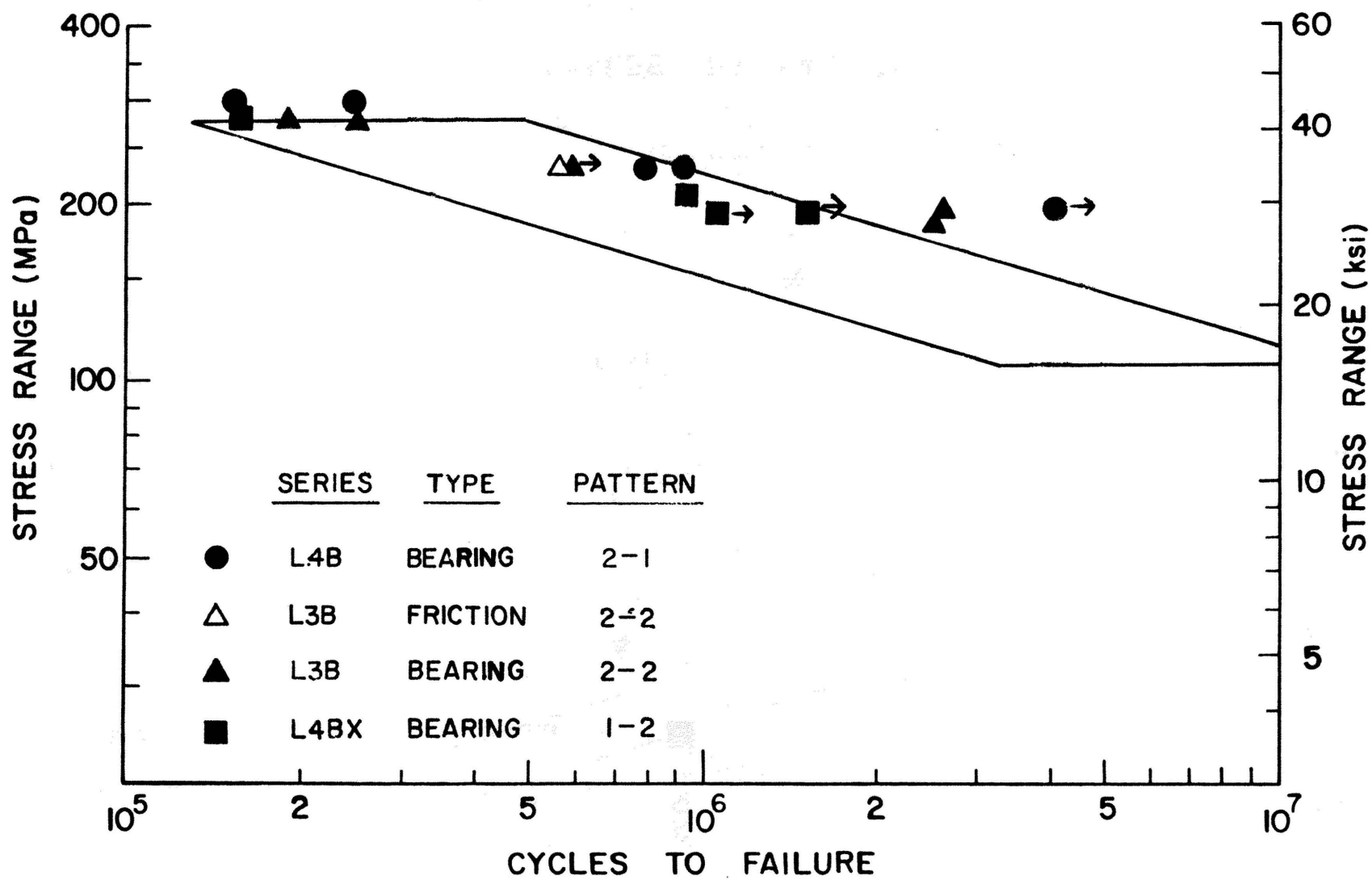


Figure 17: Fatigue strength of bearing-type joints in terms of gross area stress range (Ref. 15)



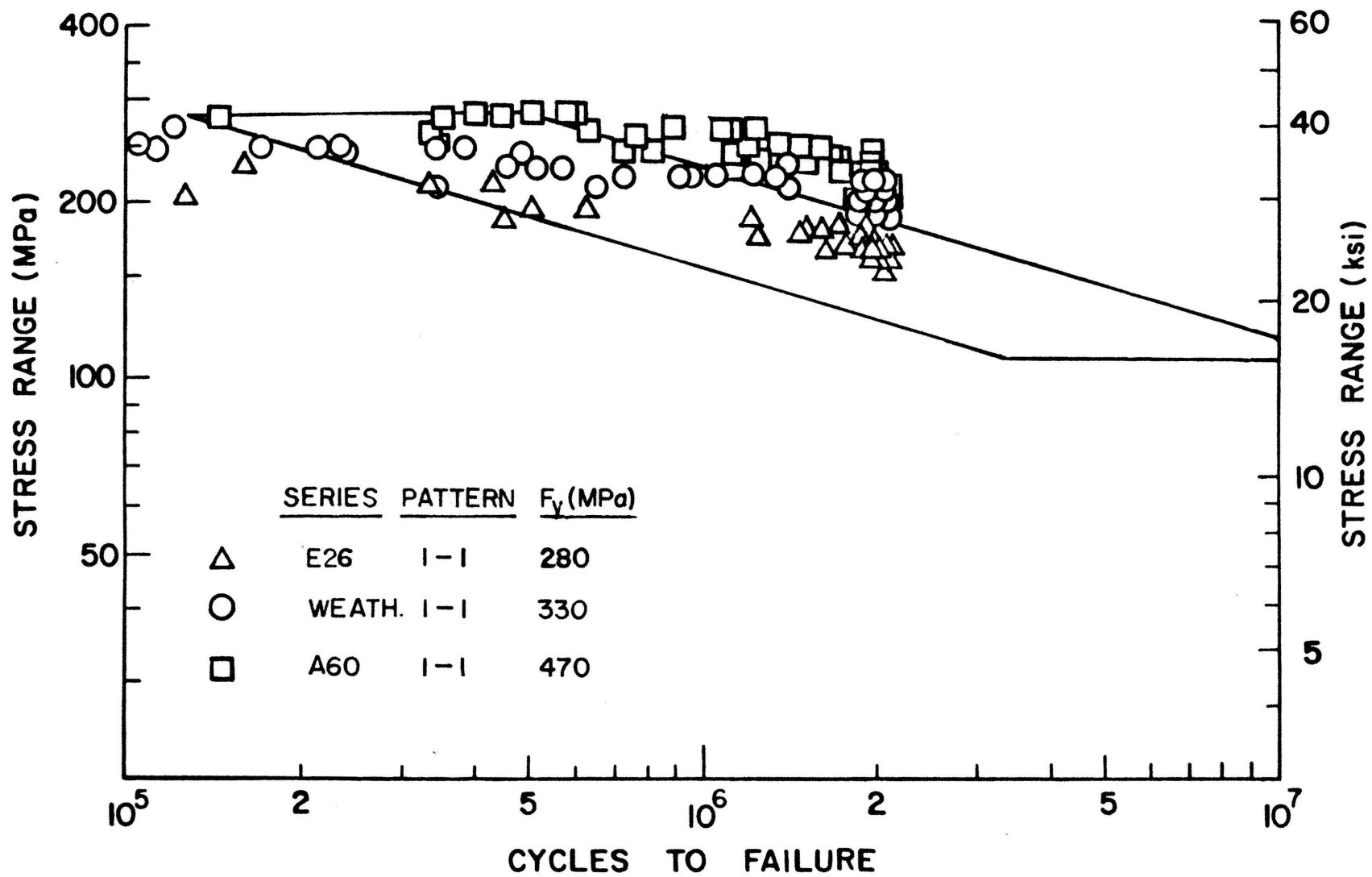


Figure 18: Effect of yield point on fatigue strength of bolted joints (Ref. 21)

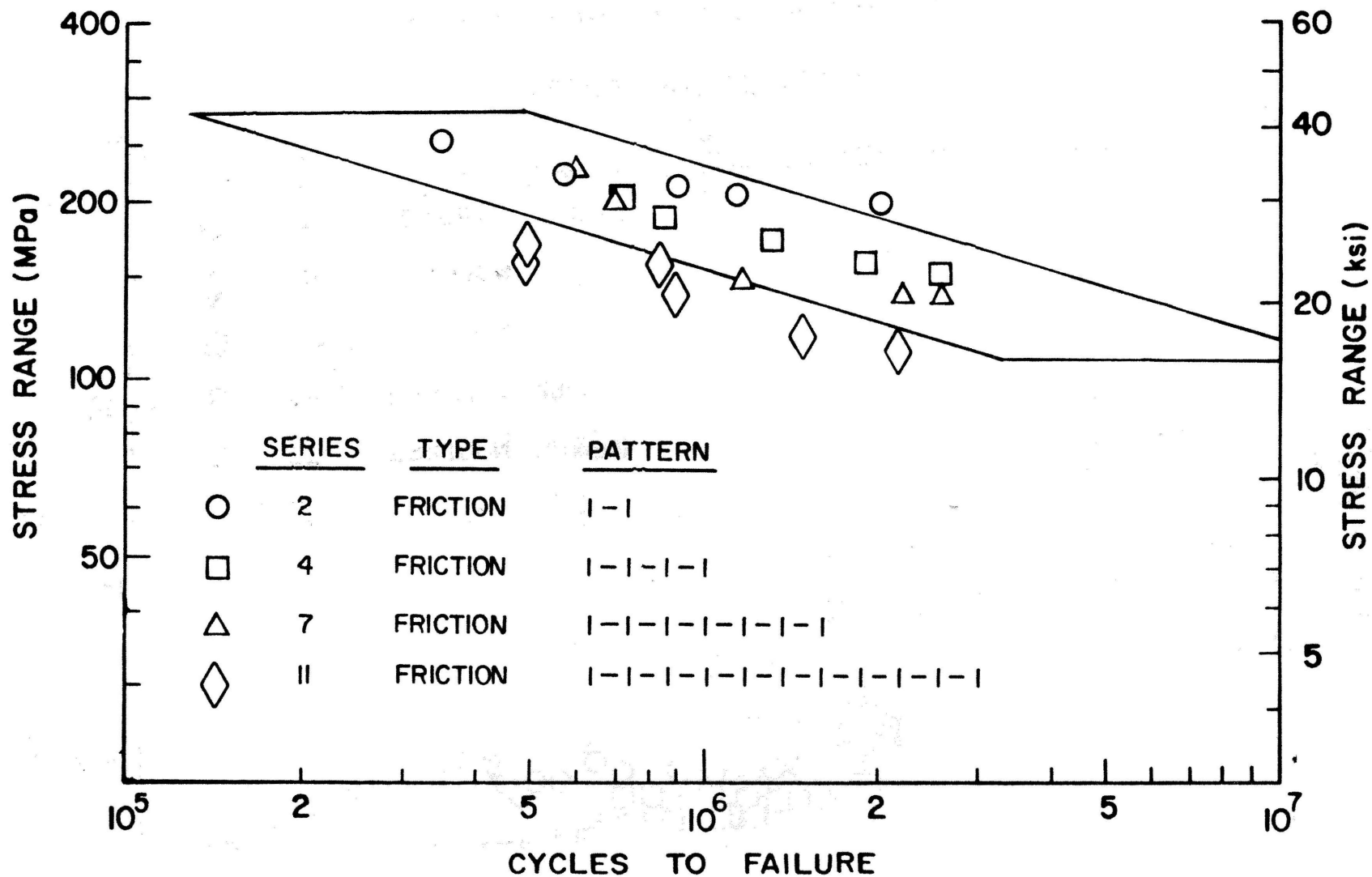


Figure 19: Effect of number of bolt rows on fatigue strength of bolted joints (Ref. 22)

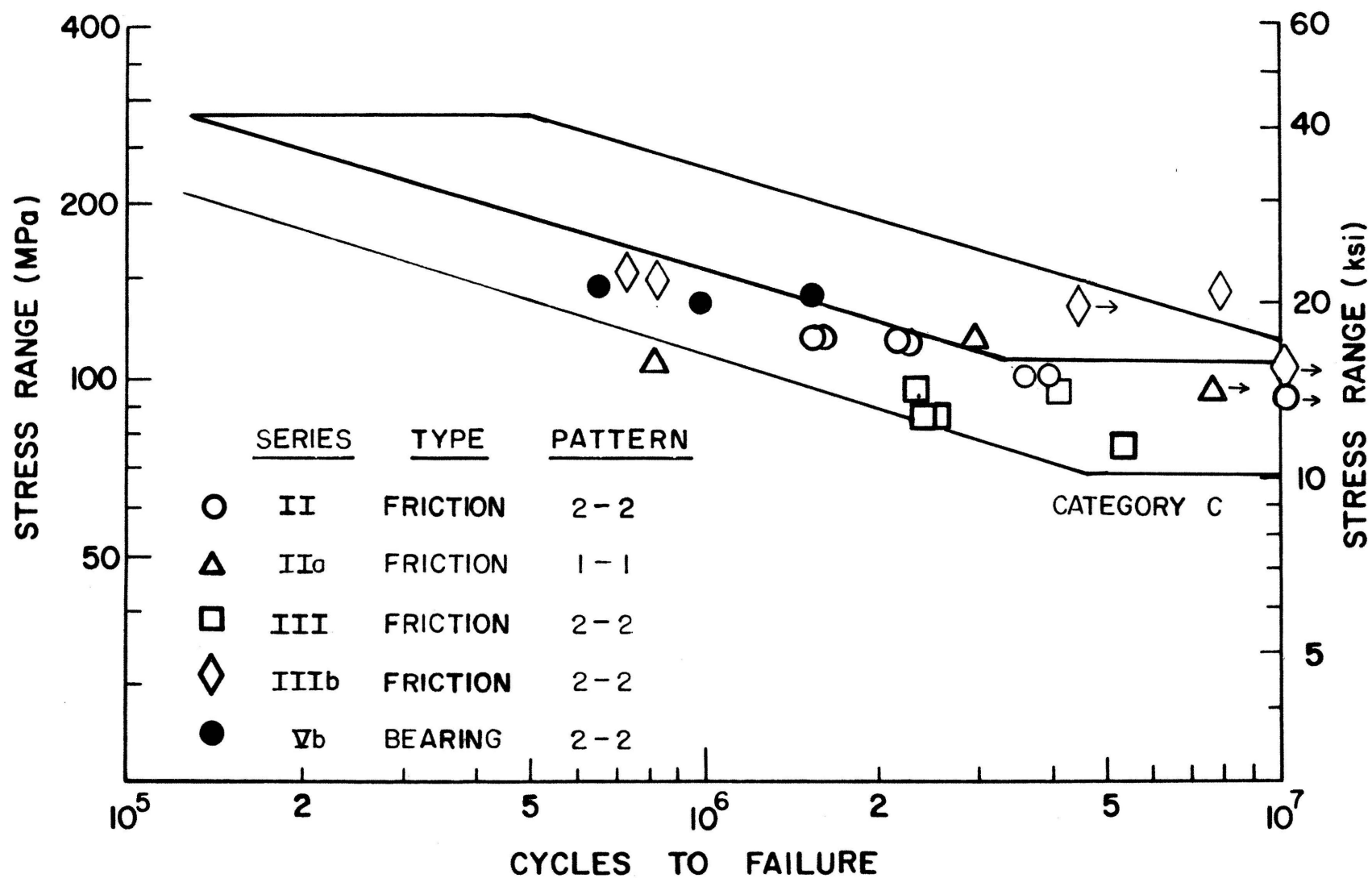


Figure 20: Effect of bolting some but not all cross sectional elements on fatigue strength of bolted joints (Ref. 20)

## CHAPTER 4: FATIGUE STRENGTH OF SERIES B BEAM SPLICES

### 4.1 Experiment Design

The Series B beam specimens, shown in Fig. 2, had three details: one splice at midspan and two cover plates in the moment gradient regions. Each beam test yielded four data points: one for each half splice (presented in this chapter), and one for each cover plate end closest to midspan (presented in Chapter 5).

Beam Splices: The fatigue test matrix for the Series B beam splices, shown in Table 10, consisted of 18 beams arranged in a three-way factorial with two levels of stress range, six-bolt and four-bolt splices, nonbonded or bonded contact surfaces, and three replicate tests per cell. Nonbonded four-bolt splices were not tested.

The specimens were cycled at stress ranges of 23 and 30 ksi (159 and 207 MPa) determined from:

$$f_r = \frac{M_r}{S} \quad (4.1)$$

in which  $M_r$  = moment range in the plane through the first bolt row (closest to the support), and  $S$  = section modulus of W14 x 30 without splice plates. The minimum stress was 1 ksi (7 MPa) in all tests.

As was done with the Series A tensile specimens, the six-bolt and four-bolt beam splices were tested to determine to what degree bolts can be replaced by adhesives without lowering the fatigue strength. The bolts-to-member strength ratios, calculated in Section 2.2, were  $M_b/M_m = 0.87$  and  $0.58$  for the six-bolt and four-bolt splices, respectively.

#### 4.2 Crack Initiation and Propagation

Three types of cracks, illustrated in Fig. 10, were observed in the nonbonded and bonded splices: (1) bolt hole cracks on the first row in the flange, closest to the support; (2) bolt hole cracks on the last row in the splice plate, closest to the beam centerline; and (3) fretting cracks in the flange ahead of the first row. No fretting cracks were found in the splice plates. Examples of these cracks are shown in Figures 21 to 23. They initiated and propagated like those in the tensile specimens, as described in Section 3.2.

The bolt hole cracks, illustrated in Fig. 24, initiated along the bore or at the intersection of the bore with the flange or splice plate surface. They propagated at first as part-through or corner cracks until their length along the bore was equal to the flange or splice plate thickness (Fig. 24). Thereafter, they propagated as through cracks across the plate. Failure occurred when the net ligament ruptured in a ductile mode.

The fretting cracks initiated by rubbing of the flange against the splice plate. They propagated as a part-through crack until they reached the inside flange surface and then as a two-ended through crack across the flange. All fretting cracks occurred in the flange, none in the splice plate.

The dimensions of all cracks are given in Tables 11 and 12, respectively, for the six-bolt and four-bolt splices.

Table 13 summarizes the number of failures in terms of type of crack and type of detail. The available data indicate that the type of crack was independent of: (1) number of bolts in the splice; (2) non-

bonded or bonded surfaces; and (3) friction type or bearing type behavior. Indeed, the distribution of types of failures was similar for all groups.

#### 4.3 Fatigue Test Data

Six-Bolt Splices: The fatigue test data for the nonbonded and bonded six-bolt splices are summarized in Table 14. The table lists for each splice the stress range on the gross and net area of the flanges, the fatigue life, and whether the splice remained in friction or slipped into bearing.

The data points were plotted in Fig. 25 on the basis of gross area stress range with open and solid triangles, respectively, for the nonbonded and bonded splices. All runouts were identified with arrows. The splices B1-2 and B12-2, labeled F in Fig. 25, failed from fretting cracks and had long lives when compared to their counterparts tested at the same stress ranges.

The nonbonded splices slipped into bearing during the first loading cycle, whereas the bonded splices behaved as friction-type joints. Bonding, in addition to bolting, increased the fatigue life, on average, by a factor of 5.2, from 1,335,000 to 6,950,000 cycles at 23-ksi (159 MPa) stress range, and by a factor of 1.4, from 474,000 to 686,000 cycles at 30-ksi (207 MPa) stress range.

The mean regression line, standard deviation, and coefficient of correlation for the 12 nonbonded half splices on beams B1-B6 are:

$$\log N = 11.4334 - 3.8980 \log f_r \quad (4.2)$$

$$S = 0.2126$$

$$r = 0.76$$

and for the 12 bonded half splices on beams B7-12:

$$\log N = 18.7083 - 8.7141 \log f_r \quad (4.3)$$

$$S = 0.1801$$

$$r = 0.95$$

The intercepts of Eqs. 4.2 and 4.3, for stress range in units of MPa, are 14.7020 and 26.0153, respectively. The two regression lines were plotted in Fig. 25.

Figure 25 also compares the data with the AASHTO Category B rhomboid, defined in Section 2.8. Nine of twelve data points for non-bonded splices fell inside the rhomboid even though they slipped into bearing and were plotted in terms of the gross area stress range. All data points for bonded splices fell inside or above the rhomboid. Bonding pushed five of six splices tested at 23-ksi (159 MPa) stress range to runout. It appears that their fatigue limit is much higher than the 16 ksi (110 MPa) specified by AASHTO for Category B details.

Table 14 compares the log-mean life of each group of replicate tests with the mean lives of Category B welded beams at the corresponding gross and net area stress ranges. The latter values were calculated from:  $\log N = 10.870 - 3.372 \log f_r^{(10)}$ . The following is concluded:

1. The mean lives of the nonbonded bearing-type splices fell about half-way between the Category B mean lives based on gross area and net area stress range.
2. The mean life of the bonded friction-type splices tested at 30-ksi (207 MPa) stress range was about equal to the Category B mean life based on gross area stress range. The mean

life of those tested at 23 ksi (159 MPa) was even longer than the Category A mean life given by  $\log N_A = 11.121 - 3.178 \log 23$ ;  $N_A = 6,215,000$ .<sup>(10)</sup>

Four-Bolt Splices: The fatigue test data for the bonded four-bolt splices are summarized in Table 15. The data points were plotted in Fig. 26 on the basis of gross area stress range. The splices B15-1 and B17-2, labeled F in Fig. 26, failed from fretting cracks. They had about average lives.

The splices tested at 23-ksi (159 MPa) stress range behaved as friction-type joints. Their data points fell inside the Category B rhomboid. Those tested at 30-ksi (207 MPa) stress range slipped into bearing, with four failure points falling below the rhomboid.

The regression analysis of the 12 bonded half splices on beams B13-B18 gave the following results:

$$\log N = 15.0542 - 6.5275 \log f_r \quad (4.4)$$

$$s = 0.1979$$

$$r = 0.90$$

The intercept of Eq. 4.4, for stress range in units of MPa, is 20.5276. The mean line was plotted in Fig. 26.

A comparison of the log-mean lives of the replicate splices with the Category B mean lives, given in Table 15, suggests the following conclusions:

1. The mean life of the bonded friction-type splices tested at 23-ksi (159 MPa) stress range was 23% shorter than the Category B mean life based on gross area, but 1.96 longer than that based on net area.



2. The mean life of the bonded bearing-type splices tested at 30-ksi (207 MPa) stress range was about the same as the Category B mean life based on net area.

Comparison of Present Splice Data: Figure 27 compares the data for Series A tensile specimens with two-bolt splices ( $P_b/P_m = 0.72$ ) with the data for Series B beams with six-bolt and four-bolt splices ( $M_b/M_m = 0.87$  and  $0.58$ ). The data for the one-bolt tensile specimens were deleted because some failed by shearing of the bolts. Each point corresponds to the mean of a group of replicate tests. Also shown are the mean lines (dashed) and the AASHTO allowable lines (solid) for Categories A and B.

The data show good correlation between the lives of tensile and beam specimens. Bonding increased the fatigue life of the splices with bolts-to-member strength ratios equal to or greater than 0.72. At 23 ksi (159 MPa), the bonded splices approached the fatigue strength of Category A. The fatigue life of the bonded splices with  $M_b/M_m = 0.58$  was significantly shorter than that of their counterparts with ratios equal to or greater than 0.72.

#### 4.4 Comparison with Previous Work

Nonbonded Splices: It appears that the only fatigue tests of beams with bolted splices reported in the literature are those performed by Kloeppel and Seeger in 1964.<sup>(20)</sup> They tested six IPE 22 (European designation) beams, 3 ft.-6 in. (1100 mm) long. They were spliced at mid span with six-bolt single-shear flange splices and a three-bolt double-shear web splice. The web splice transferred 6.4% of the design moment, as calculated by elastic analysis. The contact surfaces were

sand blasted, and the joints were friction-type. The bolts in the splice had been oversized, making the splice  $M_b/M_m = 2.5$  times stronger than the beam. As a result, the friction coefficient along the contact surfaces was only  $k = 0.35$  at maximum load, although the extreme fiber bending stress was high, 33.2 ksi (229 MPa).

The splices had not been bonded. One failed in the flange at the first bolt row, the other five were runouts. Figure 28 compares the Ref. 20 data with the present data for nonbonded six-bolt splices. The former fell inside the Category B rhomboid and had somewhat longer lives than the present data tested at about the same stress range. No previous fatigue test data for bonded beam splices were reported in the literature.

Table 10: Fatigue test matrix for  
Series B beam splices

| Stress<br>Range<br>ksi (MPa) | Six-Bolt Splices |        | Four-Bolt Splices |        |
|------------------------------|------------------|--------|-------------------|--------|
|                              | Nonbonded        | Bonded | Nonbonded         | Bonded |
| 23<br>(159)                  | B1               | B7     | ...               | B13    |
|                              | B2               | B8     | ...               | B14    |
|                              | B3               | B9     | ...               | B15    |
| 30<br>(207)                  | B4               | B10    | ...               | B16    |
|                              | B5               | B11    | ...               | B17    |
|                              | B6               | B12    | ...               | B18    |

Table 11: Dimensions of cracks in Series B beams  
with six-bolt splices

| Splice No.        | Cracked Element | Type of Crack | Zone of Crack Initiation | Distance from Hole Center Line d (in.) | Crack Angle at               |                           | Crack Length in |           | Notes |
|-------------------|-----------------|---------------|--------------------------|--|------------------------------|---------------------------|-----------------|-----------|-------|
|                   |                 |               |                          |  | Initiation $\alpha_i$ (deg.) | Failure $\alpha_f$ (deg.) | Flange (in.)    | Web (in.) |       |
| Nonbonded Splices |                 |               |                          |  |                              |                           |                 |           |       |
| B1-1              | Flange          | 1st           | I                        | 0.13                                   | 1                            | -5                        | 0.91            | ..        | 5     |
| B1-2              | Flange          | F             | ..                       | 0.50                                   | ..                           | ..                        | 3.85            | ...       |       |
| B2-1              | Flange          | 1st           | I                        | 0                                      | -3                           | -2                        | 0.88            | ..        | 5     |
| B2-2              | Plate           | 3rd           | I                        | 0                                      | 9                            | 16                        | 0.88            | ..        | 5     |
|                   | Plate           | 3rd           | II                       | -0.09                                  | -4                           | 9                         | 0.75            | ..        |       |
| B3-1              | Flange          | 1st           | I                        | 0.06                                   | -2                           | -2                        | 0.94            | ..        | 5     |
| B3-2              | Flange          | 1st           | IV                       | 0.06                                   | -2                           | 1                         | 0.88            | ..        |       |
| B4-1              | Flange          | 1st           | I                        | 0                                      | 27                           | -8                        | 0.88            | ..        | 5     |
| B4-2              | Flange          | 1st           | IV                       | 0.22                                   | 22                           | -14                       | 0.75            | ..        |       |
| B5-1              | Plate           | 3rd           | I                        | -0.03                                  | 1                            | 6                         | 0.88            | ..        | 5     |
| B5-2              | Plate           | 3rd           | II                       | 0.06                                   | 6                            | 6                         | 0.88            | ..        | 5     |
|                   | ..              | ..            | ..                       | ..                                     | ..                           | ..                        | ..              | ..        | 3     |
| B6-1              | Flange          | 1st           | IV                       | 0.13                                   | 12                           | -8                        | 0.63            | ..        |       |
|                   | Flange          | 1st           | III                      | 0                                      | 0                            | -14                       | 0.16            | ..        |       |
| B6-2              | Flange          | 1st           | I                        | 0                                      | 0                            | -13                       | 0.88            | ..        | 5     |

Table 11: Dimensions of cracks in Series B beams  
with six-bolt splices (continued)

| Splice No.     | Cracked Element | Type of Crack | Zone of Crack Initiation | Distance From Hole Center Line d (in.) | Crack Angle at               |                           | Crack Length in |           | Notes |
|----------------|-----------------|---------------|--------------------------|--|------------------------------|---------------------------|-----------------|-----------|-------|
|                |                 |               |                          |  | Initiation $\alpha_1$ (deg.) | Failure $\alpha_2$ (deg.) | Flange (in.)    | Web (in.) |       |
| Bonded Splices |                 |               |                          |  |                              |                           |                 |           |       |
| B7-1           | Flange          | 1st           | IV                       | 0.13                                   | 6                            | 12                        | 1.0             | ..        | 5     |
|                | Flange          | 1st           | II & III                 | 0.13 & 0.31                            | 11 & 21                      | ..                        | 3.22            | 3.5       | 4     |
|                | Flange          | F             | ..                       | 0.41                                   | ..                           | ..                        | 1.12            | ..        | 3     |
| B7-2           | ..              | ..            | ..                       | ..                                     | ..                           | ..                        | ..              | ..        | 3     |
| B8-1           | ..              | ..            | ..                       | ..                                     | ..                           | ..                        | ..              | ..        | 3     |
| B8-2           | ..              | ..            | ..                       | ..                                     | ..                           | ..                        | ..              | ..        | 3     |
| B9-1           | ..              | ..            | ..                       | ..                                     | ..                           | ..                        | ..              | ..        | 3     |
| B9-2           | ..              | ..            | ..                       | ..                                     | ..                           | ..                        | ..              | ..        | 3     |
| B10-1          | Flange          | 1st           | IV                       | -0.06                                  | -6                           | -6                        | 0.63            | ..        | 5     |
| B10-2          | Flange          | 1st           | I                        | -0.09                                  | 0                            | -5                        | 1.0             | ..        |       |
| B11-1          | Flange          | 1st           | IV                       | 0.06                                   | -4                           | 13                        | 0.63            | ..        | 1     |
| B11-2          | Flange          | 1st           | II                       | -0.09                                  | -8                           | 3                         | 2.25            | 0.88      |       |
| B12-1          | Flange          | 1st           | II & III                 | -0.03 & -0.09                          | -9 & -6                      | ..                        | 3.22            | 0.50      | 1, 4  |
| B12-2          | Flange          | F             | ..                       | 6.28                                   | ..                           | ..                        | 3.38            | ..        |       |

Table 11: Dimensions of cracks in Series B beams  
with six-bolt splices (continued)

---

Notes:

1. Crack grew into the web. It was stopped by drilling a hole at the web crack tip.
2. Crack grew into the web. It was stopped by drilling a hole at the web crack tip and installing a high-strength bolt.
3. Runout or test discontinued.
4. Crack extended from hole to hole.
5. Crack extended from hole to flange or plate edge

Conversion factor: 1 in. = 25.4 mm

Table 12: Dimensions of cracks in Series B beams  
with four-bolt splices

| Splice No.            | Cracked Element | Type of Crack | Zone of Crack Initiation | Distance from Hole Center Line d (in.) | Crack Angle at               |                           | Crack Length in |           | Notes |
|-----------------------|-----------------|---------------|--------------------------|--|------------------------------|---------------------------|-----------------|-----------|-------|
|                       |                 |               |                          |  | Initiation $\alpha_i$ (deg.) | Failure $\alpha_f$ (deg.) | Flange (in.)    | Web (in.) |       |
| <u>Bonded Splices</u> |                 |               |                          |  |                              |                           |                 |           |       |
| B13-1                 | Flange          | 1st           | I                        | -0.38                                  | 7                            | -19                       | 1.13            | ..        | 5     |
| B13-2                 | Flange          | 1st           | I                        | 0.38                                   | 5                            | 5                         | 1.13            | ..        | 5     |
| B14-1                 | Flange          | 1st           | II                       | -0.09                                  | -11                          | -11                       | 0.63            | ..        | 5     |
| B14-2                 | Plate           | 2nd           | I                        | 0                                      | 9                            | 16                        | 0.89            | ..        |       |
|                       | Plate           | 2nd           | II                       | -0.09                                  | -4                           | 9                         | 0.75            | ..        |       |
| B15-1                 | Flange          | F             | ..                       | 0.69                                   | ..                           | ..                        | 2.5             | 0.87      | 1     |
| B15-2                 | ..              | ..            | ..                       | ..                                     | ..                           | ..                        | ..              | ..        | 3     |
| B16-1                 | Flange          | 1st           | IV                       | 0.09                                   | 0                            | 0                         | 0.50            | ..        |       |
|                       | Flange          | 1st           | III                      | -0.09                                  | -9                           | -1                        | 1.09            | ..        |       |
| B16-2                 | Flange          | 1st           | IV                       | -0.09                                  | -23                          | -23                       | 0.38            | ..        |       |
| B17-1                 | Flange          | 1st           | II                       | 0.09                                   | -12                          | -12                       | 0.63            | ..        | 4     |
| B17-2                 | Flange          | F             | ..                       | 0.72                                   | ..                           | ..                        | 1.0             | ..        | 5     |
| B18-1                 | Plate           | 2nd           | I                        | 0.09                                   | 4                            | 7                         | 0.88            | ..        | 5     |
|                       | Plate           | 2nd           | II                       | 0.16                                   | 13                           | 5                         | 0.75            | ..        | 3     |
| B18-2                 | ..              | ..            | ..                       | ..                                     | ..                           | ..                        | ..              | ..        |       |

Note: See Table 11 for description of notes.

Conversion factor: 1 in. = 25.4 mm.

Table 13: Summary of types of cracks  
at beam splices

| Type of<br>Crack    | Six-Bolt Splices       |                      | Four-Bolt Splices   |                      |
|---------------------|------------------------|----------------------|---------------------|----------------------|
|                     | Nonbonded<br>(bearing) | Bonded<br>(friction) | Bonded<br>(bearing) | Bonded<br>(friction) |
| First row in flange | 8                      | 6                    | 3                   | 3                    |
| Last row in splice  | 1                      | 1                    | 1                   | 1                    |
| Fretting in flange  | 2                      | 0                    | 1                   | 1                    |
| Runout              | 1                      | 5                    | 1                   | 1                    |
| Total               | 12                     | 12                   | 6                   | 6                    |



Table 14: Fatigue test data for Series B beams  
with six-bolt splices

| Specimen No.             | Stress Range                          |                                      | Type of Joint at Start of Test | Fatigue <sup>a</sup> Life N<br>(x10 <sup>3</sup> ) | Log-Mean Life<br>(x10 <sup>3</sup> ) | Category B Mean Life for                       |  |
|--------------------------|---------------------------------------|--------------------------------------|--------------------------------|--|--------------------------------------|--|--|
|                          | Gross Area<br>f <sub>r</sub><br>(ksi) | Net Area<br>f <sub>rn</sub><br>(ksi) |                                |  |                                      | Gross Area Stress Range<br>(x10 <sup>3</sup> ) | Net Area Stress Range<br>(x10 <sup>3</sup> ) |
|                          |                                       |                                      |                                |  |                                      |  |  |
| <u>Nonbonded Splices</u> |                                       |                                      |                                |  |                                      |  |  |
| B1-1                     | 23                                    | 30.3                                 | Bearing                        | 758  |                                      |  |  |
| B1-2                     | 23                                    | 30.3                                 | Bearing                        | 4,156  |                                      |  |  |
| B2-1                     | 23                                    | 30.3                                 | Bearing                        | 805  | 1,335                                | 1,898  | 749  |
| B2-2                     | 23                                    | 30.3                                 | Bearing                        | 1,986  |                                      |  |  |
| B3-1                     | 23                                    | 30.3                                 | Bearing                        | 875  |                                      |  |  |
| B3-2                     | 23                                    | 30.3                                 | Bearing                        | 1,282  |                                      |  |  |
| B4-1                     | 30                                    | 39.5                                 | Bearing                        | 388  |                                      |  |  |
| B4-2                     | 30                                    | 39.5                                 | Bearing                        | 398  | > 474                                | 775  | 306  |
| B5-1                     | 30                                    | 39.5                                 | Bearing                        | 602  |                                      |  |  |
| B5-2                     | 30                                    | 39.5                                 | Bearing                        | 602-R  |                                      |  |  |
| B6-1                     | 30                                    | 39.5                                 | Bearing                        | 440  |                                      |  |  |
| B6-2                     | 30                                    | 39.5                                 | Bearing                        | 459  |                                      |  |  |
| <u>Bonded Splices</u>    |                                       |                                      |                                |  |                                      |  |  |
| B7-1                     | 23                                    | 30.3                                 | Friction                       | 3,101  |                                      |  |  |
| B7-2                     | 23                                    | 30.3                                 | Friction                       | 4,471-R  |                                      |  |  |
| B8-1                     | 23                                    | 30.3                                 | Friction                       | 10,012-R   | > 6,950                              | 1,898  | 749  |
| B8-2                     | 23                                    | 30.3                                 | Friction                       | 10,012-R   |                                      |  |  |
| B9-1                     | 23                                    | 30.3                                 | Friction                       | 9,006-R  |                                      |  |  |
| B9-2                     | 23                                    | 30.3                                 | Friction                       | 9,006-R  |                                      |  |  |

Table 14: Fatigue test data for Series B beams  
with six-bolt splices (continued)

| Specimen<br>No. | Stress Range                    |                                  | Type of<br>Joint at<br>Start of<br>Test | Fatigue <sup>a</sup><br>Life<br>N<br>( $\times 10^3$ ) | Log-Mean<br>Life<br>( $\times 10^3$ ) | Category B Mean Life for                        |   |
|-----------------|---------------------------------|----------------------------------|---|--|---------------------------------------|---|---|
|                 | Gross<br>Area<br>$f_r$<br>(ksi) | Net<br>Area<br>$f_{rn}$<br>(ksi) |   |  |                                       | Gross Area<br>Stress Range<br>( $\times 10^3$ ) | Net Area<br>Stress Range<br>( $\times 10^3$ ) |
| B10-1           | 30                              | 39.5                             | Friction                                | 523  |                                       |   |   |
| B10-2           | 30                              | 39.5                             | Friction                                | 670  |                                       |   |   |
| B11-1           | 30                              | 39.5                             | Friction                                | 546  | 686                                   | 775   | 306   |
| B11-2           | 30                              | 39.5                             | Friction                                | 1,149  |                                       |   |   |
| B12-1           | 30                              | 39.5                             | Friction                                | 564  |                                       |   |   |
| B12-2           | 30                              | 39.5                             | Friction                                | 842  |                                       |   |   |

Conversion Factor: 1 ksi = 6.895 MPa

Note: a. The symbol R designates runout, or test discontinued.

Table 15: Fatigue test data for Series B beams  
with four-bolt splices

| Specimen No.          | Stress Range                       |                                   | Type of Joint at Start of Test | Fatigue <sup>a</sup> Life N<br>(x10 <sup>3</sup> ) | Log-Mean Life<br>(x10 <sup>3</sup> ) | Category B Mean Life for                       |  |
|-----------------------|------------------------------------|-----------------------------------|--------------------------------|--|--------------------------------------|--|--|
|                       | Gross Area f <sub>r</sub><br>(ksi) | Net Area f <sub>rn</sub><br>(ksi) |                                |  |                                      | Gross Area Stress Range<br>(x10 <sup>3</sup> ) | Net Area Stress Range<br>(x10 <sup>3</sup> ) |
|                       |                                    |                                   |                                |  |                                      |  |  |
| <u>Bonded Splices</u> |                                    |                                   |                                |  |                                      |  |  |
| B13-1                 | 23                                 | 30.3                              | Friction                       | 1,232  |                                      |  |  |
| B13-2                 | 23                                 | 30.3                              | Friction                       | 1,256  |                                      |  |  |
| B14-1                 | 23                                 | 30.3                              | Friction                       | 1,433  |                                      |  |  |
| B14-2                 | 23                                 | 30.3                              | Friction                       | 1,438  | > 1,464                              | 1,898  | 749  |
| B15-1                 | 23                                 | 30.3                              | Friction                       | 1,450  |                                      |  |  |
| B15-2                 | 23                                 | 30.3                              | Friction                       | 2,130-R  |                                      |  |  |
| B16-1                 | 30                                 | 39.5                              | Bearing                        | 385  |                                      |  |  |
| B16-2                 | 30                                 | 39.5                              | Bearing                        | 540  |                                      |  |  |
| B17-1                 | 30                                 | 39.5                              | Bearing                        | 281  |                                      |  |  |
| B17-2                 | 30                                 | 39.5                              | Bearing                        | 337  | > 300                                | 775  | 306  |
| B18-1                 | 30                                 | 39.5                              | Bearing                        | 123  |                                      |  |  |
| B18-2                 | 30                                 | 39.5                              | Bearing                        | 123-R  |                                      |  |  |

Conversion factor: 1 ksi = 6.895 MPa

Note: a. The symbol R designates runout, or test discontinued.

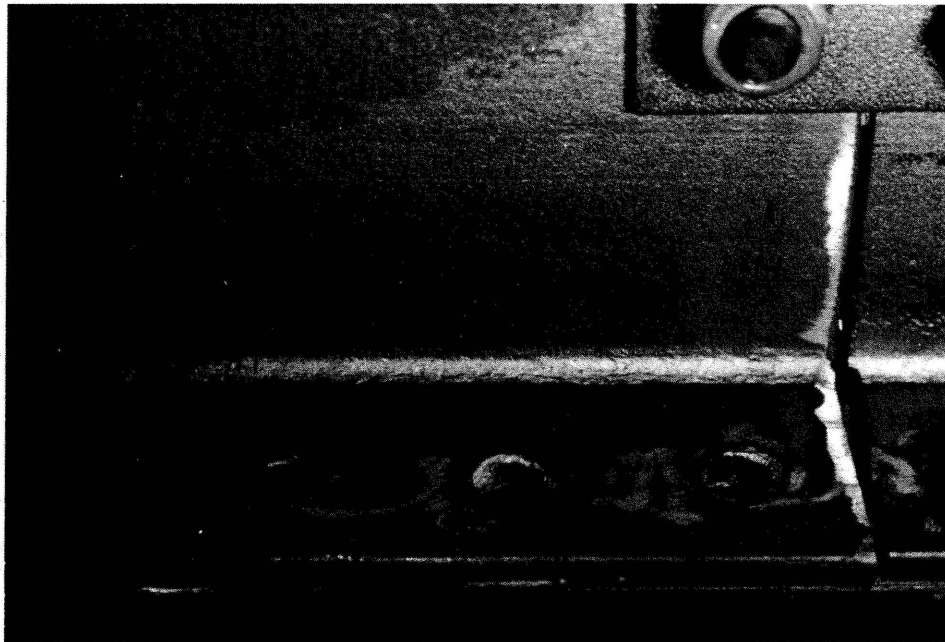


Figure 21: Typical crack initiation and propagation at first bolt row (Splice B7-1)

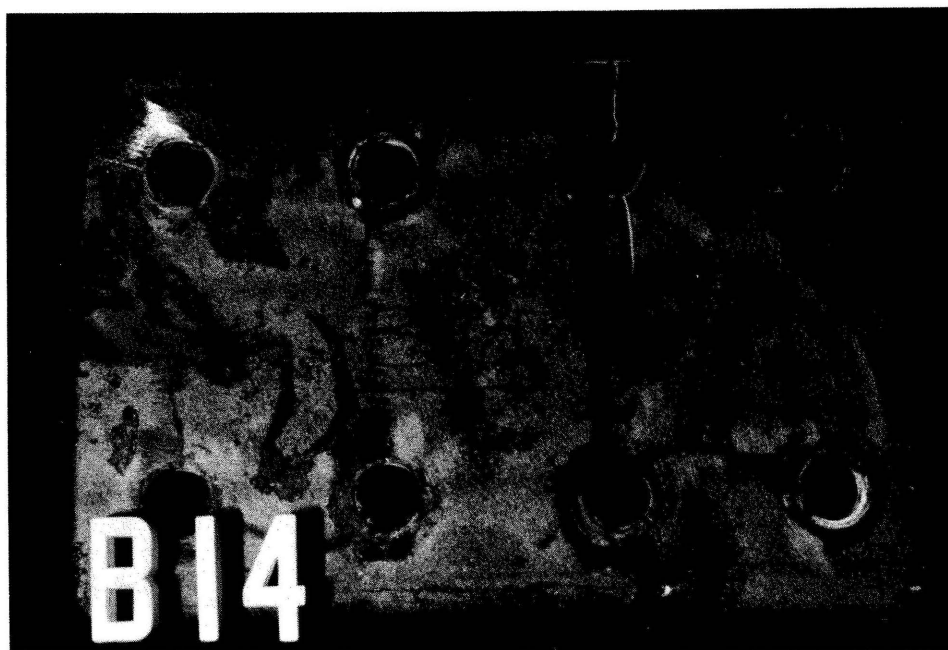


Figure 22: Fatigue crack in splice plate at second bolt row (Splice B14-2)



Figure 23: Typical fretting fatigue crack ahead of first bolt row. Crack was stopped by drilling a hole (Splice B15-1).

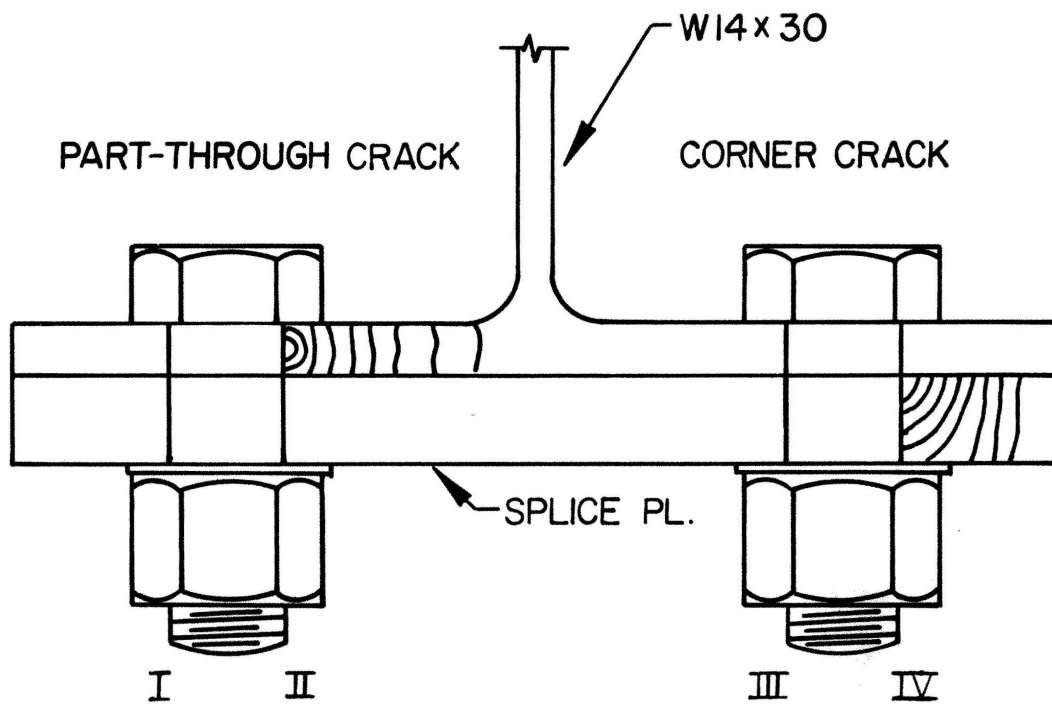


Figure 24: Typical crack initiation and propagation at bolt hole

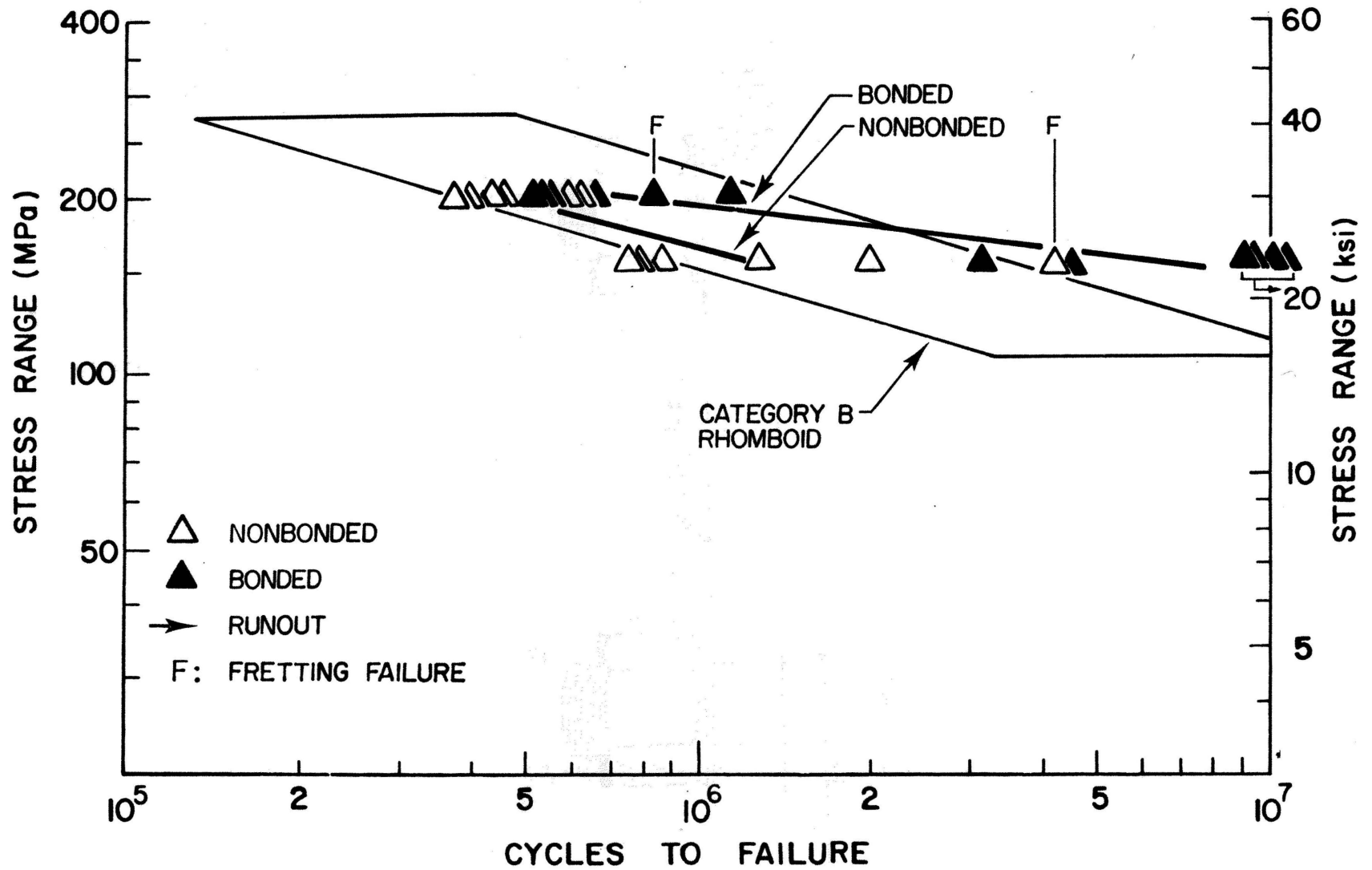


Figure 25: Fatigue test data for Series B beam specimens with six-bolt splices



Figure 26: Fatigue test data for Series B beam specimens with four-bolt splices

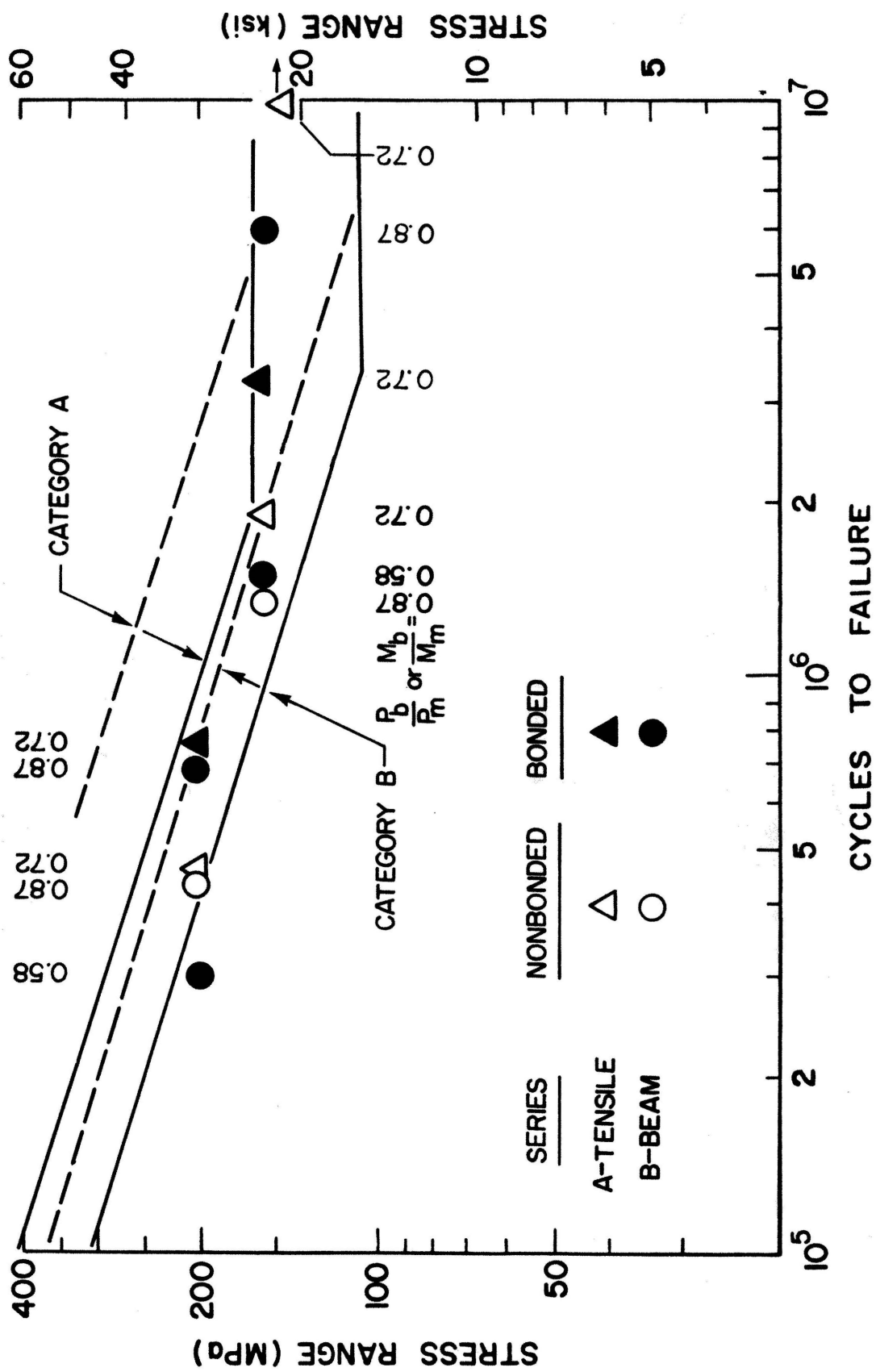


Figure 27: Comparison of fatigue test data for Series A and B splices

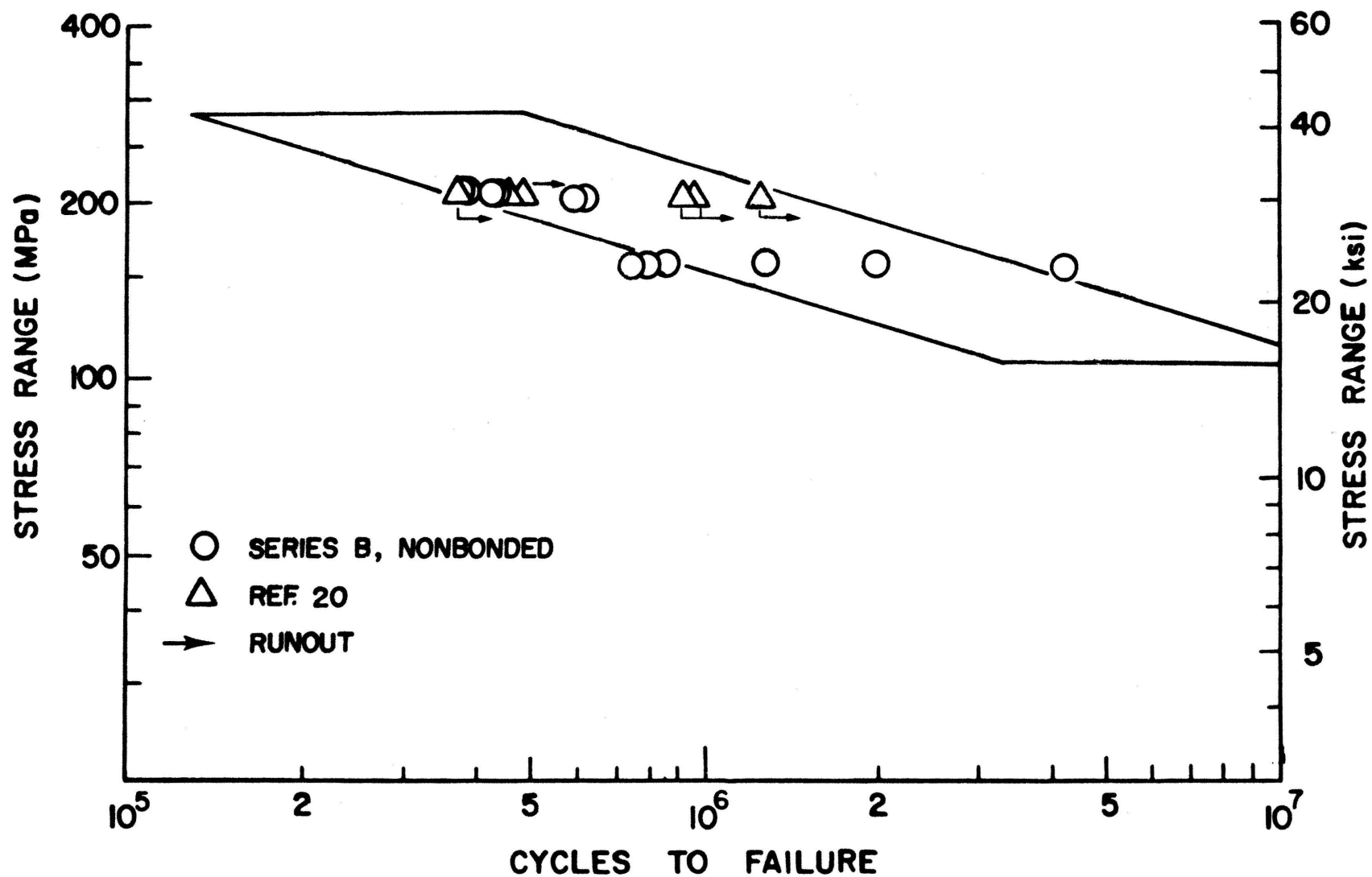


Figure 28: Comparison of previous and present fatigue test data for nonbonded beam splices

## CHAPTER 5: FATIGUE STRENGTH OF SERIES B BEAM COVER PLATES

### 5.1 Experiment Design

Two cover plates were adhesive bonded to the tension flange of all beams, except beam B16. Each beam yielded two data points for cover plate ends, for a total of 34. The test matrix is shown in Table 16.

The initial plan was to attach the cover plates to the flange with adhesive alone. After the beam tests B1 to B3 had shown that the cover plate ends were gradually debonding, the cover plate ends on beam B4, closest to mid-span, and both cover plate ends on beams B5-B18 were high-strength bolted to the flange.

The cover plates of beams B1 to B13 terminated 6 in (152 mm) from the loading points and were cycled at stress ranges of 21.0 and 27.4 ksi (145 and 189 MPa). Those on beams B14 to B18 were extended 4-1/4 in (108 mm) into the constant bending moment region and were cycled at stress ranges of 23.0 and 30.0 ksi (159 and 207 MPa), like the splices.

### 5.2 Crack Initiation and Propagation

The modes of failure and the dimensions of the cracks at the cover plates bonded to the tension flange are given in Table 17.

The six cover plates on beams B1 to B3 were bonded but not bolted to the tension flange. They gradually debonded during stress cycling. For example, an ultrasonic compression wave scan of cover plate B2-1 showed that its end had fully debonded over a 5-in (125 mm)

length after 2,000,000 cycles of 21-ksi (145 MPa) stress range. The debonded areas are shown dark in Fig. 29 and the bonded areas clear.

The midspan ends of the bonded cover plates on beam B4 were bolted, while the support ends were only bonded. After the support end of cover plate B4-1 debonded early in the test, the support end of cover plate B4-2 was secured with two high-strength C clamps.

All cover plates bonded to beams B5-B18 were also bolted at both ends. Beam B16 had no cover plates. Of these 26 cover plates, nine failed from cracks that initiated at the bolt holes in the flange, two from fretting cracks in the flange between the bolt row and the cover plate end, and 15 were runouts. No cracks were found in the cover plates.

The bolt hole cracks and the fretting cracks initiated and propagated like those in the beam splices described previously. Figure 30 shows typical bolt hole cracks at cover plate ends. To continue the test at the other details, after the cover plate end had failed, the flanges were temporarily spliced with plates and high-strength C clamps. The crack tip in the web was arrested by drilling a hole and installing a high-strength bolt.

### 5.3 Fatigue Test Data

The fatigue test data for the bonded cover plates are summarized in Table 18 and plotted in Fig. 31 against the gross area stress range in the beam section. The fatigue lives of the cover plates on beams B1-B3 whose ends had not been bolted were considered to have run out. The gradual debonding would have eventually separated the cover plate from the flange and limited the load carrying capacity to that of the W14 x 30 beam alone. The number of cycles to failure is

ambiguous in this case.

The 27 data points for the bonded cover plates with bolted ends on beams B4-B18 are shown with triangular symbols. All points fell inside or above the Category B rhomboid. The regression analysis of the 27 data points gave the following results:

$$\log N = 12.7363 - 4.5739 \log f_r \quad (5.1)$$

$$s = 0.1983$$

$$r = 0.82$$

The data for nonbolted ends were excluded. The intercept of Eq. 5.1 for stress range in units of MPa, is 16.5715. Eq. 5.1 is shown in Fig. 31.

Table 18 compares the log-mean lives of replicate specimens with the mean of Category E and B at the corresponding stress ranges. The fatigue strength of the bonded and end-bolted cover plates exceeded that of Category B. The factor increase in life over Category E for welded cover plates was at least 20 for the data at the three highest stress ranges, and 35 at the lowest stress range. Six of eight details tested at the lowest stress range [21 ksi (145 MPa)] were runouts, suggesting that the fatigue limit may lie about halfway between the AASHTO fatigue limits for Category A [24 ksi (165 MPa)] and Category B [16 ksi (110 MPa)]. Clearly, bonding and end-bolting have the potential of making cover plates in typical bridge girders fatigue proof.

#### 5.4 Comparison with Previous Work

Ref. 5 summarized the 755 fatigue tests of cover plates on steel beams that were reported since 1969. The earlier studies

established the fatigue strength of various end configurations (Category E),<sup>(10)</sup> thick cover plates on thick flanges (Category E'),<sup>(23,24)</sup> and behavior under variable amplitude loading.<sup>(25)</sup> The later studies focused on improving fatigue strength by grinding, shot-peening, TIG remelting,<sup>(26)</sup> end-welding and grinding,<sup>(27)</sup> end-bolting and retrofitting.<sup>(7,8)</sup> The fatigue test data for each series of tests are summarized in Table 19 and plotted in Fig. 32. The factor increase in life of a detail X over that of Category E is defined as

$$\frac{N_X}{N_E} = \left[ \frac{f_{r,X}}{f_{r,E}} \right]^m \quad (5.2)$$

The stress ranges for detail X and Category E at 500,000 cycles were calculated from the corresponding mean regression lines. The exponent,  $m=3.2$ , is the average slope of the S-N lines that form the basis of the AASHTO fatigue specifications. The fatigue notch factor

$$K_f = \frac{f_{r,A}}{f_{r,X}} \quad (5.3)$$

indicates by what factor on stress range the mean S-N line of a detail falls below the mean for Category A rolled beams.

Table 19 and Fig. 32 show that the various techniques improved the mean fatigue life over that of Category E by factors of: 1.5, 2.1 and 4.4 for ground, shot-peened, and TIG remelted toes of end welds, respectively; 6.5 for end-welding and grinding the cover plate to a 1:3 taper; 19 or more for bolting the ends that were left unwelded; and 18 and 13, respectively, for bridging the welded ends of non-cracked and cracked cover plates with bolted splices.

In comparison bonding and end-bolting increased the fatigue life by a factor of 20 in the finite life regime and by a factor of 35

close to the fatigue limit. The potential for increasing fatigue life by the proper use of adhesives is clearly evident. In this case, the bolts help to carry the high shear and cleavage stresses at the end of the bond line. Away from the end, the adhesive transfers the longitudinal shear stresses on its own.

The only other known fatigue tests of bonded long attachments were those reported in Ref. 4. In that study, 9 in x 9/16 in x 48 in (229 mm x 14 mm x 1220 mm) long cover plates were bonded to the tension flange of two W14 x 30 steel beams with the same adhesive used in the present study. The two beams were subjected to 6,000,000 cycles and 3,500,000 cycles of 20-ksi (138 MPa) stress range. Measured load versus midspan deflection curves had indicated a progressive decrease in beam stiffness with stress cycling caused by debonding from the ends. Matching the change in stiffness with deflection calculations performed herein suggested that the cover plate on the first beam debonded at the ends over a 12.6-in (320 mm) length. This problem was solved in the present study by bolting the ends.



Table 16: Fatigue test matrix for Series B  
bonded cover plates

| Stress Range<br>ksi (MPa) | Nonbolted Ends                   | Bolted Ends                         |
|---------------------------|----------------------------------|-------------------------------------|
| 21.0<br>(145)             | B1<br>B2<br>B3<br>..             | B7<br>B8<br>B9<br>B13               |
| 23.0<br>(159)             | ..<br>..                         | B14<br>B15                          |
| 27.4<br>(189)             | ..<br>..<br>..<br>..<br>..<br>.. | B4<br>B5<br>B6<br>B10<br>B11<br>B12 |
| 30.0<br>(207)             | ..<br>..                         | B17<br>B18                          |

Table 17: Dimensions of cracks at bonded cover plates on Series B beams

| Specimen No.                | Type of Crack | Zone of Crack Initiation | Distance from Hole Center Line d (in.) | Crack Angle at               |                           | Crack Length in |           | Notes |
|-----------------------------|---------------|--------------------------|--|------------------------------|---------------------------|-----------------|-----------|-------|
|                             |               |                          |  | Initiation $\alpha_i$ (deg.) | Failure $\alpha_f$ (deg.) | Flange (in.)    | Web (in.) |       |
| Without End Bolts           |               |                          |  |                              |                           |                 |           |       |
| B1-1                        | Debonded      | ..                       | ..                                     | ..                           | ..                        | ..              | ..        | ..    |
| B1-2                        | Debonded      | ..                       | ..                                     | ..                           | ..                        | ..              | ..        | ..    |
| B2-1                        | Debonded      | ..                       | ..                                     | ..                           | ..                        | ..              | ..        | ..    |
| B2-2                        | Debonded      | ..                       | ..                                     | ..                           | ..                        | ..              | ..        | ..    |
| B3-1                        | Debonded      | ..                       | ..                                     | ..                           | ..                        | ..              | ..        | ..    |
| B3-2                        | Debonded      | ..                       | ..                                     | ..                           | ..                        | ..              | ..        | ..    |
| With End Bolts <sup>8</sup> |               |                          |  |                              |                           |                 |           |       |
| B4-1                        | Debonded      | ..                       | ..                                     | ..                           | ..                        | ..              | ..        | 6     |
| B4-2                        | ..            | ..                       | ..                                     | ..                           | ..                        | ..              | ..        | 3,7   |
| B5-1                        | 1st           | II & III                 | -0.06 & -0.06                          | 6 & 0                        | ..                        | 3.23            | 0.87      | 1,4   |
|                             | 1st           | IV                       | 0                                      | ..                           | ..                        | 0.88            | ..        | ..    |
| B5-2                        | ..            | ..                       | ..                                     | ..                           | ..                        | ..              | ..        | 3     |
|                             |               |                          |  |                              |                           |                 |           |       |
| B6-1                        | 1st           | IV                       | -0.06                                  | 3                            | 7                         | 0.75            | ..        |       |
| B6-2                        | ..            | ..                       | ..                                     | ..                           | ..                        | ..              | ..        | 3     |
|                             |               |                          |  |                              |                           |                 |           |       |
| B7-1                        | 1st           | III                      | -0.25                                  | 8                            | 8                         | 2.6             | 1.25      | 2     |
| B7-2                        | ..            | ..                       | ..                                     | ..                           | ..                        | ..              | ..        | 3     |
|                             |               |                          |  |                              |                           |                 |           |       |
| B8-1                        | ..            | ..                       | ..                                     | ..                           | ..                        | ..              | ..        | 3     |
| B8-2                        | ..            | ..                       | ..                                     | ..                           | ..                        | ..              | ..        | 3     |
|                             |               |                          |  |                              |                           |                 |           |       |
| B9-1                        | 1st           |                          | -0.09                                  | -3                           | -3                        | 1.0             | ..        | 5     |
|                             | 1st           | II & III                 | -0.06 & 0.13                           | 11 & 16                      | ..                        | 3.24            | 4.5       | 2, 4  |
| B9-2                        | ..            | ..                       | ..                                     | ..                           | ..                        | ..              | ..        | 3     |

Table 17: Dimensions of cracks at bonded cover plates on Series B beams (continued)

| Specimen No. | Type of Crack | Zone of Crack Initiation | Distance from Hole Center Line d (in.) | Crack Angle at               |                           | Crack Length in |           | Notes |
|--------------|---------------|--------------------------|--|------------------------------|---------------------------|-----------------|-----------|-------|
|              |               |                          |  | Initiation $\alpha_i$ (deg.) | Failure $\alpha_f$ (deg.) | Flange (in.)    | Web (in.) |       |
| B10-1        | 1st           | IV                       | -0.09                                  | -10                          | 0                         | 0.88            | ..        | 5     |
| B10-2        | ..            | ..                       | ..                                     | ..                           | ..                        | ..              | ..        | 3     |
| B11-1        | ..            | ..                       | ..                                     | ..                           | ..                        | ..              | ..        | 3     |
| B11-2        | ..            | ..                       | ..                                     | ..                           | ..                        | ..              | ..        | 3     |
| B12-1        | ..            | ..                       | ..                                     | ..                           | ..                        | ..              | ..        | 3     |
| B12-2        | 1st           | I                        | 0.09                                   | 5                            | 7                         | 0.88            | ..        | 5     |
| B13-1        | ..            | ..                       | ..                                     | ..                           | ..                        | ..              | ..        | 3     |
| B13-2        | ..            | ..                       | ..                                     | ..                           | ..                        | ..              | ..        | 3     |
| B14-1        | F             | ..                       | -0.41                                  | ..                           | ..                        | 1.25            | ..        | 7     |
|              | F             | ..                       | 0.53                                   | ..                           | ..                        | 1.75            | 1.25      | 7     |
| B14-2        | ..            | ..                       | ..                                     | ..                           | ..                        | ..              | ..        | 3     |
| B15-1        | 1st           | III                      | 0.06                                   | 8                            | -4                        | 1.64            | 0.44      |       |
| B15-2        | F             | ..                       | -0.44                                  | ..                           | ..                        | 1.38            | 0.25      |       |
| B17-1        | 1st           | I                        | 0.06                                   | 0                            | 0                         | 1.0             | ..        |       |
|              | 1st           | II                       | 0.13                                   | 8                            | 0                         | 2.10            | 1.13      |       |
| B17-2        | ..            | ..                       | ..                                     | ..                           | ..                        | ..              | ..        | 3     |

Table 17: Dimensions of cracks at bonded cover plates on Series B beams (continued)

| Specimen No. | Type of Crack | Zone of Crack Initiation | Distance from Hole Center Line d (in.) | Crack Angle at               |                           | Crack Length in |           | Notes |
|--------------|---------------|--------------------------|--|------------------------------|---------------------------|-----------------|-----------|-------|
|              |               |                          |  | Initiation $\alpha_i$ (deg.) | Failure $\alpha_f$ (deg.) | Flange (in.)    | Web (in.) |       |
| B18-1        | 1st           | II                       | -0.31                                  | 5                            | 0                         | 1.68            | 0.63      | 1     |
|              | 1st           | IV                       | -0.13                                  | 5                            | 5                         | 0.50            | ..        |       |
| B18-2        | ..            | ..                       | ..                                     | ..                           | ..                        | ..              | ..        | 3     |

Notes:

1. Crack grew into the web. It was stopped by drilling a hole at the web crack tip.
2. Crack grew into the web. It was stopped by drilling a hole at the web crack tip, and installing a high-strength bolt.
3. Runout or test discontinued.
4. Crack extended from hole to hole.
5. Crack extended from hole to edge.
6. Cover plate debonded starting at the end near the support, which had not been bolted.
7. Cover plate end near support was clamped with a high-strength clamp after detail B4-1 failed.
8. Both ends of all cover plates on beams B5 to B18 were bolted to the flange.

Table 18: Fatigue test data for Series B cover plates

| Spec. No.                | Gross Area Stress Range<br>$f_r$<br>(ksi) | Fatigue <sup>a</sup> Life<br>N<br>( $\times 10^3$ ) | Log-Mean Life<br>( $\times 10^3$ ) | Mean Life of                    |                                 |
|--------------------------|---|---|------------------------------------|---------------------------------|---------------------------------|
|                          |   |   |                                    | Category E<br>( $\times 10^3$ ) | Category B<br>( $\times 10^3$ ) |
| <u>Without End Bolts</u> |   |   |                                    |                                 |                                 |
| B1-1                     | 21  | 4,156-R   | > 2,195                            | 160                             | 2,579                           |
| B1-2                     | 21  | 4,156-R   |                                    |                                 |                                 |
| B2-1                     | 21  | 1,986-R   |                                    |                                 |                                 |
| B2-2                     | 21  | 1,986-R   |                                    |                                 |                                 |
| B3-1                     | 21  | 1,282-R   |                                    |                                 |                                 |
| B3-2                     | 21  | 1,282-R   |                                    |                                 |                                 |
| <u>With End Bolts</u>    |   |   |                                    |                                 |                                 |
| B7-1                     | 21  | 2,900   | > 5,557                            | 160                             | 2,579                           |
| B7-2                     | 21  | 4,471-R   |                                    |                                 |                                 |
| B8-1                     | 21  | 10,012-R  |                                    |                                 |                                 |
| B8-2                     | 21  | 10,012-R  |                                    |                                 |                                 |
| B9-1                     | 21  | 2,568   |                                    |                                 |                                 |
| B9-2                     | 21  | 9,006-R   |                                    |                                 |                                 |
| B13-1                    | 21  | 5,502-R   | > 2,220                            | 121                             | 1,898                           |
| B13-2                    | 21  | 5,502-R   |                                    |                                 |                                 |
| B14-1                    | 23  | 2,920   |                                    |                                 |                                 |
| B14-2                    | 23  | 3,394-R   |                                    |                                 |                                 |
| B15-1                    | 23  | 1,150   |                                    |                                 |                                 |
| B15-2                    | 23  | 2,130   |                                    |                                 |                                 |
| B4-1                     | 27.4                                      | ...   | > 1,484                            | 70                              | 1,052                           |
| B4-2                     | 27.4                                      | 2,239-R   |                                    |                                 |                                 |
| B5-1                     | 27.4                                      | 1,302   |                                    |                                 |                                 |
| B5-2                     | 27.4                                      | 2,130-R   |                                    |                                 |                                 |
| B6-1                     | 27.4                                      | 684   |                                    |                                 |                                 |
| B6-2                     | 27.4                                      | 1,251-R   |                                    |                                 |                                 |
| B10-1                    | 27.4                                      | 2,277   |                                    |                                 |                                 |
| B10-2                    | 27.4                                      | 2,505-R   |                                    |                                 |                                 |
| B11-1                    | 27.4                                      | 1,311-R   |                                    |                                 |                                 |
| B11-2                    | 27.4                                      | 1,311-R   |                                    |                                 |                                 |
| B12-1                    | 27.4                                      | 842   |                                    |                                 |                                 |
| B12-2                    | 27.4                                      | 1,752-R   |                                    |                                 |                                 |
| B17-1                    | 30  | 905   | > 965                              | 53                              | 775                             |
| B17-2                    | 30  | 905-R   |                                    |                                 |                                 |
| B18-1                    | 30  | 1,029   |                                    |                                 |                                 |
| B18-2                    | 30  | 1,168-R   |                                    |                                 |                                 |

Conversion factor: 1 ksi = 6.895 MPa

Note: a. The symbol R designates runout, or test discontinued.

Table 19: Comparison of previous and present fatigue test data for cover-plate ends

| Symbol<br>in<br>Fig. 32   | Series | No. of<br>Details<br>Tested | Stress<br>Range at<br>500,000<br>Cycles<br>$f_{r,x}$ (MPa) | Fatigue<br>Notch<br>Factor<br>$K_f$ | Fatigue<br>Life<br>Increase<br>$N_x/N_E$ | Comments     |
|---|--------|-----------------------------|--|-------------------------------------|--|--------------|
| <u>Square-ended, Prismatic Cover Plates (Ref. 10)</u>                 |        |                             |  |                                     |  |              |
| ○   | CR,CW  | 103                         | 98   | 3.57                                | 0.94                                     | Welded end   |
| ●   | CR,CW  | 100                         | 109  | 3.22                                | 1.31                                     | Unwelded end |
| ①   | CT     | 30                          | 101  | 3.49                                | 1.01                                     | Welded end   |
| ①   | CB     | 30                          | 102  | 3.44                                | 1.06                                     | Welded end   |
| ⊕   | CB     | 30                          | 79   | 4.41                                | 0.48                                     | Unwelded end |
| ⊙   | CM     | 30                          | 102  | 3.45                                | 1.05                                     | Welded end   |
| ⊙   | A11    | 193                         | 100  | 3.51                                | 1.00                                     | Welded end   |
| <u>End-welded and Ground Cover Plates (Ref. 27)</u>                   |        |                             |  |                                     |  |              |
| ⬡   | CG     | 26                          | 180  | 1.94                                | 6.54                                     | Toe cracks   |
| <u>Ground, Shot-peened, and Remelted End Welds (Ref. 26)</u>          |        |                             |  |                                     |  |              |
| □   | GA     | 8                           | 115  | 3.06                                | 1.53                                     |              |
| ▤   | PA     | 16                          | 127  | 2.77                                | 2.12                                     |              |
| ■   | TA     | 16                          | 159  | 2.20                                | 4.40                                     |              |
| <u>Cover Plates Subjected to Variable Amplitude Loading (Ref. 25)</u> |        |                             |  |                                     |  |              |
| ○   | B & C  | 27                          | 98   | 3.58                                | 0.93                                     |              |
| ●   | B & C  | 45                          | 103  | 3.40                                | 1.10                                     | Var. ampl.   |
| <u>Full-Size Coverplated Beams (Refs. 23 and 24)</u>                  |        |                             |  |                                     |  |              |
| △   | B      | 38                          | 84   | 4.19                                | 0.56                                     |              |
| <u>End-Bolted Cover Plates (Ref. 7)</u>                               |        |                             |  |                                     |  |              |
| ◐   | 6-bolt | 4                           | ..   | 1.35                                | 21.4                                     | Cleaned      |
| ◑   | 6-bolt | 16                          | ..   | 1.40                                | 18.7                                     |              |
| ◒   | 4-bolt | 12                          | ..   | 1.30                                | 24.1                                     |              |
| ◓   | 2-bolt | 12                          | ..   | 1.56                                | 13.4                                     |              |
| <u>Retrofitted Cover Plates (Ref. 8)</u>                              |        |                             |  |                                     |  |              |
| ◈   | B      | 14                          | ..   | 1.42                                | 18.2                                     | Noncracked   |
| ◆   | A      | 15                          | ..   | 1.58                                | 12.9                                     | Precracked   |

Table 19: Comparison of previous and present  
fatigue test data for cover-plate ends (continued)

| Symbol<br>in<br>Fig. 32                             | Series | No. of<br>Details<br>Tested | Stress<br>Range at<br>500,000<br>Cycles<br>$f_{r,x}$ (MPa) | Fatigue<br>Notch<br>Factor<br>$K_f$ | Fatigue<br>Life<br>Increase<br>$N_X/N_E$ | Comments            |
|---|--------|-----------------------------|--|-------------------------------------|--|---------------------|
| <u>Adhesive-Bonded Cover Plates (Present Study)</u> |        |                             |  |                                     |  |                     |
| ✕   | B      | 19                          | ..   | ..                                  | 20.0                                     | $f_r = 23.0$ ksi    |
|   | B      | 8                           | ..   | ..                                  | 35.0                                     | $f_r \leq 21.0$ ksi |

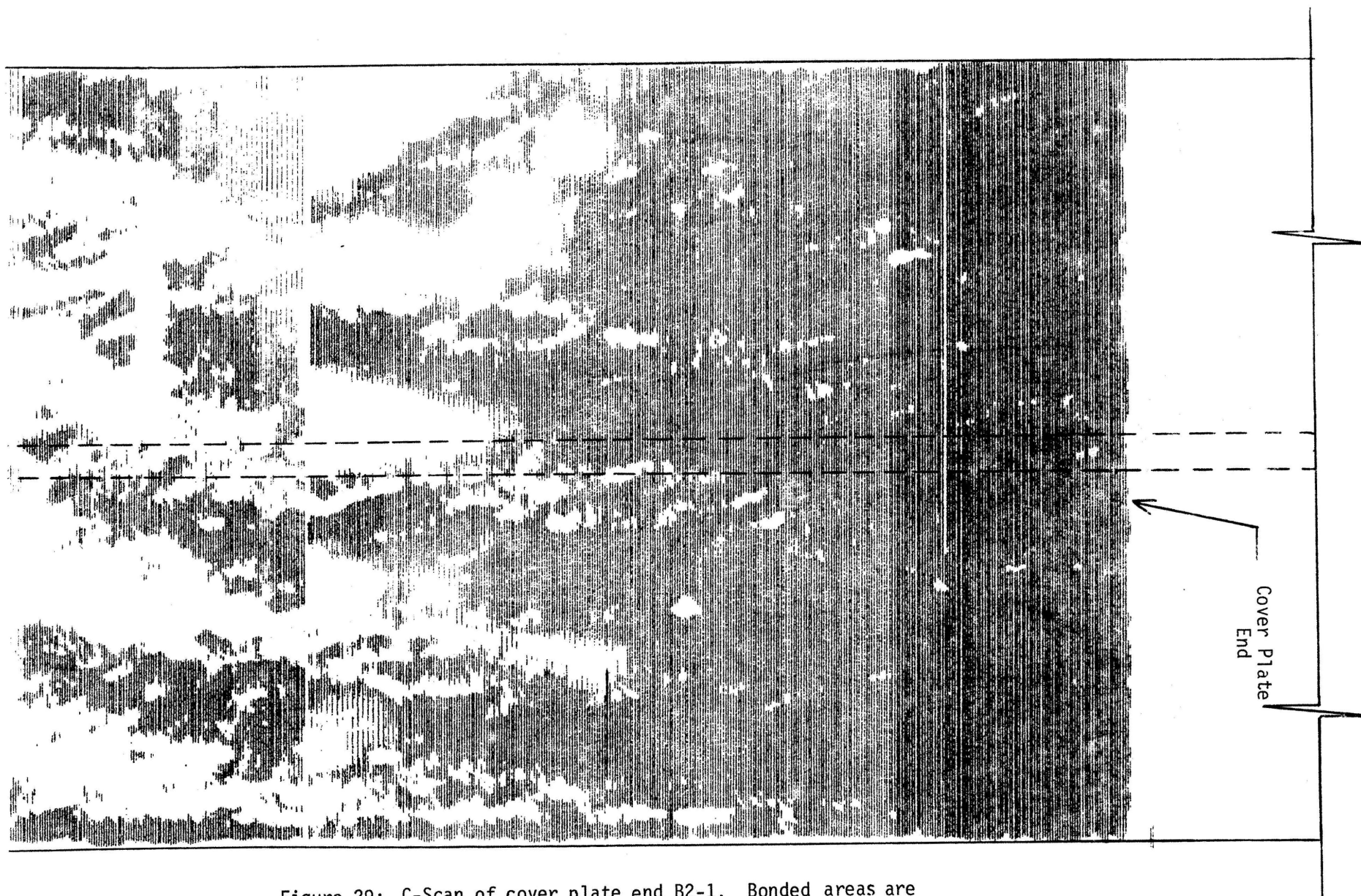


Figure 29: C-Scan of cover plate end B2-1. Bonded areas are clear, debonded areas are dark.



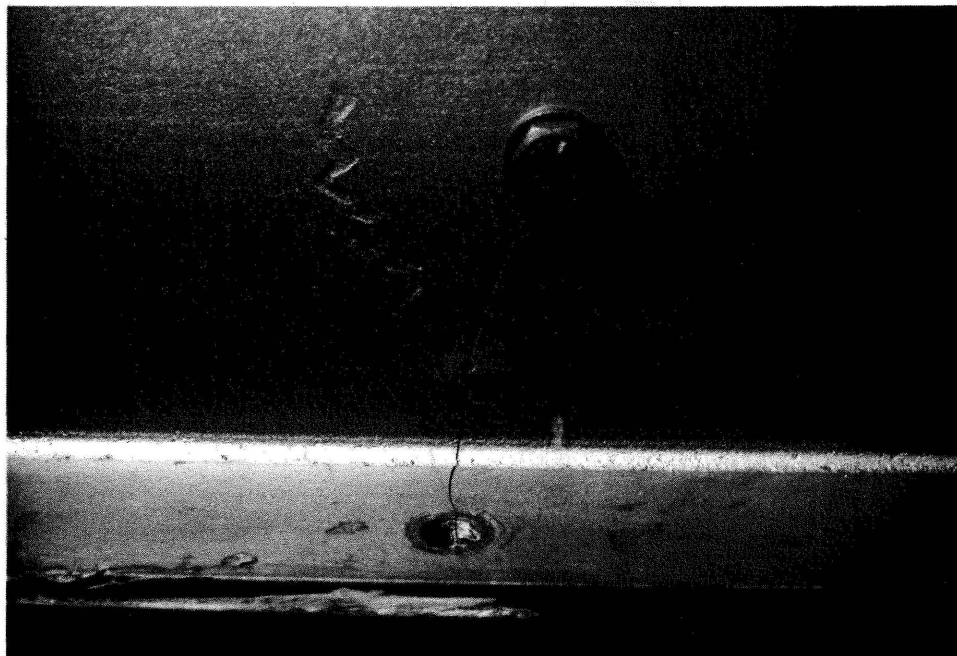


Fig. 30: Typical bolt hole cracks at cover plate ends B5-1 (top) and B9-1 (bottom). Hole and bolt at crack tip in web are part of temporary repair.

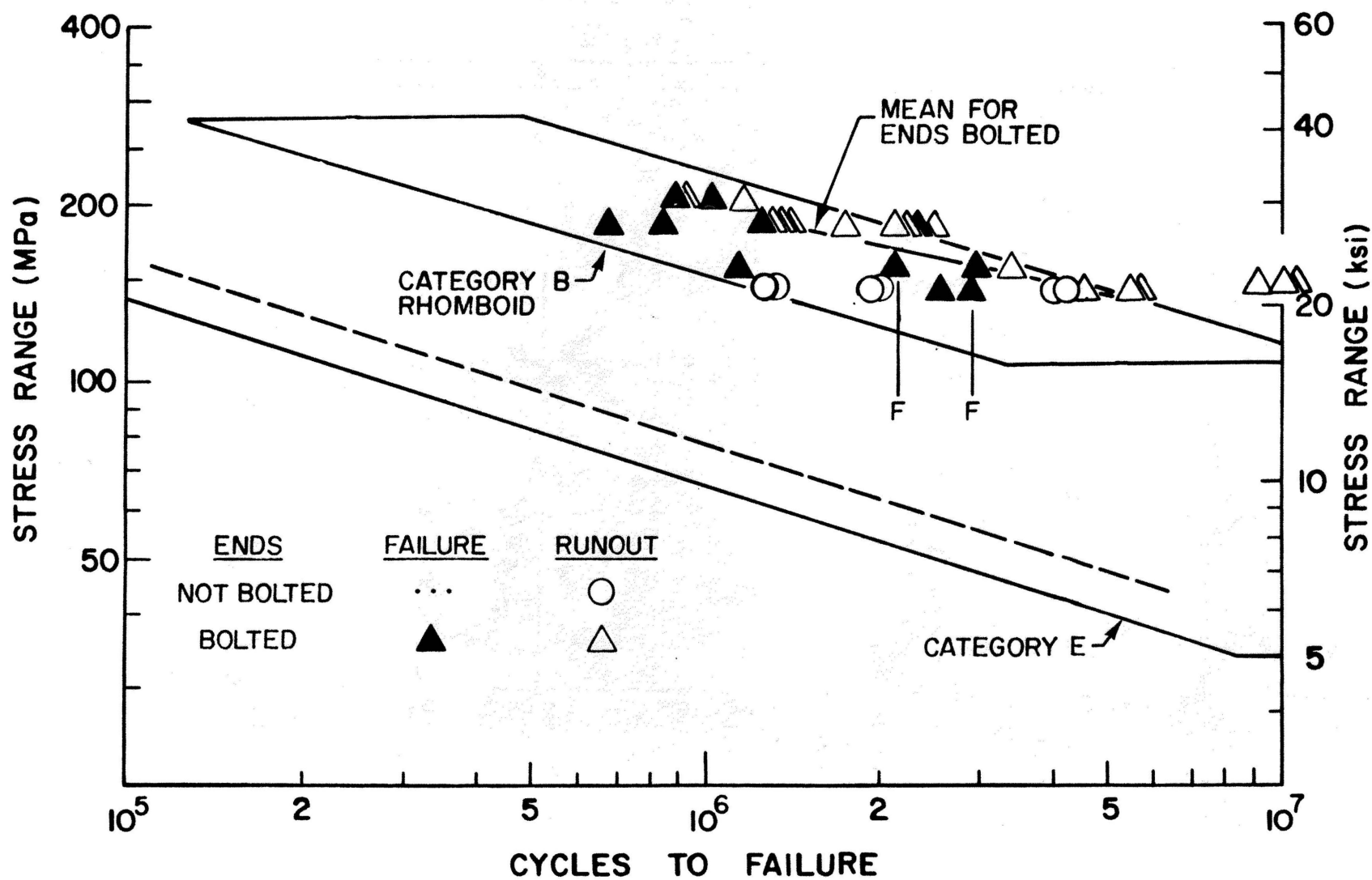


Figure 31: Fatigue test data for Series B beam cover plates

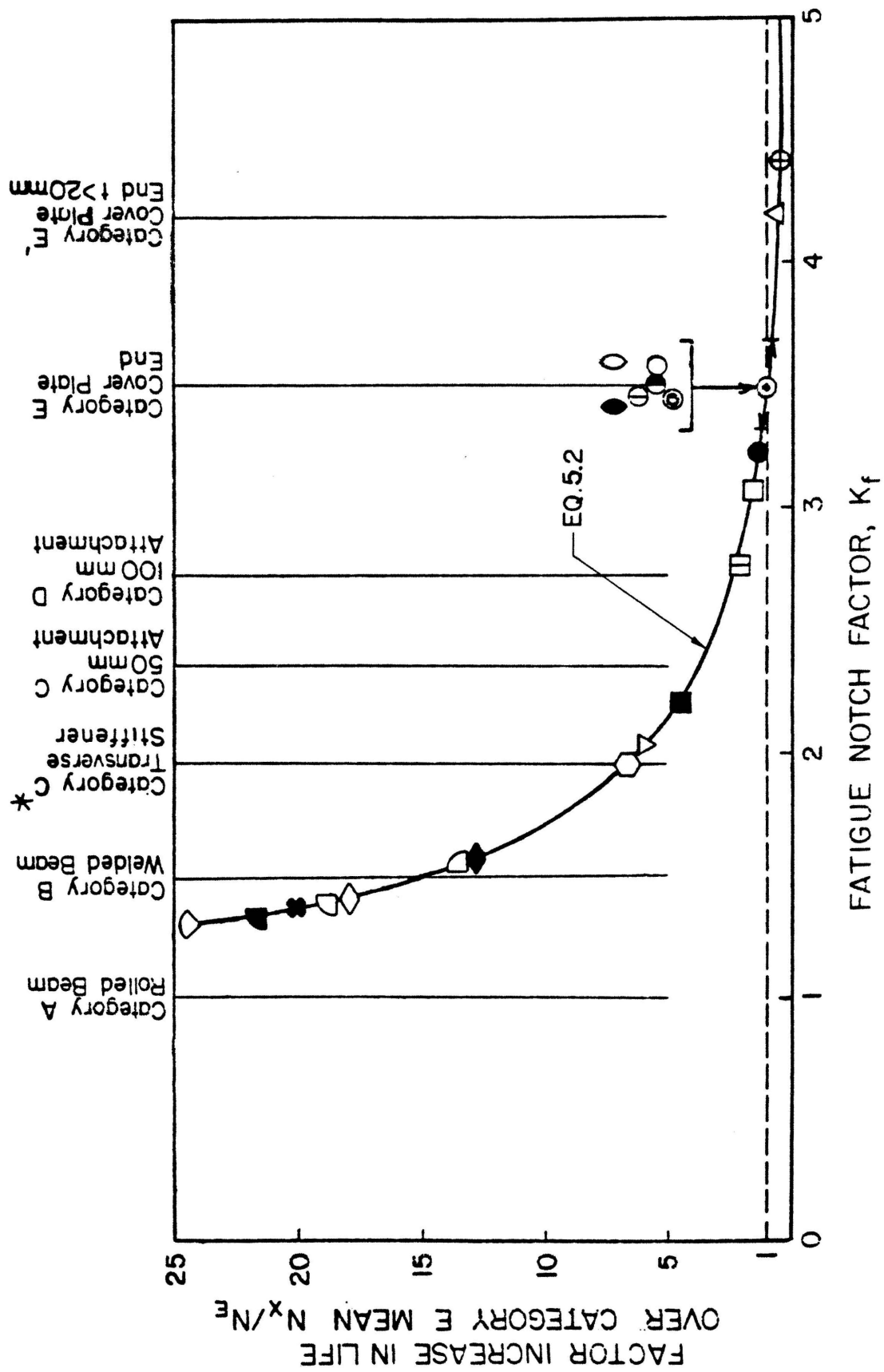


Figure 32: Comparison of mean fatigue strength of all data sets with mean of Category A through E' data. See Table 19.

## CHAPTER 6: STATIC STRENGTH OF SERIES C TENSILE SPLICES

### 6.1 Experiment Design

The experiment design, shown in Table 20, consisted of 22 specimens arranged in a two-way factorial consisting of two-bolt and one-bolt splices, nonbonded and bonded contact surfaces, and four or seven replicates per cell. The static tensile specimens are shown in Fig. 1. They were identical to the Series A fatigue test specimens.

The fabricator had blast cleaned all plates before he drilled the holes. After drilling, he ground off burrs along the plate edges and around the holes of the two-bolt splices C1-C8. The one-bolt splices C9-C16 were free of grinding marks. To obtain a uniform surface condition, for purposes of comparing the data, an additional six two-bolt splices C17-C22 were fabricated with surfaces blast cleaned after drilling. The specimens were loaded either under load control or stroke control.

### 6.2 Definition of Slip Coefficient and Slip Load

The slip coefficient,  $k_s$ , is defined as:

$$k_s = \frac{P_s}{m n T_i}$$

where:

$P_s$  = measured slip load

$m$  = number of shearing planes

$n$  = number of bolts

$T_i$  = initial bolt tension

The slip load of a splice was determined from its load-elongation curve automatically recorded during the test with an x-y plotter. It was defined as the:

1. Load at major slip of splices that slipped suddenly;
2. Load at 0.02-in (0.51 mm) slip of splices that slipped gradually.

The same criteria had been used in References 16, 28 and 29.

The load-elongation curves presented in this report were hand traced from photographic reductions of the recorded curves.

### 6.3 Static Test Data

Two-Bolt Splices: The static test data for all two-bolt splices are given in Table 21. The table lists for each splice the pertinent information on loading rate, slip, and failure.

The load-elongation curves of the nonbonded splices were plotted in Figs. 33 and 34, respectively, for specimens with grinding marks (C1-C4) and without grinding marks (C17-C19) on the contact surfaces. In the former case, the splices tested under load control exhibited major slip, whereas the splices tested under stroke control tended to slip gradually. In the latter case, all three splices slipped gradually regardless of whether they were tested under load or stroke control. After the splice slipped into bearing, the load-elongation curve rose linearly for a short distance. Thereafter, the behavior became non-linear as the plate net sections began to yield in tension and the bolts in shear. All tests ended with shearing of the bolts before the plate gross section yielded. Figure 35 shows a typical two-bolt splice after testing.

The load-elongation curves of the bonded splices were plotted in Figs. 36 and 37, respectively, for specimens with grinding marks (C5-C8) and without grinding marks (C20-C22) on the contact surfaces. All splices slipped suddenly when the adhesive bond failed. The load dropped until the splice went into full bearing and then rose again to a level at which the bolts sheared.

The mean slip coefficients and the standard deviations are summarized in Table 22. The values for the nonbonded two-bolt splices were  $\bar{k}_s = 0.352 \pm 0.051$  for specimens with grinding marks and  $\bar{k}_s = 0.653 \pm 0.091$  for specimens without grinding marks on the contact surfaces. Evidently, the ground areas reduced the slip resistance of the nonbonded surfaces and decreased the slip coefficient by almost one-half. Frank and Yura<sup>(16)</sup> reported the same finding for pilot test specimens with sand blasted surfaces whose edges had been ground after sandblasting. Their tests yielded an average slip coefficient  $\bar{k}_s = 0.353 \pm 0.050$ , which was smaller than the value of  $\bar{k}_s = 0.472 \pm 0.046$  for specimens without grinding marks.

The mean slip coefficients of the bonded two-bolt splices were  $\bar{k}_s = 1.235 \pm 0.021$  for specimens with grinding marks and  $\bar{k}_s = 1.207 \pm 0.025$  for specimens without grinding marks on the contact surfaces. The ground surfaces did not reduce the slip resistance in this case. Bonding increased the slip coefficient by a factor of 1.87.

The splices C1-C8 and C17-C22 were fabricated from steels that came from two different heats. For this reason, the tensile yield loads and ultimate shear loads of the two sets differed by about 10 kips (44.5 kN). The slip load of both sets of bonded specimens remained, however, within a narrow range [89.6 - 95.5 kips (399 - 425 kN)]. It

was higher than the net section yield load,  $P_{yn}$ , but lower than the gross section yield load,  $P_{yg}$ , of the main and splice plates.

It seems that the adhesive fails when the shear stress or shear strain in the bond line exceed certain limits. The first case would occur when the steel specimen remains elastic while the adhesive reaches its ultimate shear stress. In the second case, plastic deformations of the steel specimen would impose large shear strains on the adhesive and cause it to fail prematurely. Since the slip loads fell within the range of net and gross area yield loads, it is not possible to conclusively determine the reason for the adhesive failure in the two-bolt splices.

One-bolt Splices: The static test data for all one-bolt splices are summarized in Table 23.

The load-elongation curves of the nonbonded splices C9-C12 were plotted in Fig. 38. The splices tested under load control exhibited major slip, whereas the splices tested under stroke control tended to slip gradually. After the splice slipped into bearing, the load-elongation curve rose nonlinearly as the bolt gradually sheared before the plate net sections yielded.

The load-elongation curves for the bonded splices C13-C16 were plotted in Fig. 39. All specimens slipped suddenly when the adhesive bond failed. The load dropped until the splice went into full bearing and then rose slightly to the shearing load of the bolt. The failure was abrupt because the slip load exceeded the ultimate shear load of the bolt.

The mean slip coefficients and standard deviations are summarized in Table 22. The value for the nonbonded one-bolt splices,

$\bar{k}_S = 0.585 \pm 0.071$  agrees reasonably well with that for the two-bolt splices. Bonding increased the slip coefficient of the one-bolt splices by a factor of 2.50, to  $\bar{k}_S = 1.462 \pm 0.159$ .

The failure of the bonded one-bolt splices differed in two respects from those of the bonded two-bolt splices. First, the slip loads were smaller than the net area yield loads. Secondly, the slip loads were greater than one-half the load for the two-bolt splices. This suggests that the load carrying capacity of the adhesive bond was limited by shear stresses in the bond line, and not by shear strains induced by yielding deformations of the steel plates.

Assuming an ultimate adhesive shear stress of 4.0 ksi (27.6 MPa) under monotonic loading (see Chapter 8), the shear capacity of the bonded area of the one-bolt splice should be:

$$P_{adh.} = 4.0 \times 2 \left[ 2.5 \times 2.5 - \frac{\pi (11/16)^2}{4} \right] = 47.0 \text{ kip (209 kN)}$$

the mean failure load of the nonbonded one-bolt splices was 49.9 kip (222 kN). In comparison, the mean failure load of the bonded one-bolt splices was 55.5 kip (247 kN) which is less than the sum of the shear capacity of the adhesive and the bolt,  $P = 47.0 + 49.9 = 96.9 \text{ kip (431 kN)}$ . The two contributions are not additive.

#### 6.4 Comparison with AASHTO Specifications and Previous Work

Comparison with AASHTO Specifications: The slip load,  $P_S$ , defined in Eq. 6.1 can also be expressed in terms of a fictitious shear stress on the gross area of the bolts:  $P_S = mn f_v A_b$ . The specified bolt tension is  $T_i = 0.7 F_u A_t$ , in which  $A_t$  = tensile stress area and  $F_u$  = tensile strength of bolt. Substituting  $P_S$  and  $T_i$  in Eq. 6.1, and recalling that  $A_t/A_b = 0.75$ , gives

$$k_s = \frac{f_v}{0.525 F_u} \quad (6.2)$$



The allowable shear stress for friction-type joints is obtained by substituting the allowable slip coefficient in Eq. 6.2 and solving for:

$$F_v = 0.525 F_u k_{s,all} \quad (6.3)$$

The tensile strength is  $F_u = 120$  ksi (827 MPa) for A325 bolts and  $F_u = 150$  ksi (1034 MPa) for A490 bolts.

In 1957, AASHTO specified for the first time an allowable shear stress of 13.5 ksi (93 MPa) for A325 bolts in friction-type joints. In 1965, an allowable shear stress of 18 ksi (124 MPa) was added for A490 bolts. These values, based on early data for A7 and A440 steel specimens, applied equally to joints with blast cleaned or mill scale surfaces. They are shown in Fig. 41 with solid and dashed lines respectively.

In 1974, Fisher and Struik<sup>(30)</sup> surveyed the literature and reported that the average slip coefficient of 168 grit blasted A7, A36 and European Fe37 steel specimens tested in several studies was  $\bar{k}_s = 0.493$ , with standard deviation  $s = 0.074$ . The corresponding value for 19 grit blasted A514 steel specimens were  $\bar{k}_s = 0.331$  and  $s = 0.043$ . On the basis of the Reference 30 findings, and assuming a 5% slip probability, the allowable slip coefficient was calculated from

$$k_{s,all} = \bar{k}_s - 1.645s \quad (6.4)$$

Accordingly, it appears that AASHTO in 1979 increased the allowable shear stress of A325 bolts, based on the aforementioned data and assuming a 5% probability of slip, to:

$$\begin{aligned} F_v &= 0.525 \times 120 (0.493 - 1.645 \times 0.074) = 23.4 \text{ ksi} \\ &\approx 25 \text{ ksi (172 MPa)} \end{aligned}$$

for Class of Surface B blast-cleaned carbon and low-alloy steel, and to:

$$F_v = 0.525 \times 120 (0.331 - 1.645 \times 0.043) = 16.4 \text{ ksi}$$

$$\approx 17 \text{ ksi (117 MPa)}$$

for Class of Surface C blast-cleaned quenched and tempered steel. The corresponding values for A490 bolts are 29.25 ksi  $\approx$  31 ksi (214 MPa) and 20.5 ksi  $\approx$  21 ksi (145 MPa), respectively, for Class of Surfaces B and C. These values were also plotted in Fig. 41.

In 1981, Frank and Yura <sup>(16)</sup> developed statistically reliable slip resistance data for bolted joints with coated contact surfaces. As part of that work they proposed that the allowable shear stress for friction-type joints should be based on a 1% slip probability or a mean safety factor of 1.45, whichever gave the smaller value, that is:

$$k_{s,all} = \bar{k}_s - 2.326 s \quad (6.5)$$

or:

$$k_{s,all} = \frac{\bar{k}_s}{1.45} \quad (6.6)$$

The allowable shear stresses for the Series C splices tested herein were calculated in accordance with the AASHTO criterion (Eq. 6.4) and the Reference 16 criteria (Eqs. 6.5 and 6.6). The results are summarized in Table 22. By any criteria, the allowable shear stress for the nonbonded splices exceed the AASHTO value of  $F_v = 25 \text{ ksi}$  (172 MPa) for friction-type joints. The allowable shear stress for the bonded splices greatly exceeds even the AASHTO value of  $F_v = 40 \text{ ksi}$  (276 MPa) for bearing-type joints.

Comparison with Previous Data for Nonbonded Splices: Six previous domestic studies examined the slip resistance of tensile and beam splices fabricated from A7, A36, A572, A588 and A514 steel with blast cleaned

surfaces. The data were analyzed herein, and the results are summarized in Table 24. For each entry on the table, a data point was plotted in chronological order in Fig. 41. The vertical lines below each point indicate the data scatter. The tick marks were drawn at the 5% (1.654s) and 1% (2.326s) levels of slip probability. The second part of Table 24 summarizes the data by type of steel. The allowable shear stresses were calculated with Eqs. 6.4-6.6. The data suggest the following conclusions for bolted splices with blasted cleaned contact surfaces:

1. The mean slip resistance of the nonbonded splices tested herein was higher than that measured in most other studies.
2. The types of steels rank as follows in terms of mean slip resistance: (1) low-alloy steels,  $\bar{k}_s = 0.572 \pm 0.118$ ; (2) carbon steels,  $\bar{k}_s = 0.507 \pm 0.089$ ; and (3) quenched and tempered steels,  $\bar{k}_s = 0.43 \pm 0.106$ .
3. When calculated on the basis of a 5% slip probability, the allowable shear stresses for the low-alloy steels A572 and A588, and the quenched and tempered steel A514 compares well with the AASHTO values of  $F_v = 25$  ksi (172 MPa) and  $F_v = 17$  ksi (117 MPa), respectively. When calculated on the basis of a 1% slip probability, they are lower.
4. The allowable shear stress for the carbon steels, A7 and A36, is lower than the value of  $F_v = 25$  ksi (172 MPa) specified by AASHTO, regardless of which criterion is used to calculate it.

At present, AASHTO has set most allowable shear stresses based on a 5% slip probability and a few based on a 1% slip probability. A588 steel with mill scale surfaces is an example of the latter. It would be more meaningful to choose one criterion alone for all cases.

Bonded Specimens: It appears that the only previous work on bonded and bolted joints was a series of exploratory tests performed by Chesson.<sup>(3)</sup> He used shear and tensile specimens, shown in the inserts of Figs. 42, 44, and 45. The shear specimens consisted of a 2-1/2 x 3/4 x 3 in (64 x 19 x 76 mm) long main plate and two 2-1/2 x 3/8 x 3 in (64 x 9.5 x 76 mm) long splice plates, with 2-1/2 x 2-1/2 in (64 x 64 mm) contact surfaces. The tensile specimen had two 4-7/8 x 1 x 31-1/8 in (124 x 25.4 x 790 mm) long main plates and two 4-7/8 x 1/2 x 33 in (124 x 12.7 x 838 mm) long splice plates. All steel conformed to the requirements of ASTM A36 specification.

The shear specimens that were bolted had one 3/4 in (19 mm) diameter A325 bolt, for a bolt-to-member strength ratio of  $P_b/P_m = 0.59$ . The tensile specimens had either four or six 3/4 in (19 mm) bolts and  $P_b/P_m = 0.92$  and 1.37, respectively.

The contact surfaces were sandblasted, machine wire brushed, or flame cleaned and wire brushed. The specimens were bonded, bolted, or bonded and bolted. The adhesives were of the epoxy type consisting of AREA formulations 1101-32 and 991-67.

Figure 42 shows the load-elongation curves of bonded, bolted, or bonded and bolted shear specimens with sandblasted contact surfaces. Each curve is the average of three tests. The bonded specimen failed at an average shear stress of 2.3 ksi (16 MPa). Its failure load was much smaller than that of the bolted specimen despite the latter's low bolt-to-member strength ratio of  $P_b/P_m = 0.59$ . Bonding in addition to bolting increased the slip coefficient to  $\bar{K}_s = 0.94$  (mean of three tests), up from  $\bar{K}_s = 0.52$  for the bolted specimens. But it did not

increase the ultimate strength after bond failure, which depended on the shear capacity of the bolt alone. The bond failed at a load between net and gross section yielding of the plates.

The effect of contact surface preparations on the bonded and bolted shear specimens is shown in Figure 43. Those with sand-blasted surfaces had the highest slip coefficient,  $\bar{k}_s = 0.94$ . The others began to gradually slip at about one-half of that load.

Finally, Figure 44 compares the load-slip curves of the non-bonded four-bolt tensile specimens ( $P_b/P_m = 0.92$ ). Bonding the sand-blasted contact surfaces, in addition to bolting, increased the slip coefficients to  $\bar{k}_s = 0.62$  (one specimen tested), up from  $\bar{k}_s = 0.44$  for the bolted specimen. Again, the bond failed between net and gross section yielding of the plates. The load-elongation curves beyond slip were not reported. The six-bolt tensile specimens ( $P_b/P_m = 1.37$ ) also exhibited bond failure between net and gross section yielding, as shown in Figure 45.

In summary, the most important conclusion one can draw from the results of Chesson's exploratory tests and those described herein is that the adhesive fails before the gross area of the steel plate yields. Once the adhesive fails, the joint slips into bearing. Thereafter, the ultimate strength is limited by the tensile capacity of the member or the shear capacity of the bolts, whichever governs. It has not been possible to increase the ultimate strength of bonded and bolted joints to a value greater than the strength of a joint that is bolted only. However, bonding greatly increased the slip load of bolted joints. These conclusions apply to specimens with a wide range of bolts-to-member strength ratios,  $0.36 \leq P_b/P_m \leq 1.37$ .

Table 20: Static test matrix for  
Series C tensile specimens

| Control<br>Mode | Two-Bolt Splices                   |                                    | One-Bolt Splices |            |
|-----------------|------------------------------------|------------------------------------|------------------|------------|
|                 | Nonbonded                          | Bonded                             | Nonbonded        | Bonded     |
| Load            | C1 <sup>a</sup><br>C2 <sup>a</sup> | C5 <sup>a</sup><br>C6 <sup>a</sup> | C9<br>C10        | C13<br>C14 |
| Stroke          | C3 <sup>a</sup><br>C4 <sup>a</sup> | C7 <sup>a</sup><br>C8 <sup>a</sup> | C11<br>C12       | C15<br>C16 |
| Load            | C17                                | C20                                | ...              | ...        |
| Stroke          | C18<br>C19                         | C21<br>C22                         | ...<br>...       | ...<br>... |

Note: a. Splices with grinding marks on contact surfaces

Table 21: Static test data for Series C tensile specimens;  
Two-bolt splices

| Specimen No.      | Load Control Rate (kips/min) | Stroke Control Rate (in/min) | Slip Load $P_s$ (kips) | Slip Coefficient $k_s$ | Failure Load    |             | Elongation at Failure |           |
|-------------------|------------------------------|------------------------------|------------------------|------------------------|-----------------|-------------|-----------------------|-----------|
|                   |                              |                              |                        |                        | Adhesive (kips) | Bolt (kips) | Adhesive (in)         | Bolt (in) |
| Nonbonded Splices |                              |                              |                        |                        |                 |             |                       |           |
| C1                | 18                           | ...                          | 32.3                   | 0.42                   | ...             | 93.5        | ...                   | 0.59      |
| C2                | 60                           | ...                          | 25.3                   | 0.33                   | ...             | 95.5        | ...                   | 0.59      |
| C3                | ..                           | 0.12                         | 27.0                   | 0.36                   | ...             | 90.3        | ...                   | 0.44      |
| C4                | ..                           | 0.12                         | 22.9                   | 0.30                   | ...             | 86.6        | ...                   | 0.40      |
| C17               | 30                           | ...                          | 49.0                   | 0.64                   | ...             | 99.0        | ...                   | 0.42      |
| C18               | ..                           | 0.12                         | 57.1                   | 0.75                   | ...             | 104.0       | ...                   | 0.58      |
| C19               | ..                           | 0.12                         | 43.0                   | 0.57                   | ...             | 103.5       | ...                   | 0.54      |
| Bonded Splices    |                              |                              |                        |                        |                 |             |                       |           |
| C5                | 60                           | ...                          | 92.3                   | 1.21                   | 92.3            | 90.0        | 0.095                 | Undefined |
| C6                | 30                           | ...                          | 93.5                   | 1.23                   | 93.5            | Undefined   | 0.11                  | Undefined |
| C7                | ..                           | 0.12                         | 95.5                   | 1.26                   | 95.5            | 90.2        | 0.10                  | 0.48      |
| C8                | ..                           | 0.12                         | 94.0                   | 1.24                   | 94.0            | 87.2        | 0.10                  | 0.29      |
| C20               | 30                           | ...                          | 93.5                   | 1.23                   | 93.5            | 95.6        | 0.11                  | 0.155     |
| C21               | ..                           | 0.12                         | 91.6                   | 1.21                   | 91.6            | 100.0       | 0.10                  | Undefined |
| C22               | ..                           | 0.12                         | 89.6                   | 1.18                   | 89.6            | 99.5        | 0.09                  | Undefined |

Table 22: Mean slip data for Series C tensile specimens and allowable shear stresses for friction-type joints

| Specimen No.            | Surface Condition      | Mean Slip Coefficient<br>$\bar{\mu}_s$ | Standard Deviation<br>$s$ | Allowable Shear Stress of Bolts in Friction-Type Joints |             |                   |
|-------------------------|------------------------|--|---------------------------|---|-------------|-------------------|
|                         |                        |  |                           | 5%<br>(ksi)   | 1%<br>(ksi) | FOS=1.45<br>(ksi) |
| <u>Two-Bolt Splices</u> |                        |  |                           |   |             |                   |
| C1-C4                   | Nonbonded <sup>a</sup> | 0.352                                  | 0.051                     | 16.9  | 14.7        | 15.3              |
| C17-C19                 | Nonbonded              | 0.653                                  | 0.091                     | 31.7  | 27.8        | 28.3              |
| C5-C8                   | Bonded <sup>a</sup>    | 1.235                                  | 0.021                     | 75.6  | 74.7        | 53.6              |
| C20-C22                 | Bonded                 | 1.207                                  | 0.025                     | 73.4  | 72.3        | 52.4              |
| All                     | bonded                 | 1.23                                   | 0.023                     | 74.6  | 73.6        | 53.1              |
| <u>One-Bolt Splices</u> |                        |  |                           |   |             |                   |
| C9-C12                  | Nonbonded              | 0.585                                  | 0.071                     | 29.5  | 26.4        | 25.4              |
| C13-C16                 | Bonded                 | 1.462                                  | 0.159                     | 75.6  | 68.7        | 63.5              |
| <u>All Splices</u>      |                        |  |                           |   |             |                   |
| All <sup>b</sup>        | Nonbonded              | 0.614                                  | 0.081                     | 30.3  | 26.8        | 26.7              |
| All                     | Bonded                 | 1.31                                   | 0.150                     | 66.9  | 60.4        | 56.9              |

Note: a. Splices with grinding marks on contact surfaces.

b. Specimens C1-C4 were excluded because of grinding marks on contact surfaces.



Table 23: Static test data for Series C tensile specimens;  
One-bolt splices

| Specimen No.             | Load Control Rate (kips/min) | Stroke Control Rate (in/min) | Slip Load $P_S$ (kips) | Slip Coefficient $k_S$ | Failure Load    |             | Elongation at Failure |           |
|--------------------------|------------------------------|------------------------------|------------------------|------------------------|-----------------|-------------|-----------------------|-----------|
|                          |                              |                              |                        |                        | Adhesive (kips) | Bolt (kips) | Adhesive (in)         | Bolt (in) |
| <u>Nonbonded Splices</u> |                              |                              |                        |                        |                 |             |                       |           |
| C9                       | 30                           | ...                          | 22.8                   | 0.60                   | ...             | 48.3        | ...                   | 0.38      |
| C10                      | 30                           | ...                          | 25.7                   | 0.68                   | ...             | 51.7        | ...                   | 0.33      |
| C11                      | ..                           | 0.12                         | 20.2                   | 0.53                   | ...             | 48.0        | ...                   | 0.32      |
| C12                      | ..                           | 0.12                         | 20.1                   | 0.53                   | ...             | 51.7        | ...                   | 0.37      |
| <u>Bonded Splices</u>    |                              |                              |                        |                        |                 |             |                       |           |
| C13                      | 30                           | ...                          | 49.7                   | 1.31                   | 49.5            | 46.5        | 0.04                  | Undefined |
| C14                      | 30                           | ...                          | 52.7                   | 1.39                   | 52.5            | 46.5        | 0.04                  | Undefined |
| C15                      | ..                           | 0.12                         | 55.8                   | 1.47                   | 55.5            | 45.5        | 0.05                  | 0.36      |
| C16                      | ..                           | 0.12                         | 64.0                   | 1.68                   | 64.0            | 40.5        | 0.05                  | 0.30      |

Table 24: Slip coefficients and allowable shear stresses for friction-type bolted joints with blast cleaned surfaces

| Reference                             | Type of Steel | No. of Tests<br>n | Mean Slip Coefficient<br>$\bar{k}_s$ | Standard Deviation<br>s | Allowable Shear Stress for A325 Bolts |             |                   |
|---------------------------------------|---------------|-------------------|--------------------------------------|-------------------------|---------------------------------------|-------------|-------------------|
|                                       |               |                   |                                      |                         | 5%<br>(ksi)                           | 1%<br>(ksi) | FOS=1.45<br>(ksi) |
| <u>Nonbonded Specimens</u>            |               |                   |                                      |                         |                                       |             |                   |
| Hechtman 1955                         | A7            | 3                 | 0.47                                 | 0.108                   | 18.4                                  | 13.8        | 20.4              |
| Douty 1965                            | A7            | 7                 | 0.560                                | 0.068                   | 28.2                                  | 25.3        | 24.3              |
| Chesson 1966                          | A36           | 5                 | 0.488                                | 0.064                   | 24.1                                  | 21.5        | 21.2              |
| Fisher 1968                           | A514          | 17                | 0.332                                | 0.041                   | 16.7                                  | 14.9        | 14.4              |
| Frank 1981                            | A36           | 21                | 0.495                                | 0.097                   | 21.1                                  | 17.0        | 21.5              |
|                                       | A514          | 24                | 0.50                                 | 0.077                   | 23.5                                  | 20.2        | 21.7              |
|                                       | A572          | 68                | 0.561                                | 0.097                   | 25.3                                  | 21.1        | 24.4              |
|                                       | A588          | 5 <sup>b</sup>    | 0.86                                 | 0.038                   | 50.2                                  | 48.6        | 37.3              |
| Yura 1981                             | A588          | 20 <sup>a</sup>   | 0.518                                | 0.10                    | 22.2                                  | 18.0        | 22.5              |
|                                       |               | 7 <sup>d</sup>    | 0.614                                | 0.081                   | 30.3                                  | 26.8        | 26.7              |
| Present 1983 Study                    | A588          | 2 <sup>e</sup>    | 0.640                                | ...                     | ...                                   | ...         | 27.8              |
| <u>Summary of Nonbonded Specimens</u> |               |                   |                                      |                         |                                       |             |                   |
|                                       | A7            | 10                | 0.533                                | 0.087                   | 24.5                                  | 20.8        | 23.1              |
|                                       | A36           | 26                | 0.492                                | 0.091                   | 21.5                                  | 17.6        | 21.4              |
|                                       | A7, A36       | 36                | 0.507                                | 0.089                   | 22.7                                  | 18.9        | 22.0              |
|                                       | A572          | 68                | 0.561                                | 0.097                   | 25.3                                  | 21.1        | 24.4              |
|                                       | A588          | 34                | 0.594                                | 0.150                   | 21.9                                  | 15.4        | 25.9              |
|                                       | A572, A588    | 102               | 0.572                                | 0.118                   | 23.8                                  | 18.7        | 24.8              |
|                                       | A514          | 41                | 0.430                                | 0.106                   | 16.1                                  | 11.5        | 18.7              |

- Notes:
- Specimens tested at Federal Highway Administration.
  - Specimens tested at University of Texas.
  - For A490 bolts multiply shear stress by 150 ksi/120 ksi = 1.25.
  - Mean slip coefficient for tensile splices.
  - Mean slip coefficient for beam splices.

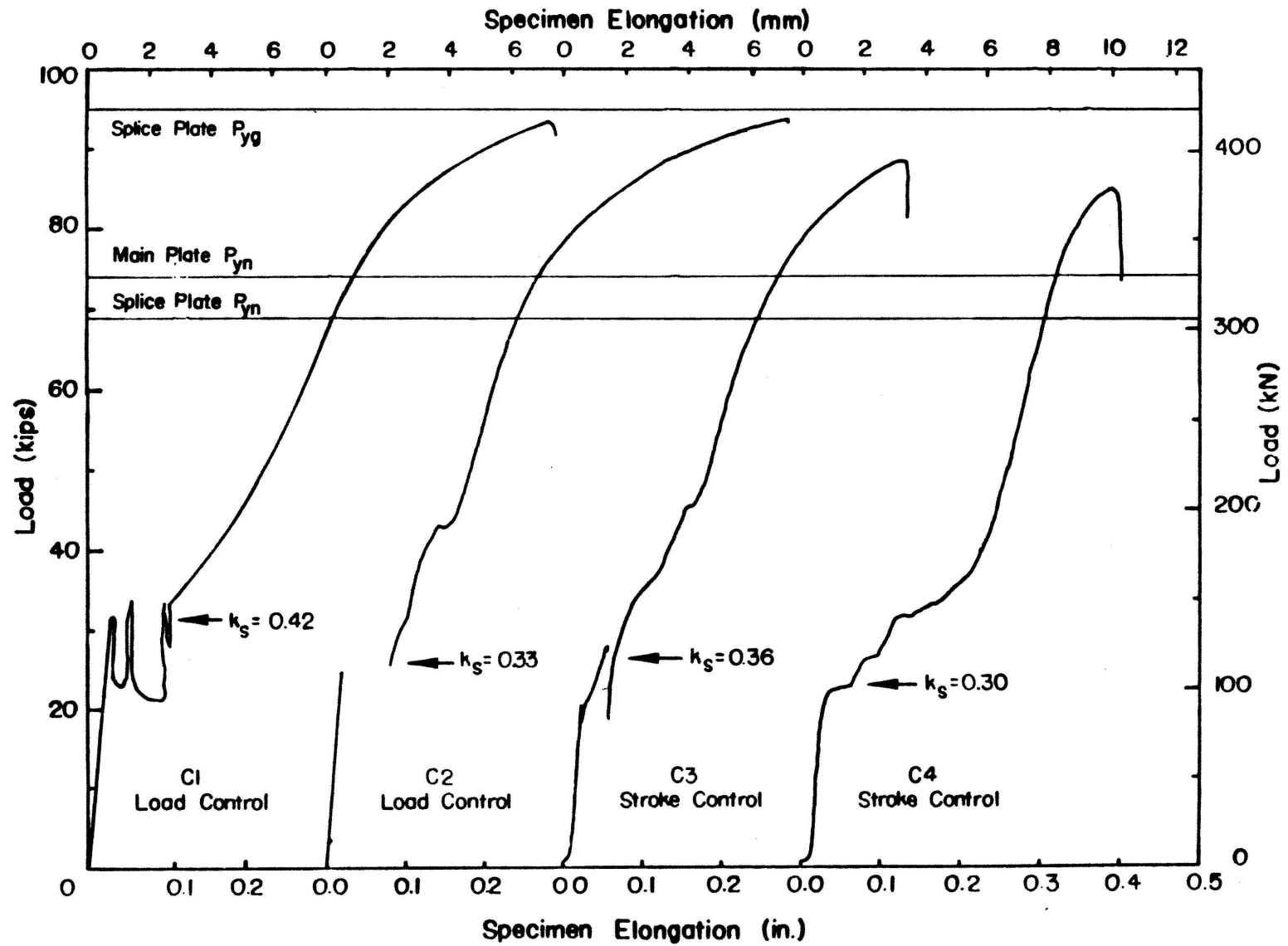


Figure 33: Load-elongation curves of nonbonded two-bolt splices C1-C4

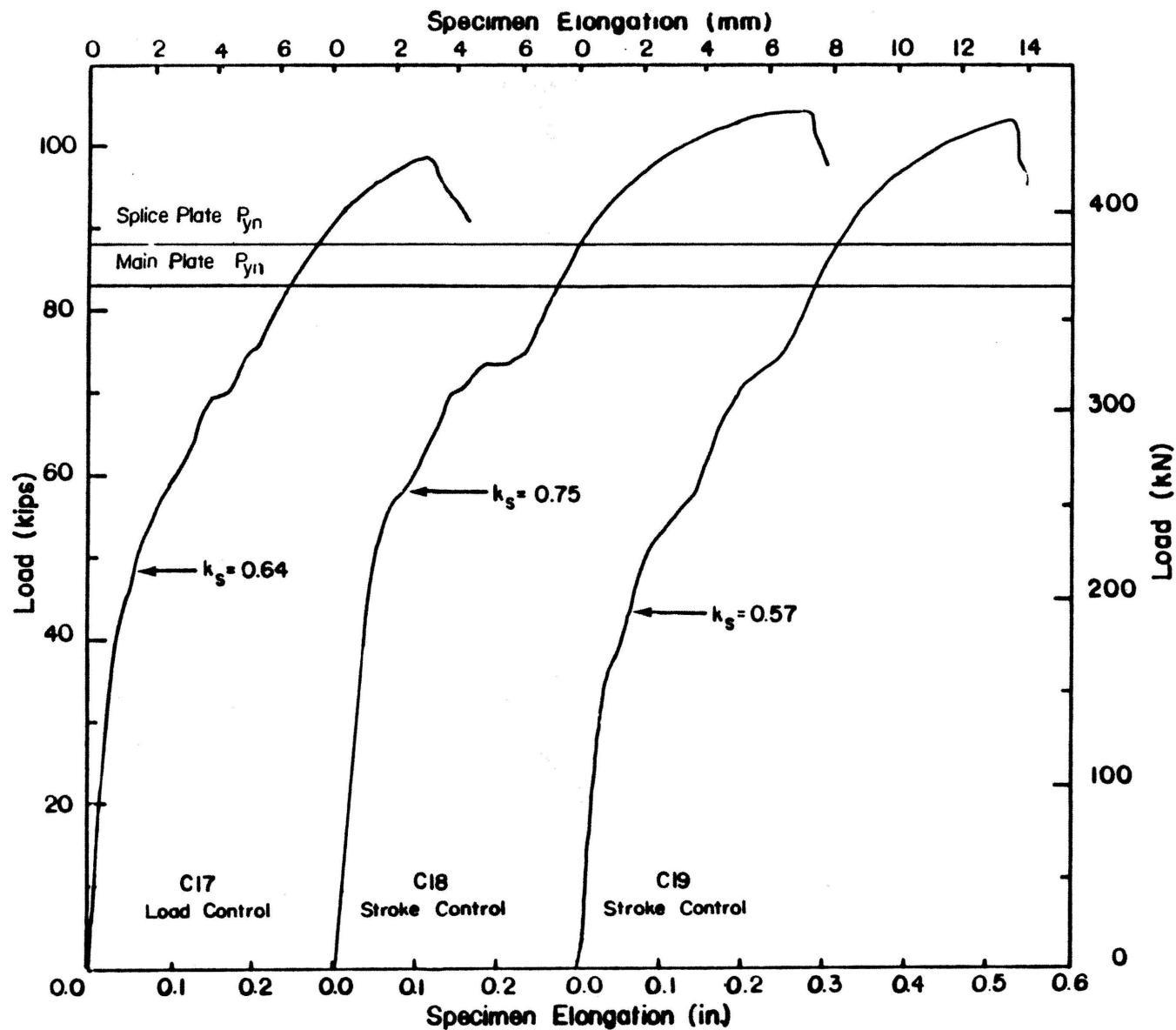


Figure 34: Load-elongation curves of nonbonded two-bolt splices C17-C19

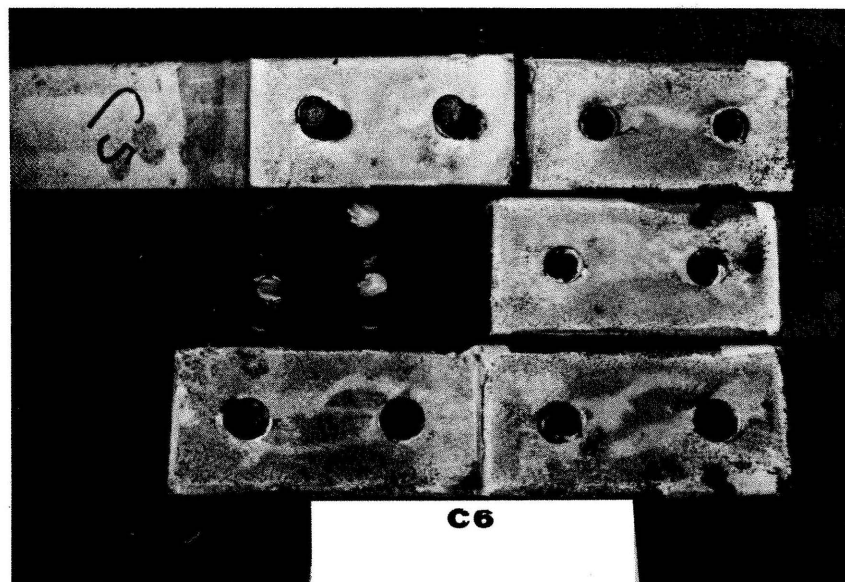
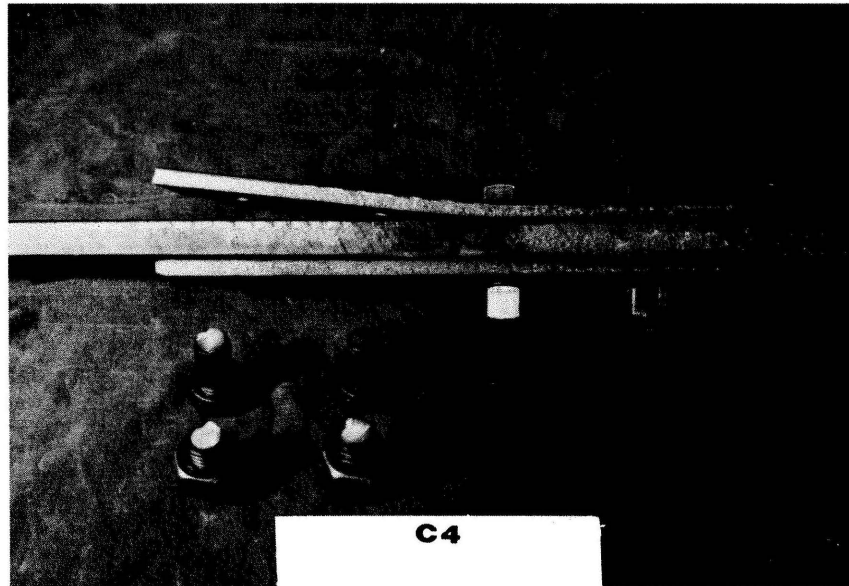


Figure 35: Typical Series C two-bolt splices at failure; specimen C4 (top) and C6 (bottom)

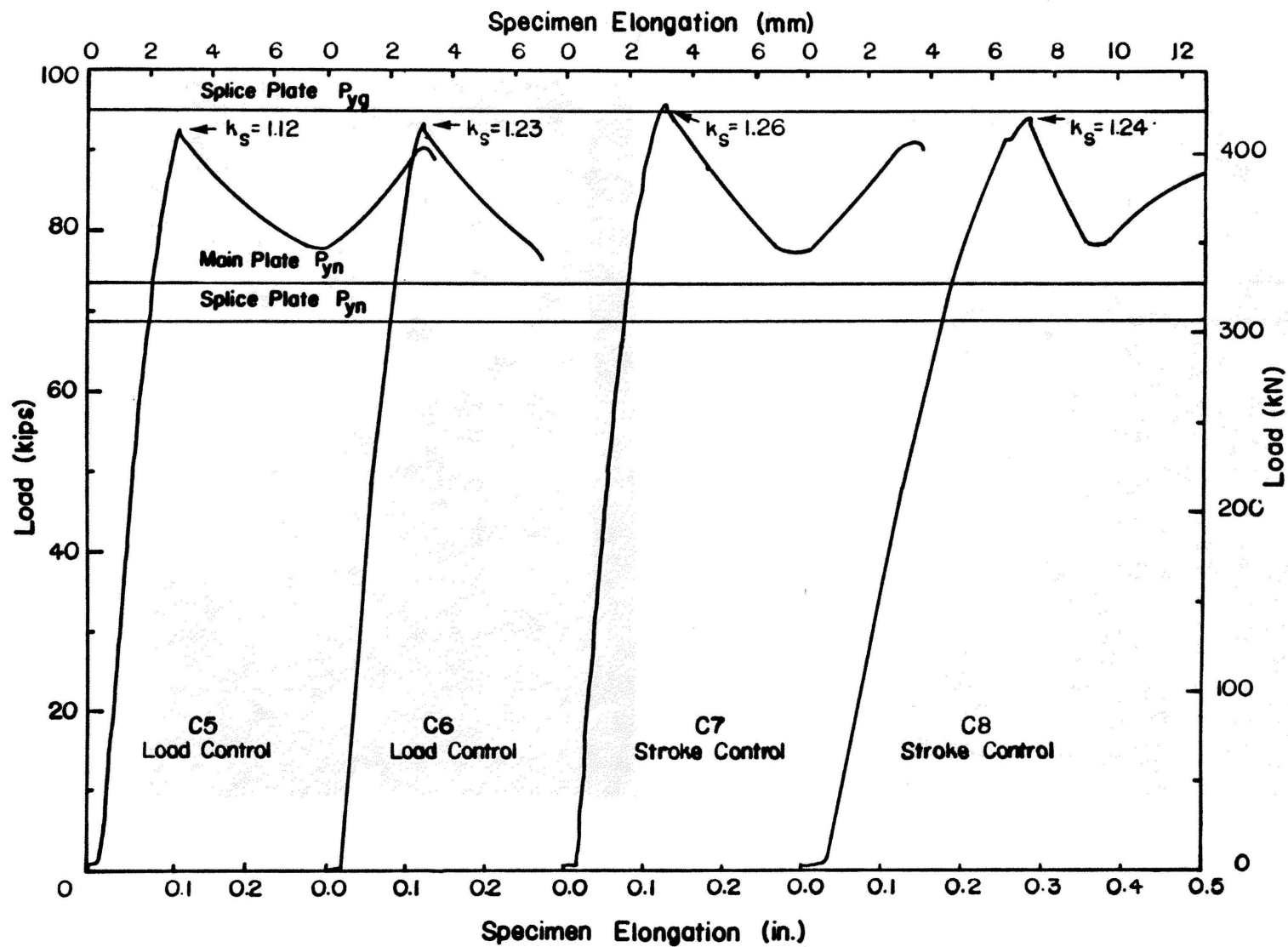


Figure 36: Load-elongation curves of bonded two-bolt splices C5-C8.

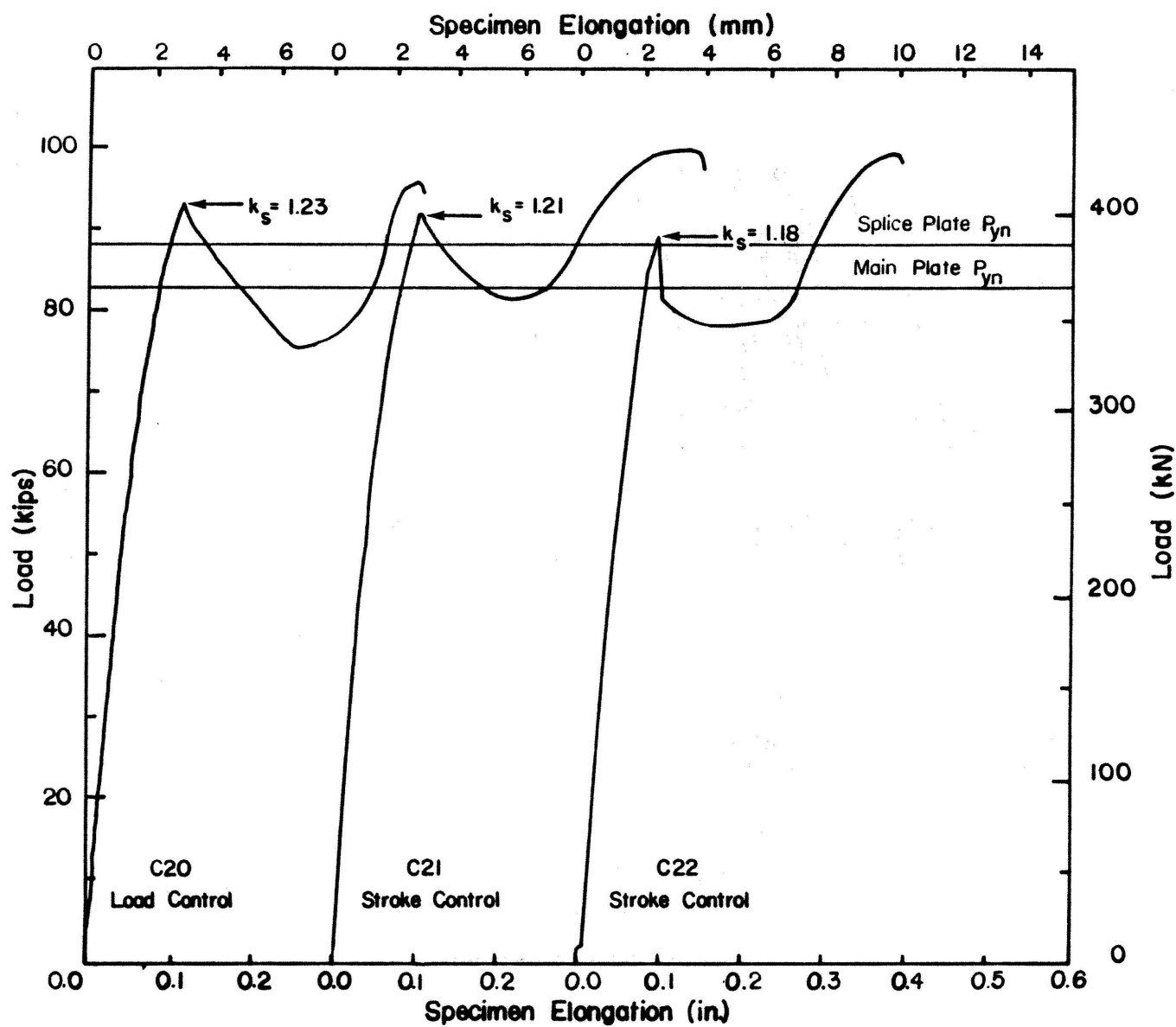


Figure 37: Load-elongation curves of bonded two-bolt splices C20-C22

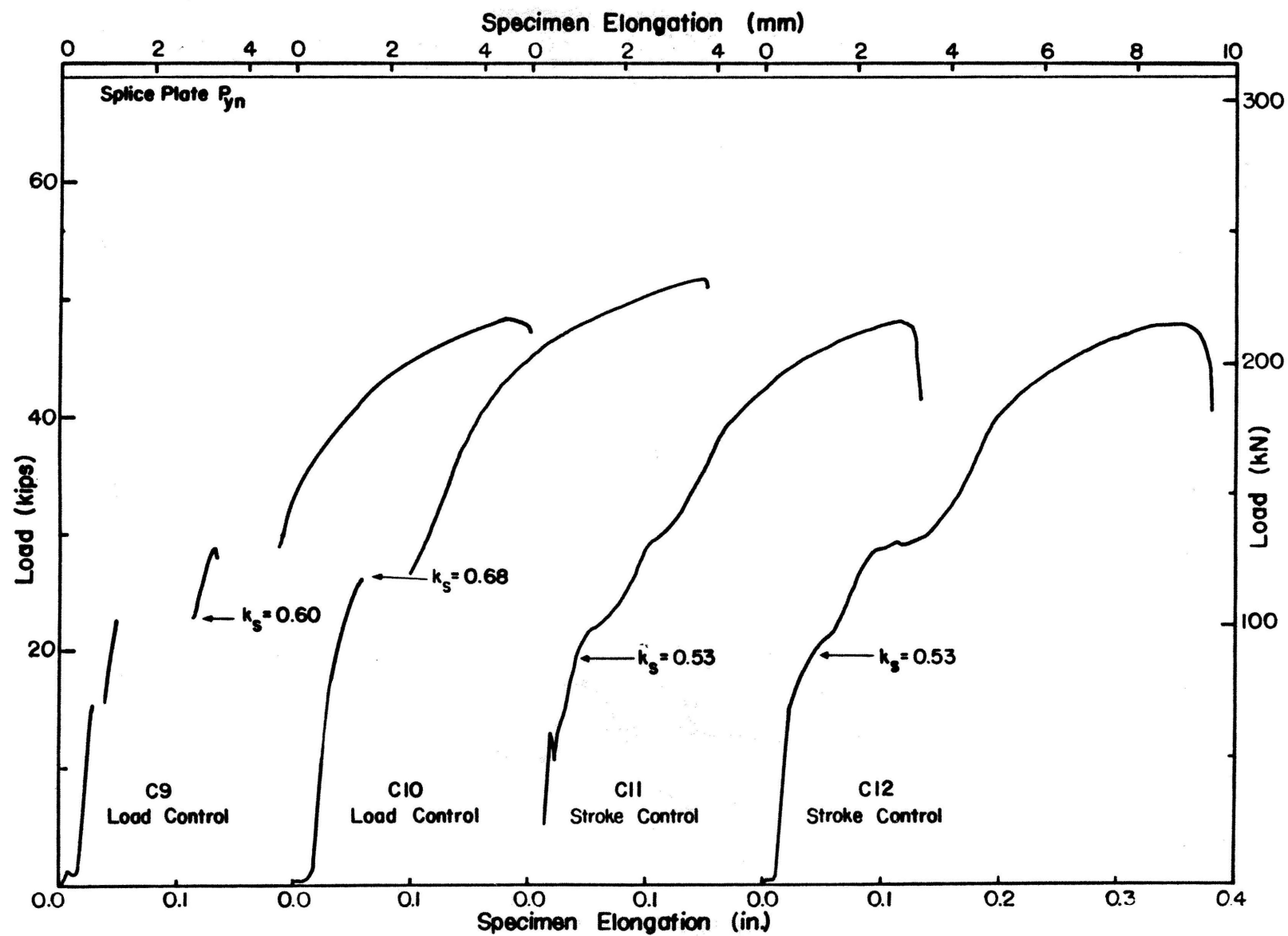


Figure 38: Load-elongation curves of nonbonded one-bolt splices C9-C12.



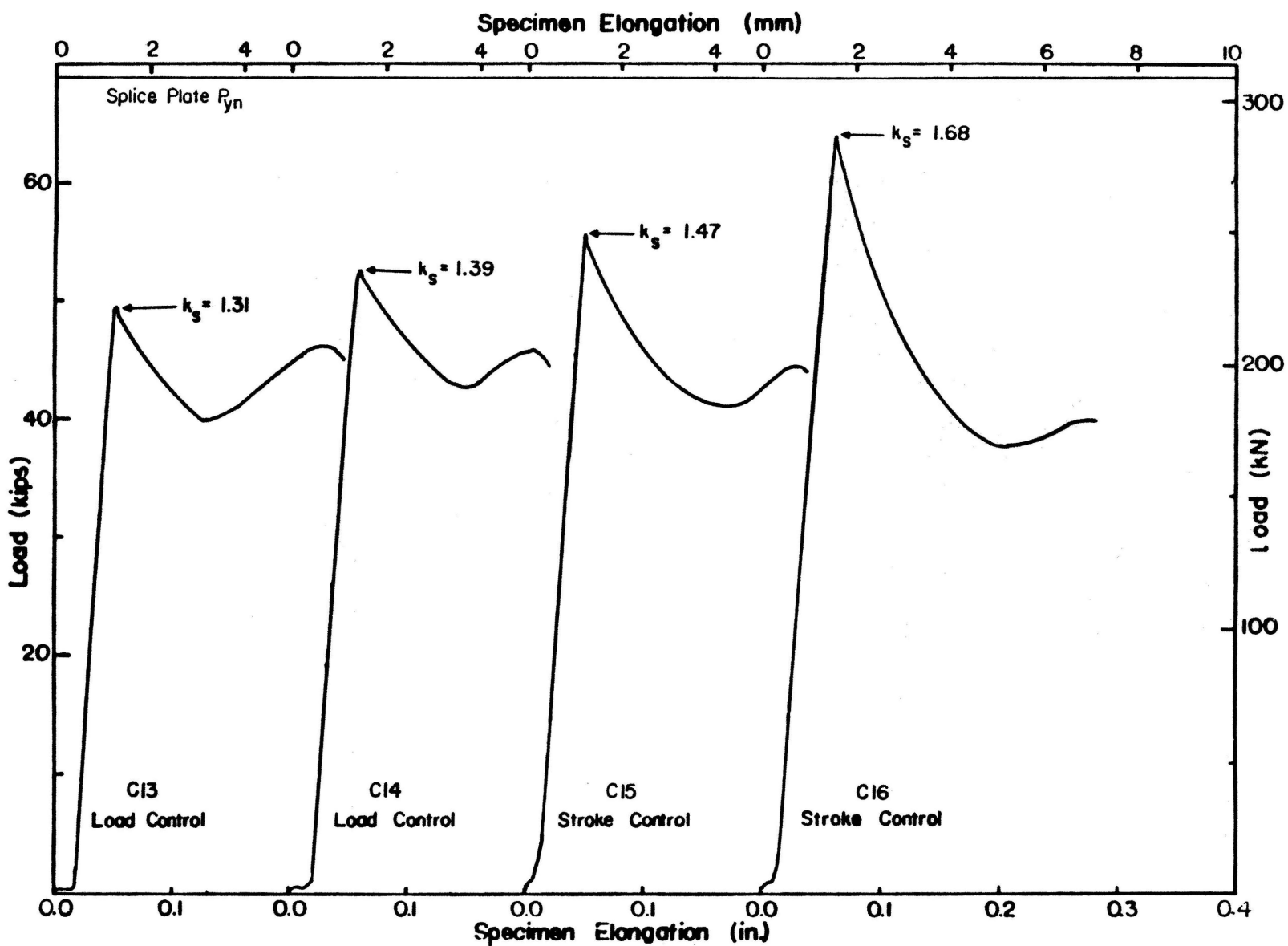


Figure 39: Load-elongation curves of bonded one-bolt splices C13-C16

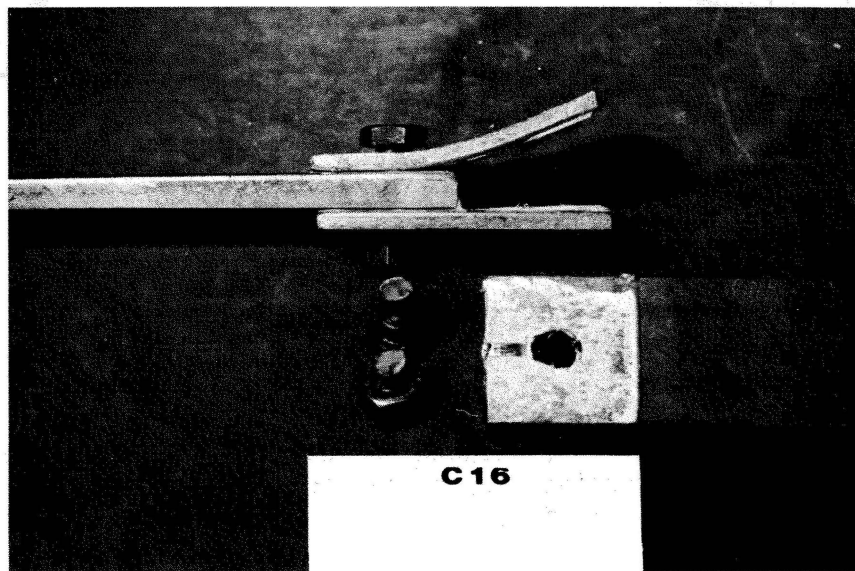
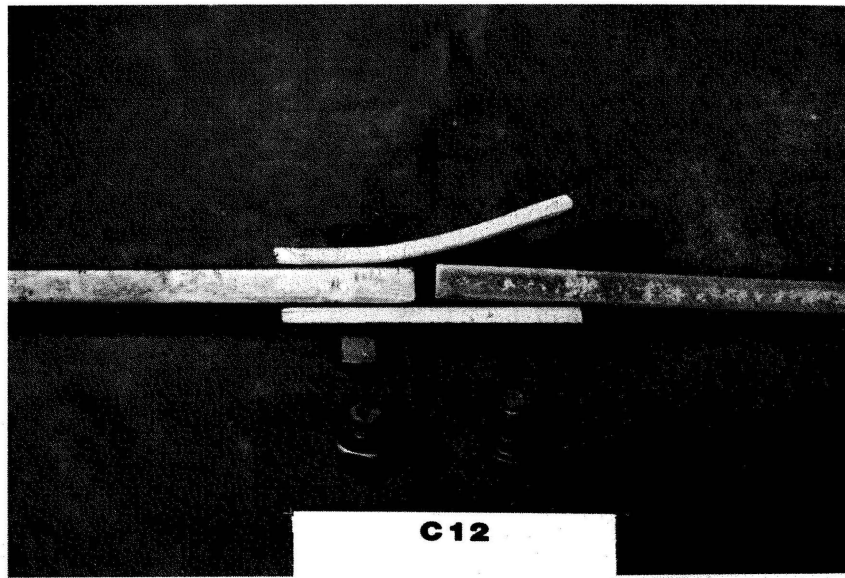


Figure 40: Typical Series C one-bolt splices at failure; specimen C12 (top) and C16 (bottom)

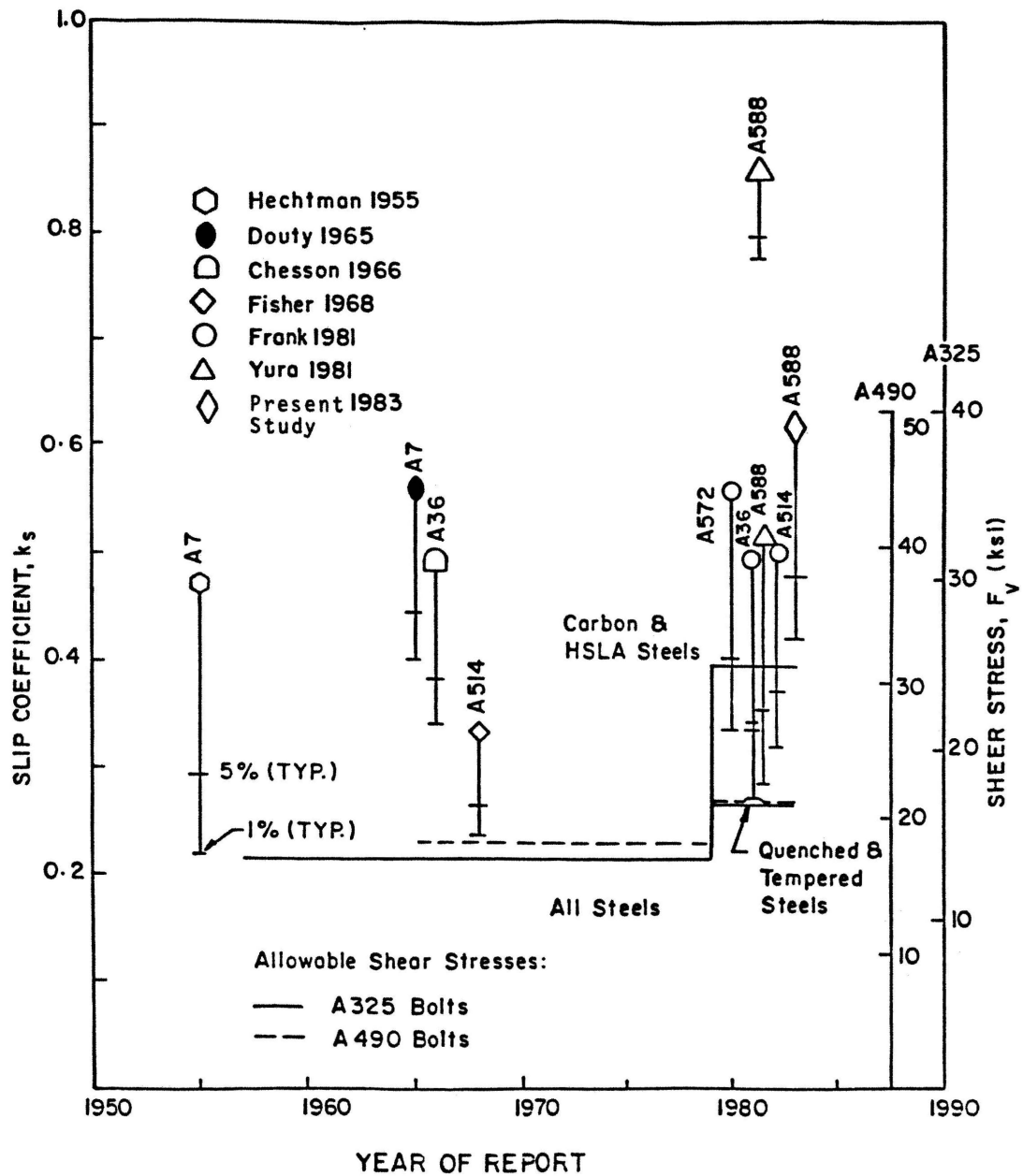


Figure 41: Slip coefficients and allowable shear stresses for friction-type bolted joints with blast cleaned surfaces

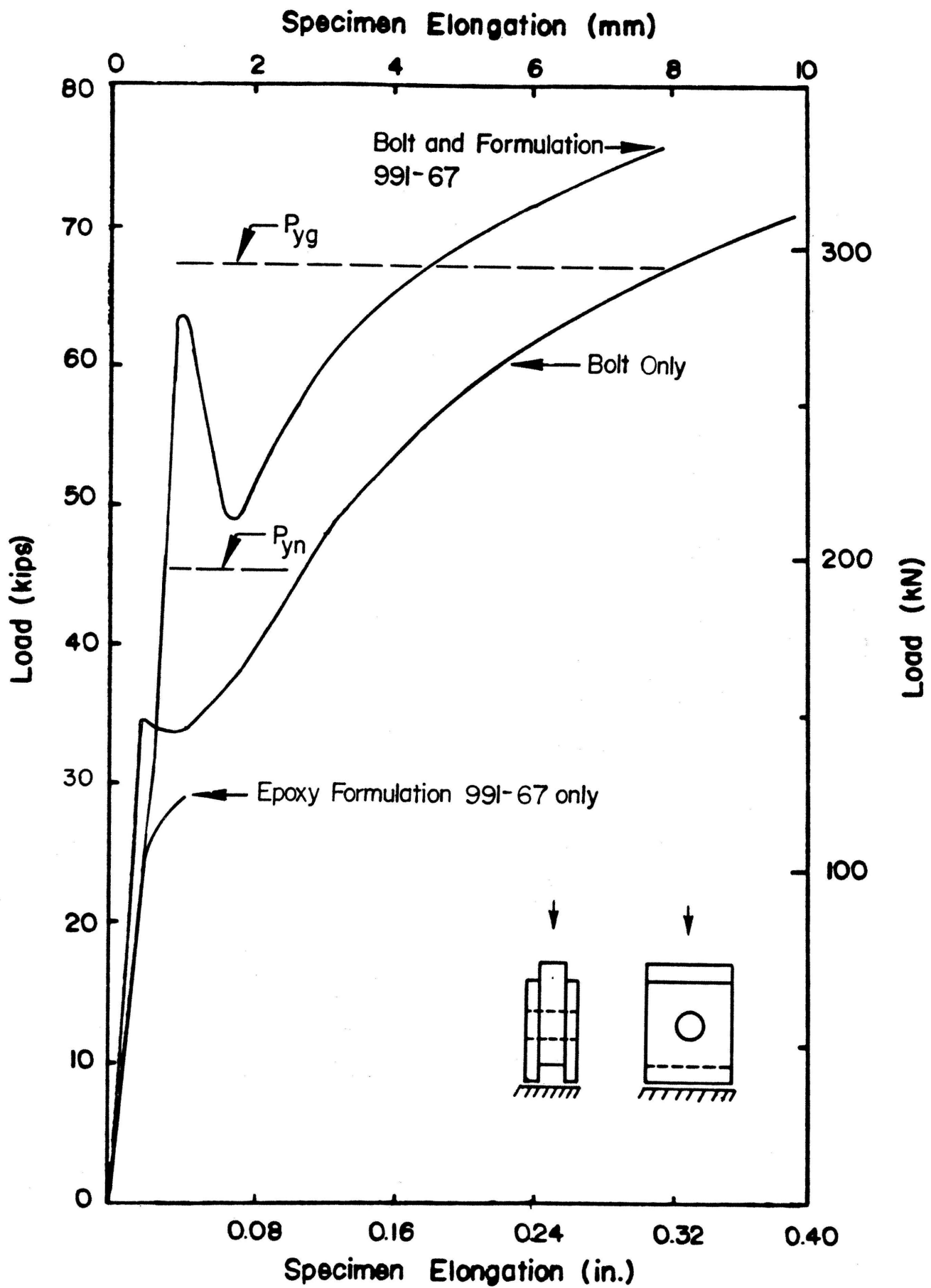


Figure 42: Load-elongation curves for shear tests (Ref. 3)

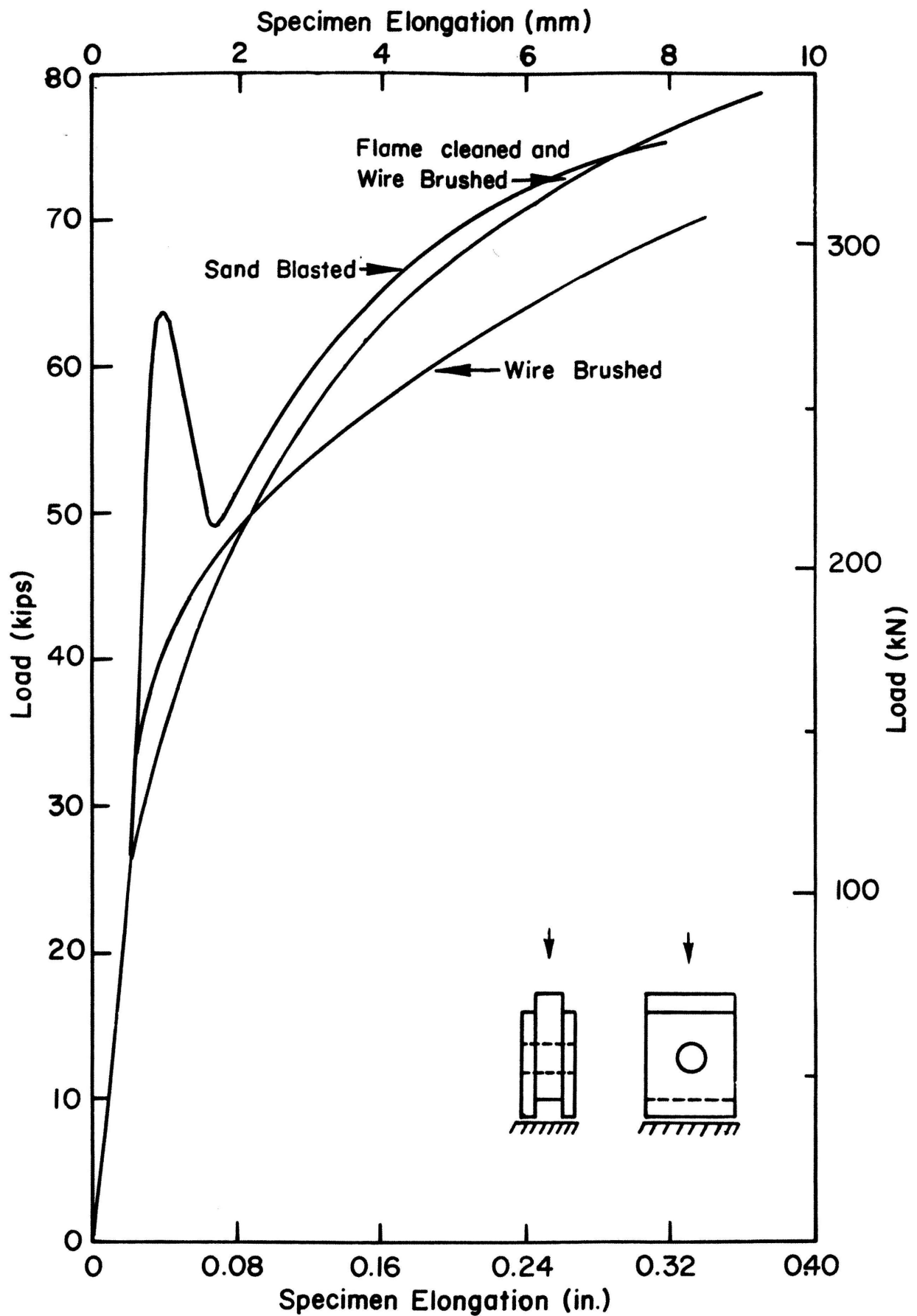


Figure 43: Load-elongation curves for shear tests with bolt and epoxy formulation 991-67 (Ref. 3)

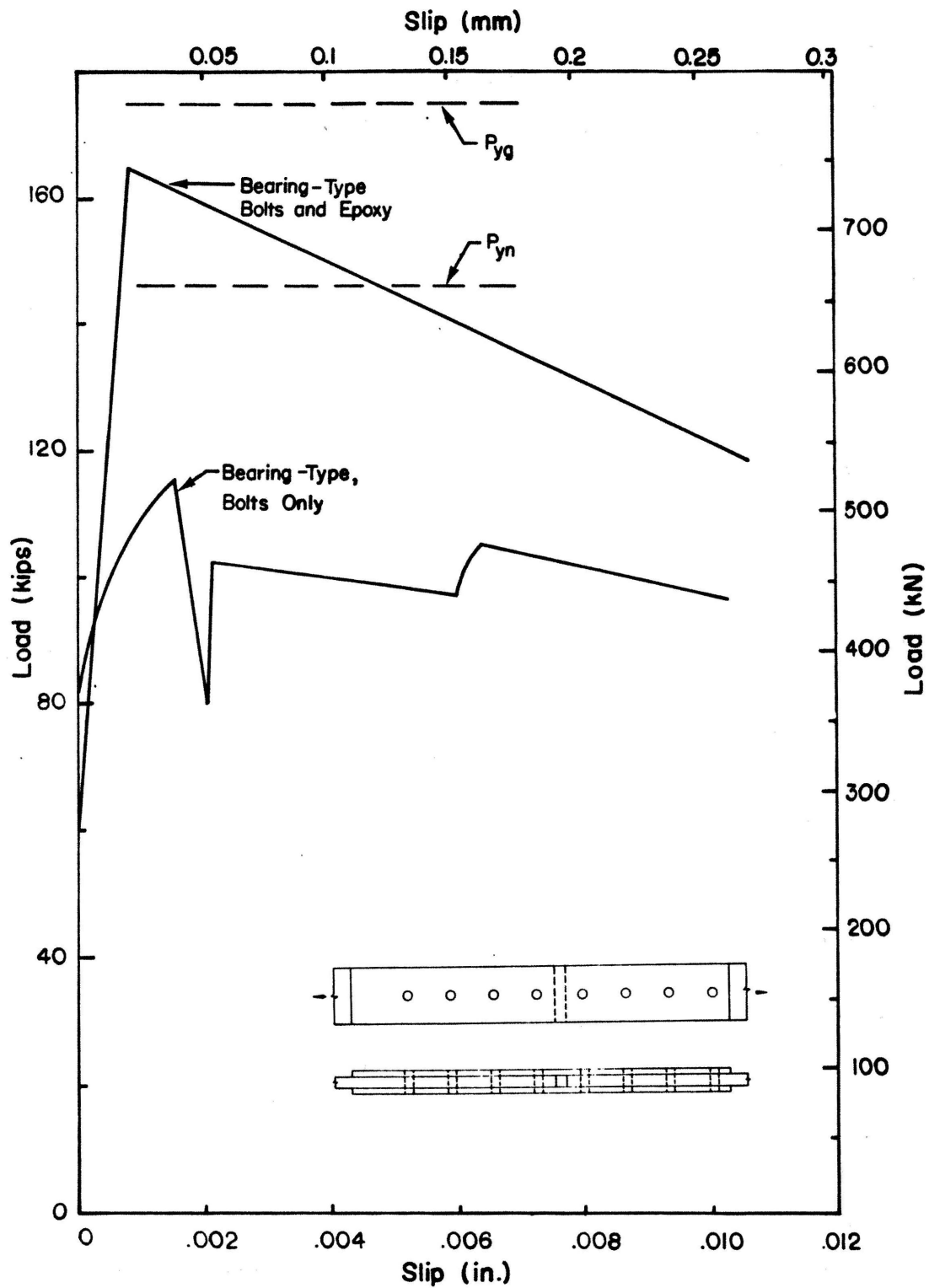


Figure 44: Load-slip curves for bearing-type specimens (Ref. 3)

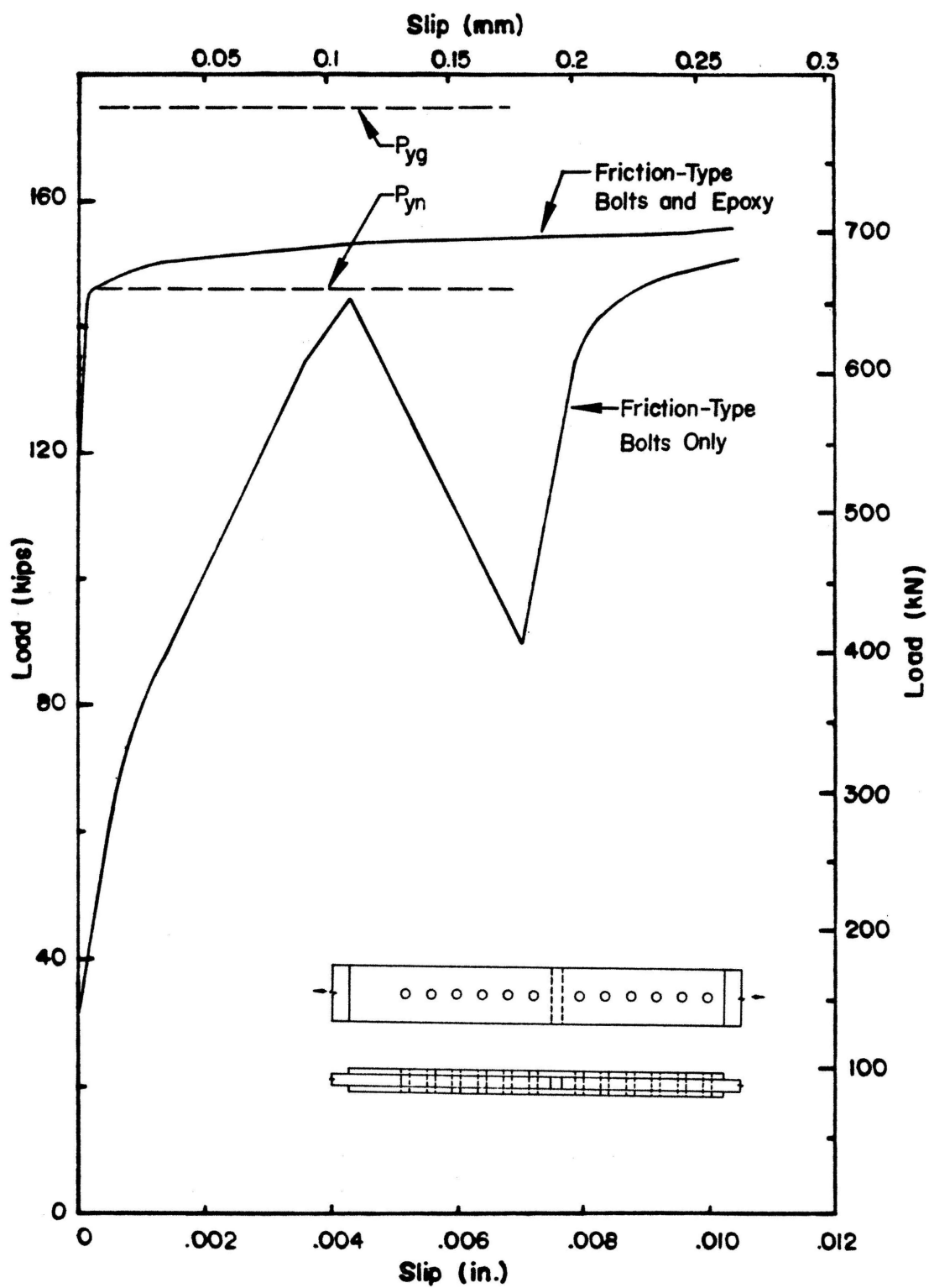


Figure 45: Load-slip curves for friction-type specimens (Ref. 3)

## CHAPTER 7: STATIC STRENGTH OF SERIES D BEAM SPLICES

### 7.1 Experiment Design

The experiment design, shown in Table 25, consisted of six beams with two-bolt, four-bolt, and six-bolt splices with contact surfaces either nonbonded or bonded. The beam specimens are shown in Fig. 2. The fabricator had ground off burrs around the bolt holes and the edges of the contact surfaces. This reduced the slip resistance of the nonbonded splice D1, which was tested first. The contact surfaces of the four-bolt and six-bolt splices were thereafter sand-blasted to restore the full contact area to blast cleaned condition.

### 7.2 Definition of Slip Coefficient

The slip coefficient,  $k_s$ , is given by:

$$k_s = \frac{M_s/d}{mnT_i} \quad (7.1)$$

where:

$M_s$  = measured slip moment

$d$  = beam depth

$m$  = number of shearing planes

$n$  = number of bolts

$T_i$  = initial bolt tension

The slip moment was determined from the load-slip curve for each splice half. All splices slipped suddenly.

### 7.3 Static Test Data

The static test data are presented in plots of: (1) applied load versus slip between flange and splice plate; and (2) applied load versus midspan deflection of the beam. The former (Figures 46 and



47) illustrates the slip behavior of each half of the splice. The letter (Figs. 48 to 50) illustrates the overall beam behavior.

For purposes of comparison, Figs. 48 to 50 show the theoretical load-deflection curve of a W 14 x 30 beam assuming elastoplastic behavior. Tick marks were drawn at the load levels corresponding to the ultimate shear strength of the bolt ( $F_{uv}$ ), yield moment of the beam net section ( $M_{yn} = F_y S_n$ ), yield moment of the beam gross section ( $M_y = F_y S$ ), and plastic moment of the beam gross section ( $M_p = F_y Z$ ). The ultimate bolt shear strength was calculated using an average shear strength of 62.5% of the tensile strength of A325 bolts,  $F_{uv} = 0.625 \times 120 = 75$  ksi (517 MPa), based on laboratory tests reported in Reference 30. The yield and plastic moments were calculated using the measured yield strength,  $F_y = 56.6$  ksi (390 MPa), given in Table 1.

The static test data for all beam splices are summarized in Table 26. The table lists for each splice the slip moment, slip coefficient, ultimate moment, and type of failure.

Slip Resistance of Nonbonded Splices: The load-slip curves for the two-bolt (D1), four-bolt (D3), and six-bolt (D5) nonbonded beam splices were plotted in Fig. 46. Splice D1, which had grinding marks on the contact surfaces, slipped into bearing at a slip coefficient,  $k_s = 0.38$ , comparable to the mean slip coefficient,  $\bar{k}_s = 0.352$ , for the two-bolt tensile splices C1-C4 with grinding marks given in Table 22.

Splices D3 and D5, whose contact surfaces were free of grinding marks had a mean slip coefficient,  $\bar{k}_s = 0.64$ , comparable to the mean slip coefficient,  $\bar{k}_s = 0.614$ , for their tensile splice counter parts (Table 22).

Slip Resistance of Bonded Splices: The load-slip curves for the two-bolt (D2), four-bolt (D4), and six-bolt (D6) bonded beam splices were plotted in Fig. 47.

Splices D2 and D4 exhibited about the same slip resistance with a mean of  $\bar{k}_s = 1.04$ . At first one would have expected that this value might be comparable to the mean for the bonded one-bolt tensile splices C13-C16,  $\bar{k}_s = 1.462$  (Table 22). All had low bolts-to-member strength ratios of  $M_b/M_m = 0.29$  and  $0.58$ , and  $P_b/P_m = 0.36$ , respectively; all slipped before the member net section yielded, suggesting that the slip occurred when the shear strength of the adhesive was exceeded. The mode of loading was the reason why the tensile splices failed at relatively higher shear stresses than the beam splices. The adhesive in the tensile splices was subjected to shear stresses. On the other hand, the adhesive in the beam splices was subjected to shear stresses plus cleavage stresses at the leading edge of the splice plate. The curvature of the beam and the splice plate's tendency to remain straight ahead of the first bolt row placed the adhesive under tension, a phenomenon commonly called cleavage. Cleavage stresses greatly reduce the shear strength of adhesives. This condition cannot be avoided in beam splices. But it can be mitigated by: (1) reducing the thickness and hence the flexural rigidity of the splice plate; and (2) adding inside splice plates that are forced to follow the curvature of the flange.

The slip coefficient of splice D6,  $k_s = 0.74$ , was lower than that of the other two splices. In this case net section yielding (Fig. 47) limited the slip resistance in a manner similar to that observed for the two-bolt tensile splices.

Ultimate Strength of Beam Splices: Figures 48 to 50, respectively, show the load versus midspan deflection curves of the beams with two-bolt, four-bolt, and six-bolt splices. Initially the curves rose at the calculated slope for a W14 x 30 beam. After the major slip occurred, all splices behaved as bearing type joints. Since the adhesive failed when the splices slipped, the ultimate strength was the same for the nonbonded and bonded beams. This behavior was the same as that of Series C tensile specimens.

The beams D1 and D2 with two-bolt splices failed when the bolts sheared at 102 and 108 ksi (703 and 745 MPa), respectively. The beams D3-D6 failed by local buckling of the compression flange when the moment between the loadpoints approached the plastic moment of the W14 x 30 beam at the measured yield strength of  $F_y = 56.6$  ksi (390 MPa).

The midspan deflection at failure of the beams with bonded splices was less than that of the nonbonded splices because the compression flange splices of the bonded beams did not slip during the test. The splice plate of the compression flange is forced to follow the curvature of the flange over its entire length. Hence the adhesive bond ahead of the first bolt row is not subjected to cleavage stresses as it would be in the splice plate of the tension flange.

Figure 51 shows the nonbonded and bonded four-bolt splices at the end of the test. The contact surfaces of the tension flange splices of these beams are shown in Figure 52.

#### 7.4 Comparison with Previous Work

The only data for high strength bolted moment connections found in the literature were those reported by Johnson, et. al,<sup>(34)</sup> and by Douty and McGuire.<sup>(32)</sup> The former were obtained from tests of

S10 x 25 beam splices with wire brushed contact surfaces. The results are not comparable to those from the present study because of the different surface conditions.

Douty and McGuire<sup>(32)</sup> tested eight W16 x 36 beams made of A7 steel with blast cleaned contact surfaces. The bolts-to-member strength ratios were  $M_b/M_m = 1.12$  to  $2.24$ . The mean slip coefficient and standard deviation of the seven splices that slipped into bearing were,  $\bar{k}_s = 0.560 \pm 0.068$ . This value was plotted with a solid symbol in Fig. 41. It compares well with all other data obtained from tensile specimen tests.

There are no previous data in the literature on bolted and bonded moment connections.

Table 25: Static test matrix for Series D beam splices

| Contact Surfaces | Two-Bolt Splice | Four-Bolt Splice | Six-Bolt Splice |
|------------------|-----------------|------------------|-----------------|
| Nonbonded        | D1 <sup>a</sup> | D3               | D5              |
| Bonded           | D2 <sup>a</sup> | D4               | D6              |

Note: a. Splices with grinding marks on contact surfaces.

Table 26: Static test data for Series B beam splices

| Specimen No. | Contact Surfaces | No. of Bolts in Splice | Slip Moment (kip.in) | Slip <sup>a</sup> Coefficient $k_s$ | Ultimate Moment (kip.in) | Type of Failure     |
|--------------|------------------|------------------------|----------------------|-------------------------------------|--------------------------|---------------------|
| D1           | Nonbonded        | 2                      | 293<br>293           | 0.38<br>0.38                        | 1,248                    | Bolts sheared       |
| D2           | Bonded           | 2                      | 780<br>780           | 1.00<br>1.00                        | 1,326                    | Bolts sheared       |
| D3           | Nonbonded        | 4                      | 854<br>854           | 0.55<br>0.55                        | 2,457                    | Lateral instability |
| D4           | Bonded           | 4                      | 1,677<br>1,747       | 1.08<br>1.13                        | 2,340                    | Lateral instability |
| D5           | Nonbonded        | 6                      | 1,691<br>1,755       | 0.73<br>0.75                        | 2,570                    | Lateral instability |
| D6           | Bonded           | 6                      | 1,716<br>1,950       | 0.74<br>0.84                        | 2,496                    | Lateral instability |

Conversion factor: 1 kip in = 0.113 KN m

Notes: a. Slip coefficients were determined for each half of the splice.

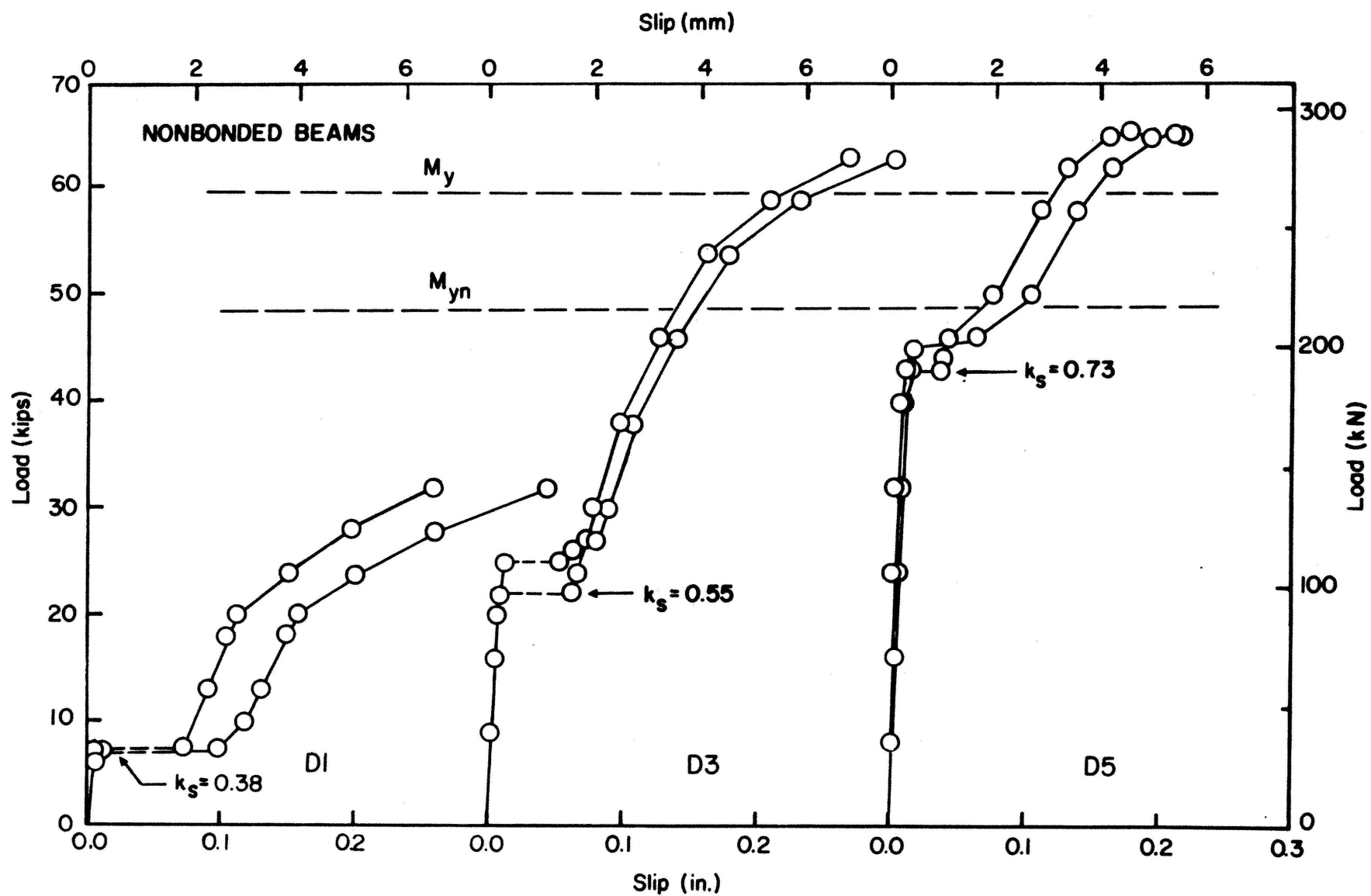


Figure 46: Load-slip curves of nonbonded beam splices

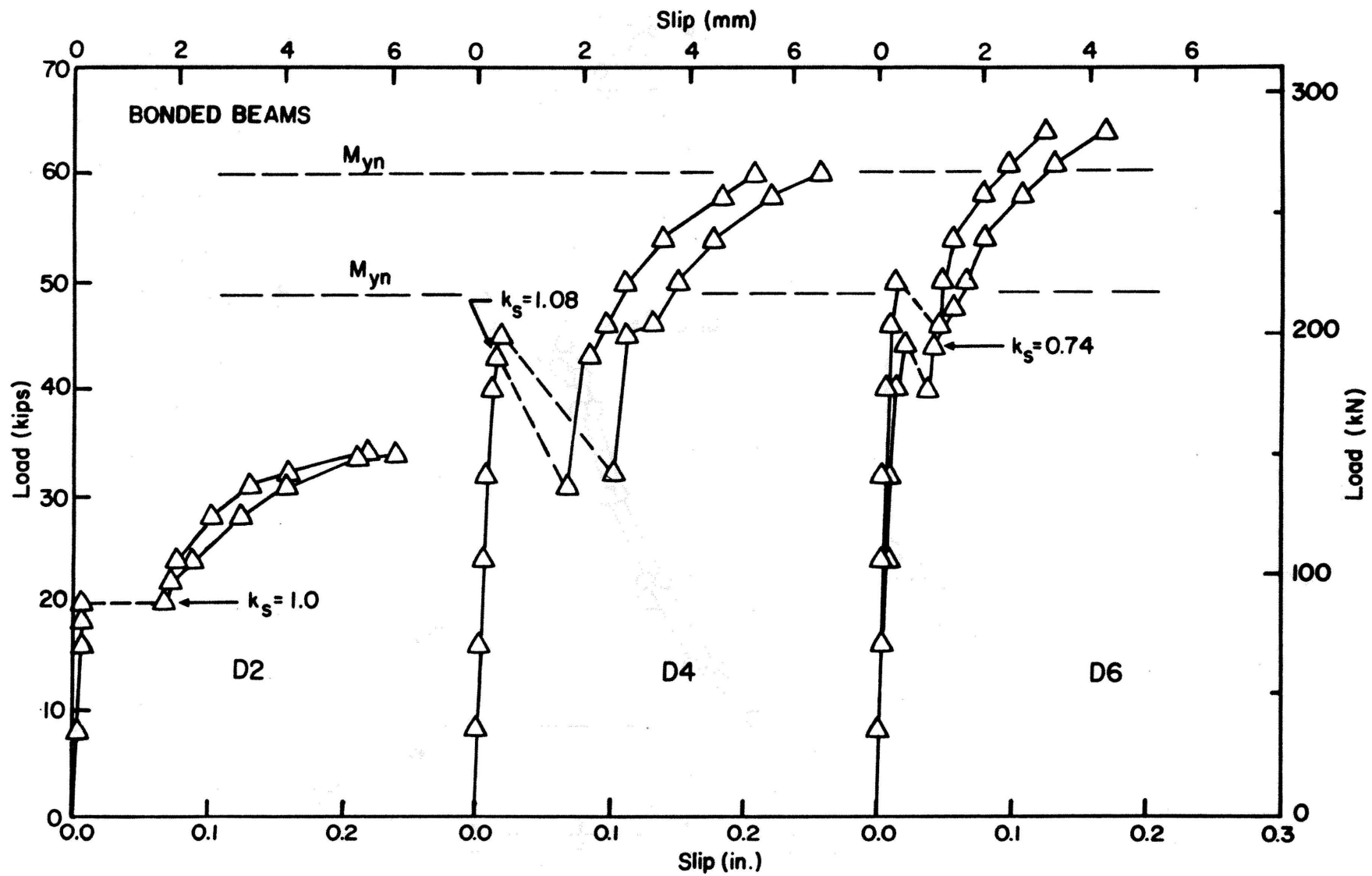


Figure 47: Load-slip curves of bonded beam splices



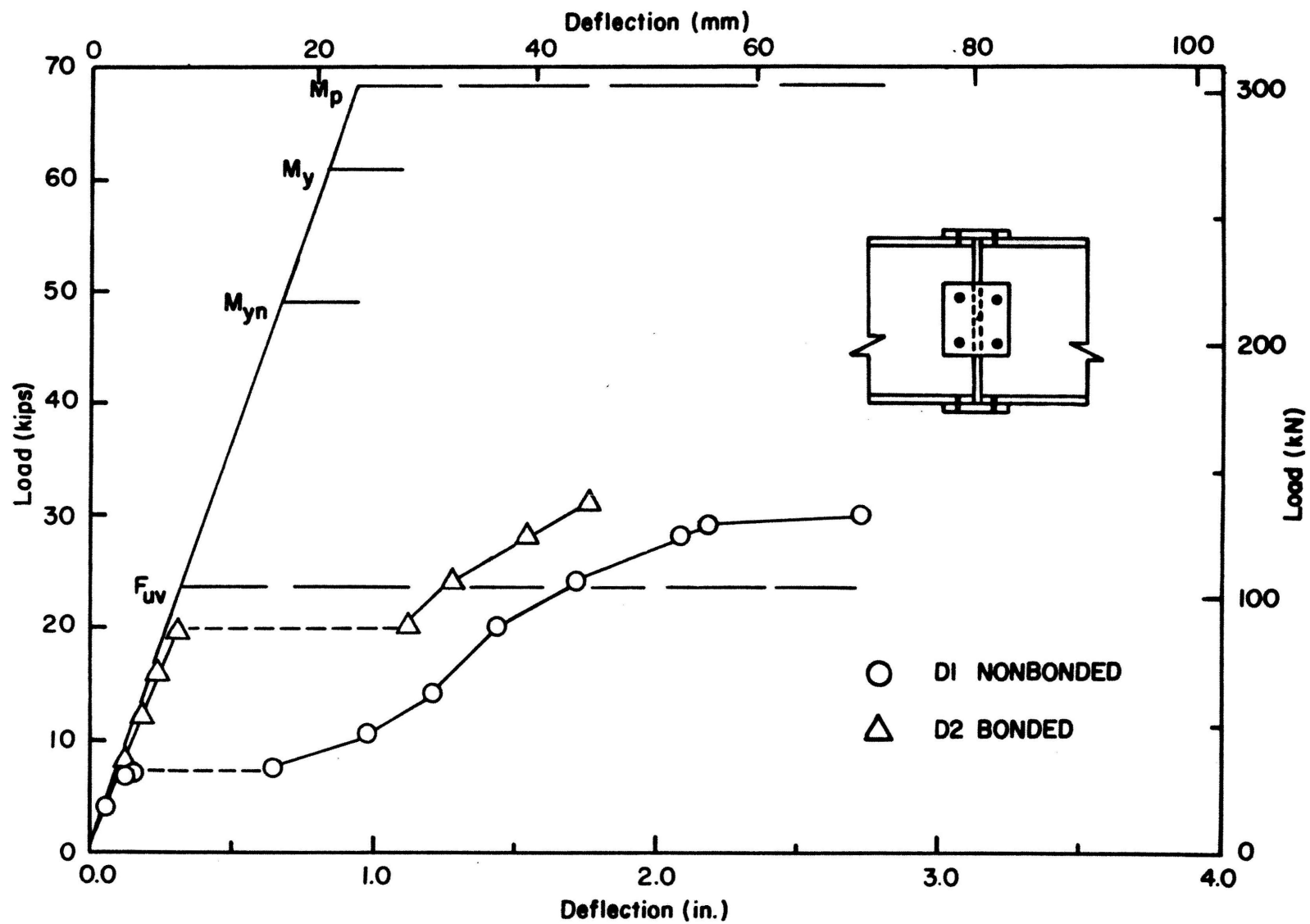


Figure 48: Load-deflection curves of two-bolt beam splices

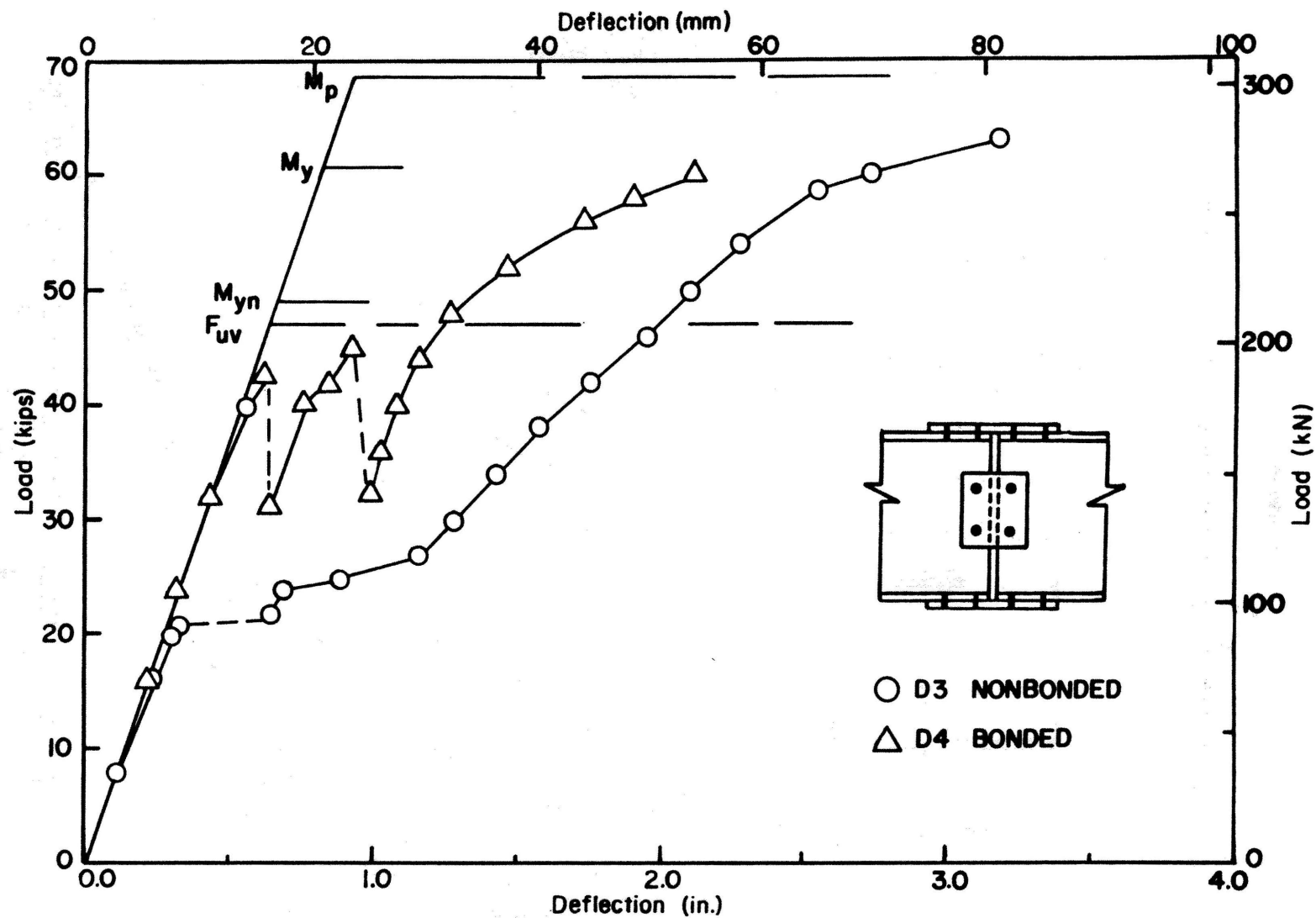


Figure 49: Load-deflection curves of four-bolt beam splices

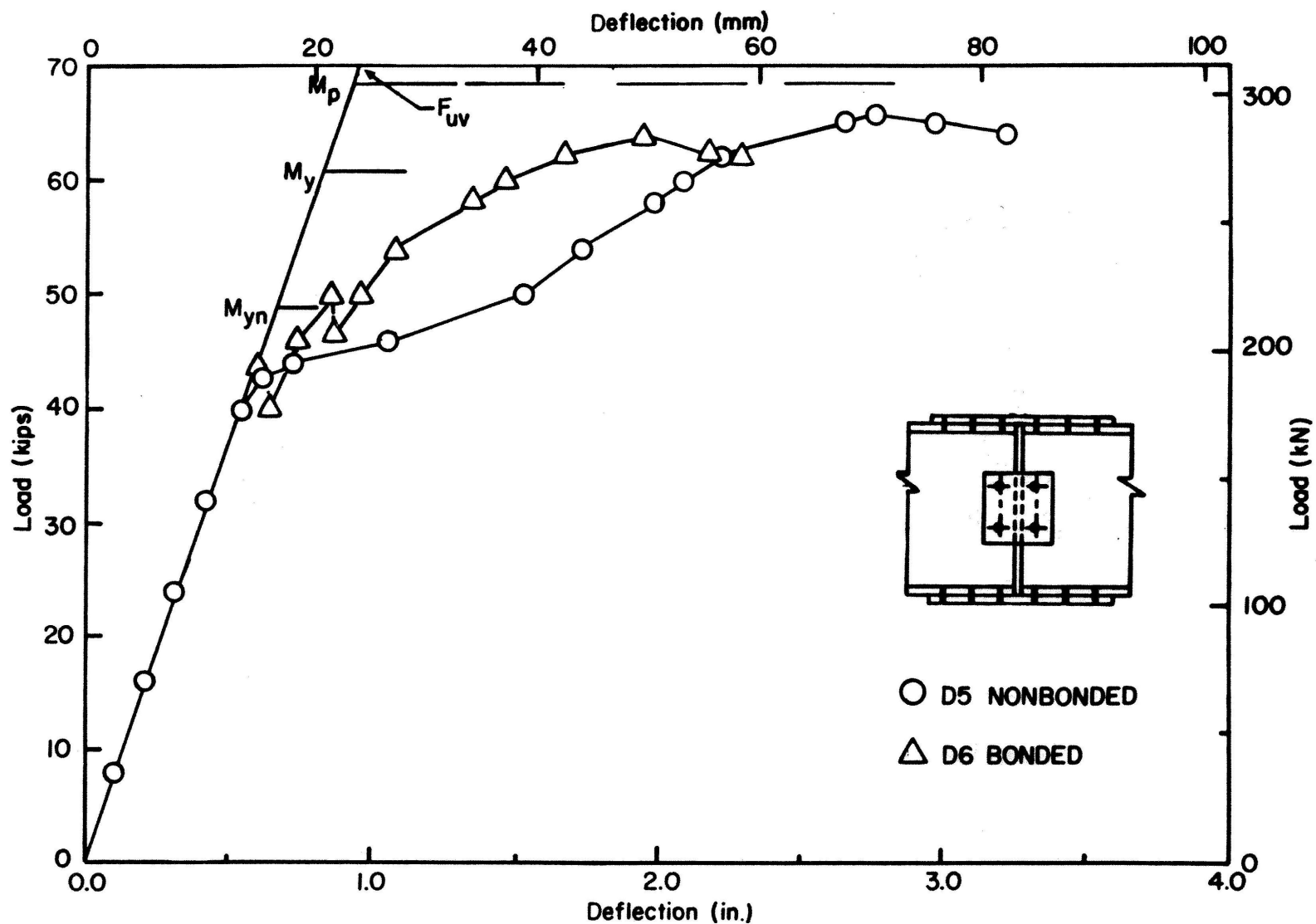


Figure 50: Load-deflection curves of six-bolt beam splices

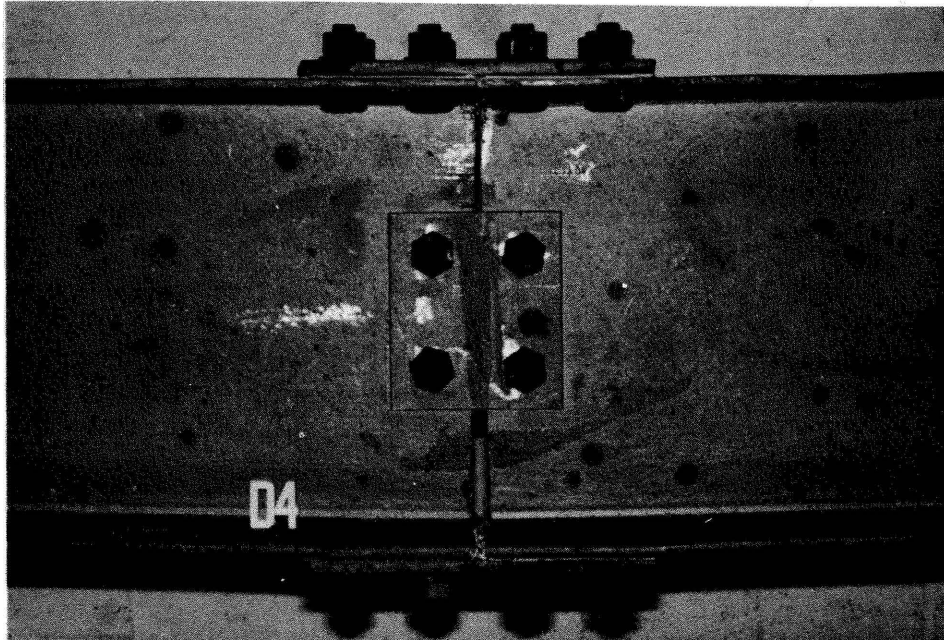
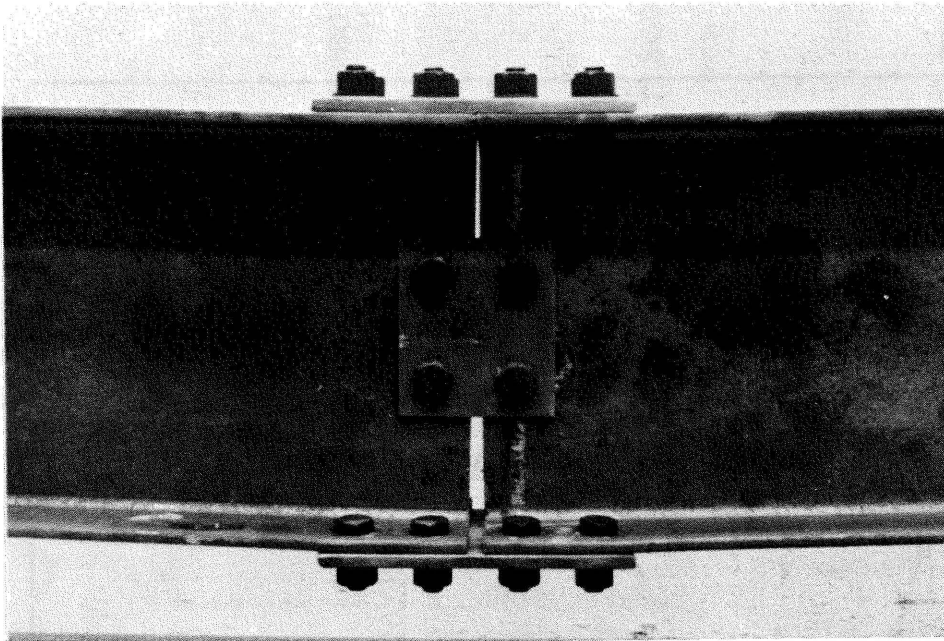


Figure 51: Four-bolt beam splices at end of test;  
Splice D3 (top) and D4 (bottom)

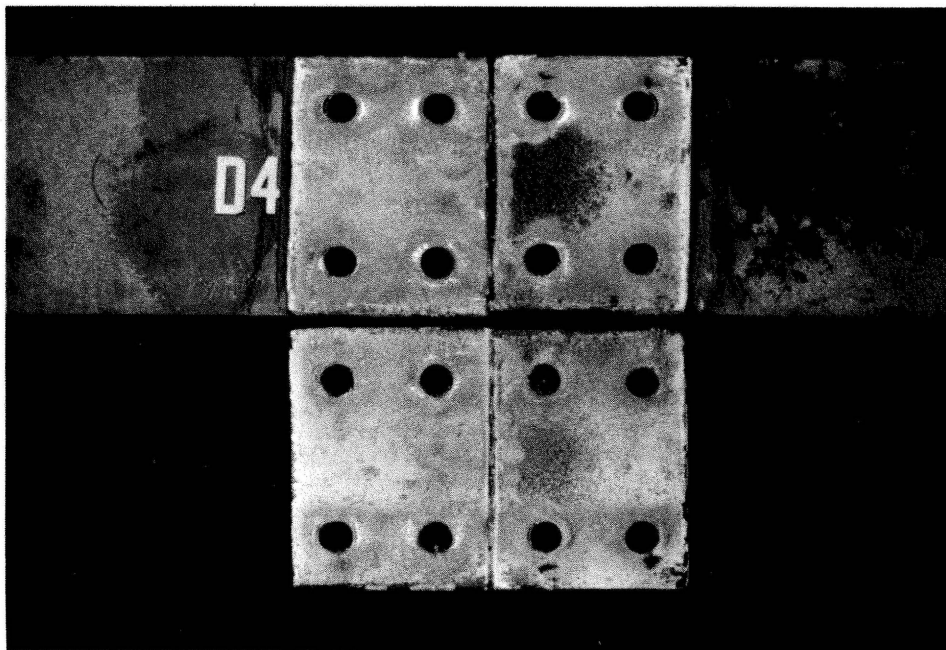
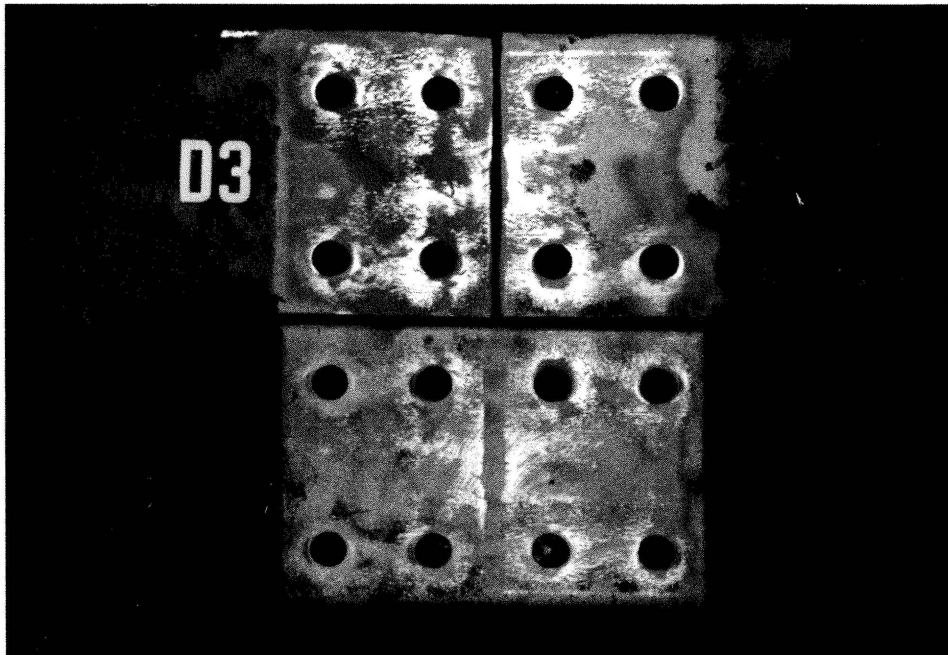


Figure 52: Tension flange contact surfaces of beam splices D3 (top) and D4 (bottom)

## CHAPTER 8: CREEP STRENGTH OF SERIES E TENSILE SPECIMENS

### 8.1 Experiment Design

The experiment considered three main variables: shear stress, environment, and lap length. Table 27 shows the test matrix, and Fig. 3 the double-strap test specimen. The objectives were to determine: (1) the shear stress reduction needed to avoid creep failure; (2) the effect of outdoor environment; and (3) the effect of lap length on creep behavior.

Stress levels were set at 20% intervals at higher stresses (down to 60% of maximum), and then at 10% intervals at the lower stresses as the creep threshold was approached. Using indoor and outdoor environments gave a simple comparison to observe the effect of service environments. The short lap lengths, 1/2 in (13 mm) and 1 in (25 mm), kept testing loads within the capacity of the small spring-loaded frames that were used for the tests of longer duration. At each combination of the three variables (each cell of the test matrix), at least three specimens were tested to allow for statistical and material variations. At stress levels above 50% of maximum shear stress, failures occurred too quickly to make outdoor tests meaningful. In the indoor environment, tests below 30% stress level would not have failed before the end of the project.

### 8.2 Creep Measurements

Creep displacement and air temperature were periodically measured during all 50% to 30% indoor tests and 40% to 20% outdoor tests.

Creep was measured by extending a depth micrometer, accurate to 0.0005 in (0.013 mm), through holes on either side of the cross bar down to the top plates and recording changes in spring length. Subsequent calculations revealed that these changes in spring length caused load reductions of up to 8% of the original load before the specimen failed. Early measurements with an electronic thermometer showed that, even in midday sun, the temperature of the steel specimens differed no more than 2°F (1°C) from the air temperature. Thereafter, only air temperature was recorded.

After each specimen failed, the length and width of the failed bonds were measured with calipers, accurate to 0.0005 in (0.013 mm). The mean shear stress on the adhesive was then calculated, dividing the recorded load by the bonded area. This gave the shear stress value recorded in the tables and figures.

### 8.3 Creep Test Data

Creep Strength: Tables 28 and 29 give the pertinent information on all creep specimens tested indoors and outdoors, respectively. The specimen number consists of a batch number (for each batch of adhesive mixed), and then a sequence number within that batch. Specimens were grouped by lap length and nominal stress level.

Adhesives can fail in adhesion or in cohesion. Adhesion failures occur between the adhesive and the face of the adherend. Cohesive failures occur within the adhesive itself. All specimens in the creep tests failed mainly in adhesion, most of them at the face of the main adherend with the adhesive remaining on the strap piece, as shown in Fig. 53a. The few that failed along both metal surfaces usually failed along the main adherend surface near the end of the main adherend,

and along the strap surface near the end of the strap (Fig. 53b). The small percentages of cohesive failure shown in the tables represent observations of small specks of adhesive remaining on the metal surfaces (Fig. 53c).

The shear stress values in the tables give an average stress over the bond area, assuming a uniform stress in the bond. This assumption is reviewed in Section 8.4. In the 100% tests, specimens with a 1/2-in (13 mm) lap length had a mean shear stress of 3,890 psi (26.8 MPa), with a standard deviation of 330 psi (2.3 MPa). Those with a 1-in (25 mm) lap had a 4,050-psi (27.9 MPa) mean and 300-psi (2.1 MPa) standard deviation. The difference between the two means was statistically insignificant at the 5% level. For convenience, an ultimate strength value of 4,000 psi (27.6 MPa) was used to determine the actual stress level, expressed as a percentage in Column 7 of Tables 28 and 29.

In the longer duration tests, specimens were observed periodically for failures. When failure occurred between two observations, it was assumed to have occurred midway between the observations. Figure 54 shows shear stress and time to failure plotted on a semi-log graph. The time to failure increased with decreasing stress, as expected. The 1/2-in (13 mm) and 1-in (25 mm) lap lengths gave similar results in terms of shear stress, indicating that the differences in lap length were too small to show the effect of shear stress distribution on bond creep strength.

Environment had a substantial effect on the time to failure. The tests indicated that temperature, in particular, greatly decreased the creep strength of the adhesive. The outdoor specimens tested at



50%, 40% and 30% stress levels failed much more quickly than the indoor specimens tested at the same levels (Fig. 54). These three sets of tests were performed during the summer, with temperatures reaching as high as 106°F (41°C) on the roof where the outdoor specimens were placed, while the indoor temperatures remained at about 80°F (26°C).

To verify that temperature had a great effect on creep strength, two more specimens (Nos. 47-4 and 49-4) were set outdoors on January 4, 1983. These specimens, tested at 40% stress level, lasted on average 1,512 hours, whereas their counterparts exposed on July 19, 1982 had lasted 1 hour (No. 38-3) to 39 hours (No. 39-1). The data points for the two specimens exposed outdoors during the cold winter months fell inside the data band for the indoor tests (Fig. 54), suggesting that temperature was indeed the environmental factor responsible for the short creep lives of the outdoor specimens.

Creep Rate: Figs. 55 through 58 show creep displacement vs. time for several longer duration tests, with temperature and relative humidity (outdoor tests only) plotted below. Relative humidity and night temperatures for the outdoor tests were obtained from local climatological data at Washington National Airport.<sup>(35)</sup> The creep displacement for each specimen is plotted as an individual line and labeled with specimen number and lap length in parenthesis. The dashed line at the end represents the unknown behavior from the last measurement until failure. The creep values shown represent total creep displacement. Since a double strap joint has two lap details, the creep in each adhesive bond area can be approximated by dividing the total creep in half. Using a bond-line thickness of 0.010 in (0.25 mm), the shear strain can be approximated by  $\gamma = \arctan \left[ C_T / (2 \times 0.010 \text{ in}) \right]$ .

where  $C_T$  is the total measured creep displacement.

Figures 55 and 56 show indoor creep rates, while Figs. 57 and 58 show outdoor rates. The indoor specimens (Figs. 55 and 56) exhibited steady creep rates, though the rates vary from one specimen to another, as the temperature remained relatively constant. The outdoor specimens (Fig. 58) showed excessive creep following the day-night temperature fluctuations. The rates increased during daytime highs and decreased markedly during nighttime lows. In the 40% outdoor tests (Fig. 57), the one specimen that lasted through the first day and night also showed this step-like behavior. Figures 56 and 57 show the difference in creep rate between the indoor and outdoor tests at the 40% stress level. Even with time scales differing by a factor of 25, the slopes of the daytime curves of the outdoor specimens are much steeper than those of the indoor specimens. In the long-duration low stress level tests, the temperature effect continued to show itself as creep rates dropped with the coming of cooler fall and winter weather.

Humidity did not appear to have a detrimental effect on creep behavior. In fact, creep rates appeared to increase when humidity decreased (Figs. 57 and 58), the opposite of what would be expected. This must be due to the overriding effects of temperature. As temperature increases, relative humidity decreases. Any potential effects of humidity were hidden by the much larger effect of temperature.

The tests did not reveal a threshold stress level, below which no creep occurred. They indicated that such a threshold level depends on the environment. Previous studies have proposed that proper joint design can produce a bond that will not creep. This is discussed further in the next section.

#### 8.4 Comparison with Previous Studies

Temperature: Previous studies concur with the present findings that temperature radically affects the behavior of adhesives. Rioux pointed out that one must know the glass transition temperature ( $T_g$ ) of an adhesive, that is the temperature at which it changes from a glassy to a flexible state, in order to accurately predict its structural behavior.<sup>(36)</sup> A closely related property, the heat deflection temperature (HDT), is the temperature at which a beam spanning 4 in (100 mm) deflects 0.01 in (0.25 mm) under a constant stress of 264 psi (1.820 MPa).<sup>(37)</sup> Within the transition zone near the  $T_g$  and the HDT, all mechanical and physical properties change drastically. Rioux specified that adhesives used for structural bonding should have an HDT 25°F (14°C) to 40°F (22°C) above the maximum service temperature.<sup>(36)</sup> Information on the HDT of Versilok 201 was not available from the manufacturer, nor was it determined in the present study.

Other sources indicate that the HDT for acrylics ranges from 165°F (74°C) to 212°F (100°C).<sup>(38)</sup> This would satisfy Rioux's requirements for many service applications. However, the present tests indicated that, even well below the HDT, temperature increases can significantly decrease the creep strength of an adhesive. Figures 56 and 57 show, indeed, the radical change in behavior of specimens tested at the same nominal stresses, but varying temperatures. Previous findings bear this out. The Modern Plastics Encyclopedia states that increasing temperature significantly lowers creep strength and shortens the time to rupture at a given stress.<sup>(38)</sup> Creep behavior at maximum service temperatures will need to be one of the major determinants in choosing adhesives for structural use.

Humidity: Previous studies, conducted at the General Dynamics Materials Research Laboratory, have determined that moisture in an adhesive bond will tend to soften the adhesive, making it weaker and more prone to creep.<sup>(39)</sup> The specimens in that test were conditioned for 9 months or more in an environment of 150°F (66°C) and 100% relative humidity, so that moisture actually penetrated the adhesive. The present tests did not expose the specimens to such extreme conditions, nor for such long periods of time. Relative humidity only occasionally exceeded 85%, and even these higher values usually occurred at night, when temperatures were low (see Figs. 57 and 58). Under these conditions, moisture apparently did not significantly penetrate the bonds. Temperature had a much larger effect, masking any minor effects from humidity which may have occurred.

Bond Length: Hart-Smith reported that joint strength is proportional to bond length only for very short overlaps, where the entire bond acts plasticly, transferring a uniform stress over its whole area. For longer lap lengths, joint strength depends on material properties and thickness of the adhesive, independent of bond area.<sup>(40,41)</sup> He proposed that adhesive bonds can be designed, with respect to these material properties, to avoid creep completely. His proposed design assumes an "elastic trough" between two plastic zones at the ends of the bond giving a shear stress distribution sometimes referred to as a "bath tub" curve (Figure 59). The plastic zones transfer most of the load, while stresses at the center of the elastic trough drop to very low values. Since these low stresses produce proportionately low strains, no creep occurs.

The present results show that lap lengths of 1/2 in (13 mm) to 1 in (25 mm) were too short to produce the "elastic trough" effect with this adhesive. Joint strengths proportional to bond area for both lap lengths indicate that the entire bond acted plastically, transferring a uniform shear stress. Furthermore, since creep occurred in all tests, the bonds could not have had a creep-arresting elastic trough.

Hart-Smith's<sup>(41)</sup> formula for calculating the length of creep resistant bonds, Eq. 8.1, consists of two terms. The first gives the length of the plastic zones,  $l_p$ , and is obtained by equating the plastic adhesive strength to the ultimate strength of the adherend. The second term gives the length of the elastic zone (trough),  $l_e$ , which is a function of the adhesive properties, bond thickness, and thickness of the lap adherend. Smaller applied loads would shorten the length of the plastic zone, while the required elastic trough length remains constant for all loads.

$$l = l_p + l_e = 2 \left[ \frac{t F_u}{2 F_{vp}} + \frac{3}{\sqrt{\frac{2 G}{E t n}}} \right] \quad (8.1)$$

Thickness of lap or strap adherends:  $t = 0.25$  in (6.4 mm)

Ultimate strength of adherends:  $F_u = 70,000$  psi (483 MPa)

Plastic adhesive shear stress (max.

shear stress):  $F_{vp} = 4,000$  psi (27.6 MPa)

Adhesive shear modulus:  $G = 100$  ksi (690 MPa)

Young's modulus of adherend:  $E = 30,000$  ksi (207 GPa)

Thickness of adhesive layer:  $n = 0.010$  in (0.25 mm)

Applying Eq. 8.1 with the aforelisted values to the Series E creep specimens gives the following length for creep:

$$\begin{aligned}
 l &= 2 \left[ \frac{0.25 \times 70}{2 \times 4} + \frac{3}{\sqrt{\frac{2 \times 100}{30,000 \times 0.25 \times 0.010}}} \right] \\
 &= 4.4 + 3.7 \\
 &= 8.1 \text{ in (205 mm)}
 \end{aligned}$$

The shear modulus was conservatively taken as the lower value of the range 100–200 ksi (690–1380 MPa) reported by the adhesive manufacturer. The total length of the strap adherends would be 16.2 in (410 mm).

Equation 8.1 is used in the aircraft industry for designing bonded joints of their adherends. Its applicability to bonded joints of thick adherends typical of those found in bridge structures would have to be verified.

Table 27: Creep test matrix for Series  
D double strap specimens

| Shear Stress<br>Level<br>(Percent) | Indoor Environment |      | Outdoor Environment |      |
|------------------------------------|--------------------|------|---------------------|------|
|                                    | Lap Length         |      | Lap Length          |      |
|                                    | 1/2 in             | 1 in | 1/2 in              | 1 in |
| 100                                | 7 <sup>a</sup>     | 6    | -                   | -    |
| 80                                 | 6                  | 6    | -                   | -    |
| 60                                 | 6                  | 6    | -                   | -    |
| 50                                 | 3                  | 3    | 3                   | 3    |
| 40                                 | 3                  | 3    | 3                   | 3    |
| 30                                 | 3                  | 3    | 3                   | 3    |
| 20                                 | -                  | -    | 3                   | 3    |

Note: a. Number of replicate specimens

Conversion factor: 1 in = 25.4 mm

Table 28: Results of indoor creep tests

| Specimen No.                     | Nominal Stress Level | Curing Time<br>(hrs.) | Percent Failure in Cohesion | Shear Stress |       | Actual Stress Level (%) | Time to Failure (min.) | Date of Testing |     |
|----------------------------------|----------------------|-----------------------|-----------------------------|--------------|-------|-------------------------|------------------------|-----------------|-----|
|                                  |                      |                       |                             | (MPa)        | (psi) |                         |                        | Begin           | End |
| <u>1/2-in (13 mm) Lap Length</u> |                      |                       |                             |              |       |                         |                        |                 |     |
| 20-2                             | 100                  | 90                    | 5                           | 27.0         | 3920  | 98                      | -                      | 5/17/82-5/17/82 |     |
| 20-3                             | 100                  | 90                    | 5                           | 29.1         | 4220  | 106                     | -                      | 5/17/82-5/17/82 |     |
| 20-4                             | 100                  | 90                    | 0                           | 24.6         | 3570  | 89                      | -                      | 5/17/82-5/17/82 |     |
| 21-1                             | 100                  | 90                    | 0                           | 31.5         | 4570  | 114                     | -                      | 5/17/82-5/17/82 |     |
| 21-2                             | 100                  | 90                    | 5                           | 28.0         | 4060  | 102                     | -                      | 5/17/82-5/17/82 |     |
| 21-3                             | 100                  | 90                    | 0                           | 27.6         | 4000  | 100                     | -                      | 5/17/82-5/17/82 |     |
| 21-4                             | 100                  | 90                    | 0                           | 27.7         | 4020  | 100                     | -                      | 5/17/82-5/17/82 |     |
|                                  |                      |                       |                             |              |       |                         |                        |                 |     |
| 26-1                             | 80                   | 31                    | 5                           | 21.4         | 3110  | 78                      | 3.3                    | 5/19/82-5/19/82 |     |
| 26-3                             | 80                   | 31                    | 5                           | 21.0         | 3040  | 76                      | 6.2                    | 5/19/82-5/19/82 |     |
| 26-4                             | 80                   | 31                    | 5                           | 21.0         | 3050  | 76                      | 2.7                    | 5/19/82-5/19/82 |     |
| 27-2                             | 80                   | 31                    | 0                           | 23.2         | 3370  | 84                      | 0.3                    | 5/19/82-5/19/82 |     |
| 27-3                             | 80                   | 31                    | 5                           | 21.8         | 3160  | 79                      | 0.5                    | 5/19/82-5/19/82 |     |
| 27-4                             | 80                   | 31                    | 0                           | 21.9         | 3170  | 79                      | 3.2                    | 5/19/82-5/19/82 |     |
|                                  |                      |                       |                             |              |       |                         |                        |                 |     |
| 32-1                             | 60                   | 168                   | 0                           | 19.9         | 2890  | 72                      | 37                     | 5/28/82-5/29/82 |     |
| 33-1                             | 60                   | 168                   | 0                           | 19.0         | 2750  | 69                      | 112                    | 5/28/82-5/29/82 |     |
| 33-2                             | 60                   | 168                   | 5                           | 15.1         | 2190  | 55                      | 1,490                  | 6/14/82-6/15/82 |     |
| 35-3                             | 60                   | 91                    | 0                           | 18.7         | 2710  | 68                      | 1,360                  | 5/28/82-5/29/82 |     |
| 35-4                             | 60                   | 91                    | 5                           | 19.4         | 2810  | 70                      | 21                     | 5/28/82-5/29/82 |     |
| 36-1                             | 60                   | 210                   | 0                           | 17.0         | 2460  | 62                      | 600                    | 6/14/82-6/15/82 |     |



Table 28: Results of indoor creep tests (continued)

| Specimen No.                   | Nominal Stress Level | Curing Time<br>(hrs.) | Percent Failure in Cohesion | <u>Shear Stress</u> |       | Actual Stress Level<br>(%) | Time to Failure<br>(min.) | <u>Date of Testing</u> |     |
|--------------------------------|----------------------|-----------------------|-----------------------------|---------------------|-------|----------------------------|---------------------------|------------------------|-----|
|                                |                      |                       |                             | (MPa)               | (psi) |                            |                           | Begin                  | End |
| 32-3                           | 50                   | 1000                  | 0                           | 12.2                | 1770  | 44                         | 6,900                     | 7/6/82-7/11/82         |     |
| 36-2                           | 50                   | 1000                  | 5                           | 12.6                | 1830  | 46                         | 8,040                     | 7/6/82-7/11/82         |     |
| 36-4                           | 50                   | 1000                  | 0                           | 12.8                | 1850  | 46                         | 3,780                     | 7/6/82-7/9/82          |     |
| 45-3                           | 40                   | 93                    | 0                           | 11.9                | 1730  | 43                         | 8,880                     | 8/3/82-8/9/82          |     |
| 45-2                           | 40                   | 93                    | 0                           | 11.2                | 1630  | 41                         | 10,800                    | 8/3/82-8/10/82         |     |
| 45-1                           | 40                   | 93                    | 5                           | 11.0                | 1600  | 40                         | 61,200                    | 8/3/82-9/14/82         |     |
| 47-3                           | 30                   | 1000                  | 5                           | 9.2                 | 1340  | 34                         | 21,000                    | 9/15/82-9/29/82        |     |
| 47-1                           | 30                   | 1000                  | 5                           | 8.1                 | 1180  | 30                         | 472,000                   | 9/15/82-8/8/83         |     |
| 47-2                           | 30                   | 1000                  | 5                           | 8.8                 | 1270  | 32                         | 327,000                   | 9/15/82-4/30/83        |     |
| <u>1-in (25 mm) Lap Length</u> |                      |                       |                             |                     |       |                            |                           |                        |     |
| 22-1                           | 100                  | 68                    | 0                           | 29.4                | 4270  | 107                        | -                         | 5/17/82-5/17/82        |     |
| 22-2                           | 100                  | 68                    | 5                           | 28.2                | 4090  | 102                        | -                         | 5/17/82-5/17/82        |     |
| 22-4                           | 100                  | 68                    | 5                           | 26.5                | 3850  | 96                         | -                         | 5/17/82-5/17/82        |     |
| 23-1                           | 100                  | 68                    | 5                           | 28.5                | 4130  | 103                        | -                         | 5/17/82-5/17/82        |     |
| 23-3                           | 100                  | 68                    | 0                           | 24.1                | 3490  | 87                         | -                         | 5/17/82-5/17/82        |     |
| 23-4                           | 100                  | 68                    | 0                           | 24.3                | 3520  | 88                         | -                         | 5/17/82-5/17/82        |     |
| 25-3                           | 80                   | 46                    | 0                           | 21.8                | 3160  | 79                         | 2.0                       | 5/19/82-5/19/82        |     |
| 25-1                           | 80                   | 46                    | 0                           | 21.9                | 3180  | 80                         | 4.3                       | 5/19/82-5/19/82        |     |
| 28-1                           | 80                   | 116                   | 5                           | 20.9                | 3030  | 76                         | 10.0                      | 5/24/82-5/24/82        |     |
| 28-2                           | 80                   | 116                   | 5                           | 21.0                | 3040  | 76                         | 2.3                       | 5/24/82-5/24/82        |     |
| 28-3                           | 80                   | 116                   | 0                           | 21.3                | 3090  | 77                         | 4.2                       | 5/24/82-5/24/82        |     |
| 29-1                           | 80                   | 116                   | 0                           | 22.1                | 3210  | 80                         | 9.0                       | 5/24/82-5/24/82        |     |

Table 28: Results of indoor creep tests (continued)

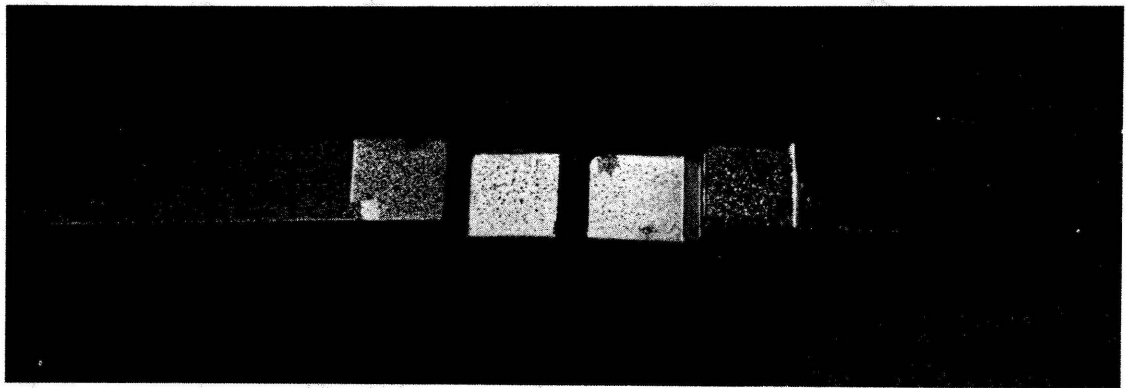
| Specimen No. | Nominal Stress Level | Curing Time<br>(hrs.) | Percent Failure in Cohesion | <u>Shear Stress</u> |       | Actual Stress Level<br>(%) | Time to Failure<br>(min.) | <u>Date of Testing</u> |     |
|--------------|----------------------|-----------------------|-----------------------------|---------------------|-------|----------------------------|---------------------------|------------------------|-----|
|              |                      |                       |                             | (MPa)               | (psi) |                            |                           | Begin                  | End |
| 30-1         | 60                   | 168                   | 5                           | 15.8                | 2290  | 57                         | 1,020                     | 5/28/82-5/29/82        |     |
| 35-1         | 60                   | 91                    | 0                           | 16.3                | 2360  | 59                         | 3,720                     | 5/28/82-5/31/82        |     |
| 35-2         | 60                   | 91                    | 0                           | 16.2                | 2350  | 59                         | 1,700                     | 5/28/82-5/29/82        |     |
| 30-2         | 60                   | 168                   | 5                           | 15.9                | 2300  | 58                         | 2,400                     | 6/14/82-6/16/82        |     |
| 31-1         | 60                   | 287                   | 0                           | 16.7                | 2420  | 60                         | 960                       | 6/14/82-6/15/82        |     |
| 34-1         | 60                   | 210                   | 10                          | 16.8                | 2440  | 61                         | 2,400                     | 6/14/82-6/16/82        |     |
| 31-2         | 50                   | 1000                  | 0                           | 13.4                | 1950  | 49                         | 6,900                     | 7/6/82-7/11/82         |     |
| 34-2         | 50                   | 1000                  | 0                           | 13.7                | 1990  | 50                         | 9,540                     | 7/6/82-7/13/82         |     |
| 34-4         | 50                   | 1000                  | 10                          | 13.8                | 2000  | 50                         | 4,260                     | 7/6/82-7/9/82          |     |
| 44-1         | 40                   | 93                    | 5                           | 11.0                | 1600  | 40                         | 10,800                    | 8/3/82-8/10/82         |     |
| 44-3         | 40                   | 93                    | 10                          | 10.9                | 1580  | 40                         | 16,800                    | 8/3/82-8/15/82         |     |
| 44-2         | 40                   | 93                    | 5                           | 11.7                | 1690  | 42                         | 21,000                    | 8/3/82-8/18/82         |     |
| 48-4         | 30                   | 1000                  | 5                           | 8.1                 | 1180  | 30                         | 400,000                   | 9/15/82-6/20/82        |     |
| 49-1         | 30                   | 1000                  | 5                           | 7.9                 | 1140  | 29                         | 413,000                   | 9/15/82-6/29/83        |     |
| 49-2         | 30                   | 1000                  | 5                           | 8.3                 | 1200  | 30                         | 373,000                   | 9/15/82-6/1/83         |     |

Table 29: Results of outdoor creep tests

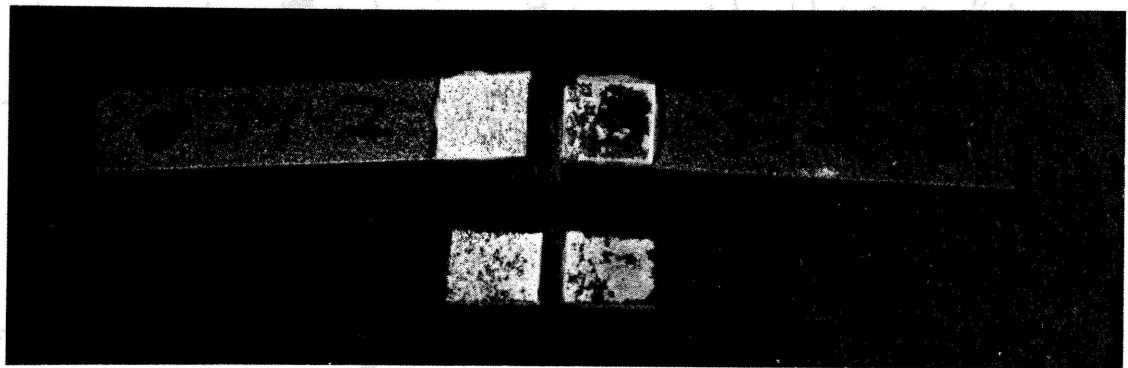
| Specimen No.                     | Nominal Stress Level | Curing Time<br>(hrs.) | Percent Failure in Cohesion | Shear Stress |       | Actual Stress Level (%) | Time to Failure (min.) | Date of Testing |     |
|----------------------------------|----------------------|-----------------------|-----------------------------|--------------|-------|-------------------------|------------------------|-----------------|-----|
|                                  |                      |                       |                             | (MPa)        | (psi) |                         |                        | Begin           | End |
| <u>1/2-in (13 mm) Lap Length</u> |                      |                       |                             |              |       |                         |                        |                 |     |
| 39-2                             | 50                   | 90                    | 0                           | 12.8         | 1850  | 46                      | 265                    | 7/19/82-7/19/82 |     |
| 40-1                             | 50                   | 90                    | 10                          | 12.0         | 1740  | 44                      | 180                    | 7/19/82-7/19/82 |     |
| 40-3                             | 50                   | 90                    | 0                           | 12.7         | 1840  | 46                      | 145                    | 7/19/82-7/19/82 |     |
| 39-1                             | 40                   | 1000                  | 0                           | 9.9          | 1430  | 36                      | 2,310                  | 7/19/82-7/20/82 |     |
| 39-3                             | 40                   | 1000                  | 0                           | 10.8         | 1570  | 39                      | 160                    | 7/19/82-7/19/82 |     |
| 40-2                             | 40                   | 1000                  | 0                           | 9.9          | 1430  | 36                      | 300                    | 7/19/82-7/19/82 |     |
| 47-4                             | 40                   | 3672                  | 0                           | 10.3         | 1500  | 38                      | 85,000                 | 1/4/83-3/4/83   |     |
| 43-1                             | 30                   | 1000                  | 10                          | 8.0          | 1160  | 29                      | 6,180                  | 7/27/82-7/31/82 |     |
| 48-2                             | 30                   | 285                   | 5                           | 10.1         | 1460  | 37                      | 2,940                  | 8/16/82-8/18/82 |     |
| 48-1                             | 30                   | 285                   | 10                          | 9.6          | 1390  | 35                      | 7,200                  | 8/16/82-8/21/82 |     |
| 46-1                             | 20                   | 240                   | -                           | -            | -     | -                       | 614,000-R              | 8/9/82-10/9/83  |     |
| 46-2                             | 20                   | 240                   | 5                           | 6.1          | 890   | 22                      | 507,000                | 8/9/82-7/27/83  |     |
| 46-3                             | 20                   | 240                   | 10                          | 5.7          | 820   | 21                      | 79,200                 | 8/9/82-10/3/82  |     |
| <u>1-in (25 mm) Lap Length</u>   |                      |                       |                             |              |       |                         |                        |                 |     |
| 37-1                             | 50                   | 90                    | 5                           | 13.1         | 1900  | 48                      | 170                    | 7/19/82-7/19/82 |     |
| 37-3                             | 50                   | 90                    | 0                           | 13.2         | 1910  | 48                      | 120                    | 7/19/82-7/19/82 |     |
| 38-2                             | 50                   | 90                    | 5                           | 12.5         | 1820  | 46                      | 90                     | 7/19/82-7/19/82 |     |

Table 29: Results of outdoor creep tests (continued)

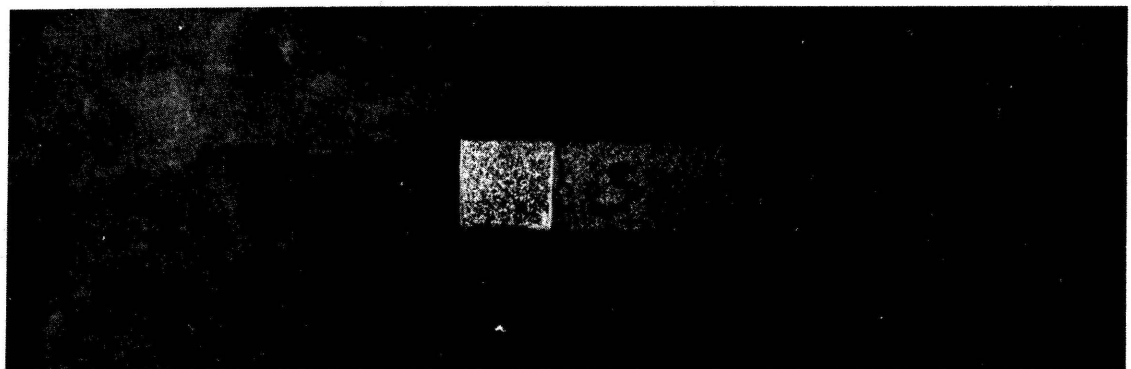
| Specimen No. | Nominal Stress Level | Curing Time<br>(hrs.) | Percent Failure in Cohesion | Shear Stress |       | Actual Stress Level (%) | Time to Failure (min.) | Date of Testing |     |
|--------------|----------------------|-----------------------|-----------------------------|--------------|-------|-------------------------|------------------------|-----------------|-----|
|              |                      |                       |                             | (MPa)        | (psi) |                         |                        | Begin           | End |
| 37-2         | 40                   | 90                    | 5                           | 10.7         | 1550  | 39                      | 360                    | 7/19/82-7/19/82 |     |
| 38-1         | 40                   | 90                    | 5                           | 11.2         | 1630  | 41                      | 395                    | 7/19/82-7/19/82 |     |
| 38-3         | 40                   | 90                    | 5                           | 10.8         | 1570  | 39                      | 60                     | 7/19/82-7/19/82 |     |
| 49-4         | 40                   | 3672                  | -                           | 10.7         | 1560  | 39                      | 96,500                 | 1/4/83-3/12/83  |     |
| 41-1         | 30                   | 112                   | 5                           | 8.3          | 1200  | 30                      | 3,120                  | 7/27/82-7/29/82 |     |
| 42-2         | 30                   | 112                   | 10                          | 8.5          | 1230  | 31                      | 11,880                 | 7/27/82-8/4/82  |     |
| 48-3         | 30                   | 285                   | 10                          | 8.4          | 1220  | 30                      | 3,180                  | 8/16/82-8/18/82 |     |
| 41-3         | 20                   | 112                   | 5                           | 5.5          | 790   | 20                      | 477,000                | 7/27/82-6/23/83 |     |
| 41-4         | 20                   | 112                   | 0                           | 5.7          | 830   | 21                      | 488,000                | 7/21/82-7/1/83  |     |
| 42-1         | 20                   | 112                   | -                           | -            | -     | -                       | 632,000-R              | 7/27/82-10/9/83 |     |



(a) Adhesive failure along face of main adherend (glue remaining on strip piece)

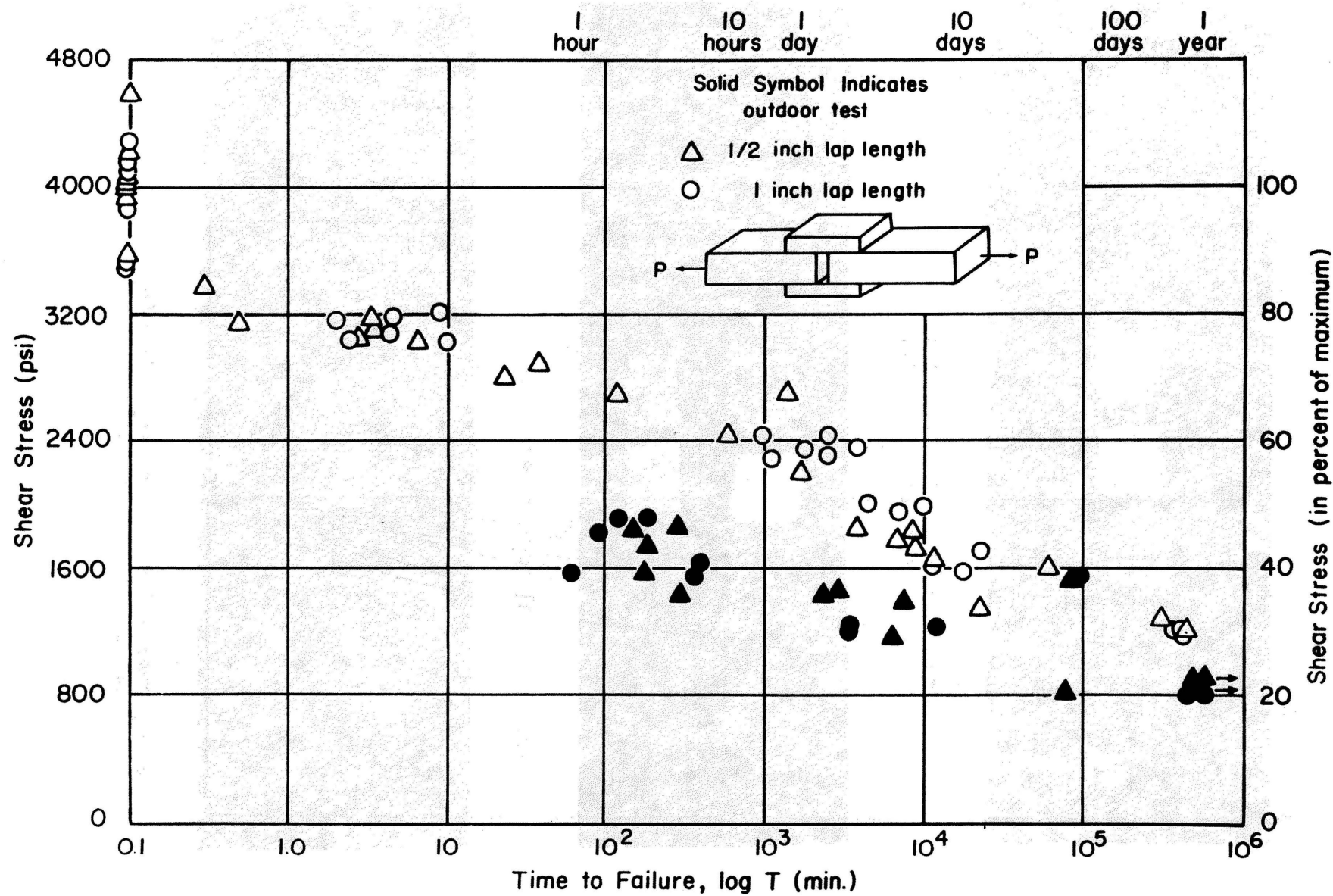


(b) Failure along both metal faces



(c) Specks of glue on metal face, showing small amounts of cohesive failure

Figure 53: Specimens showing various modes of failure



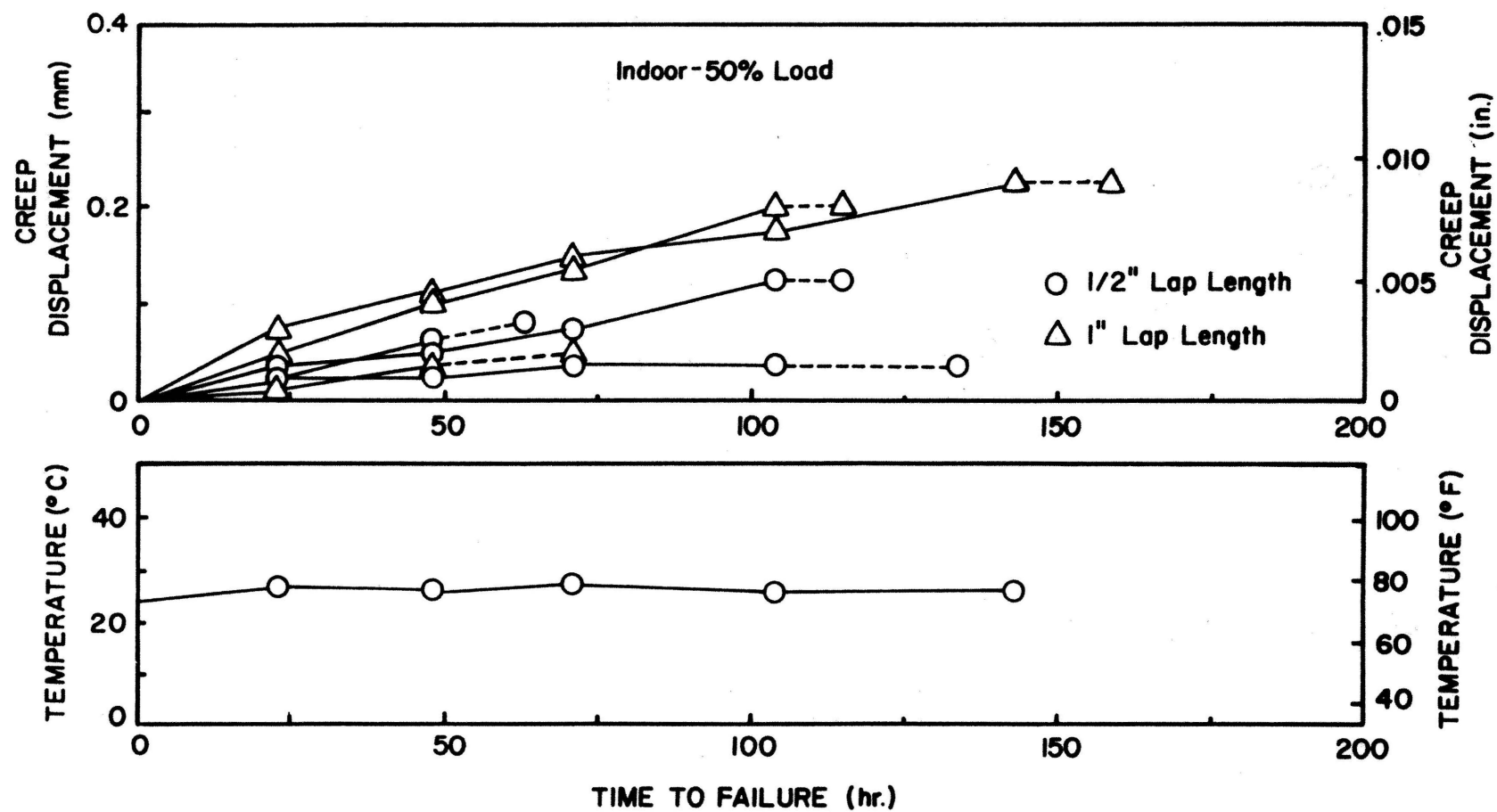


Figure 55: Creep displacements of indoor specimens at 50% stress level

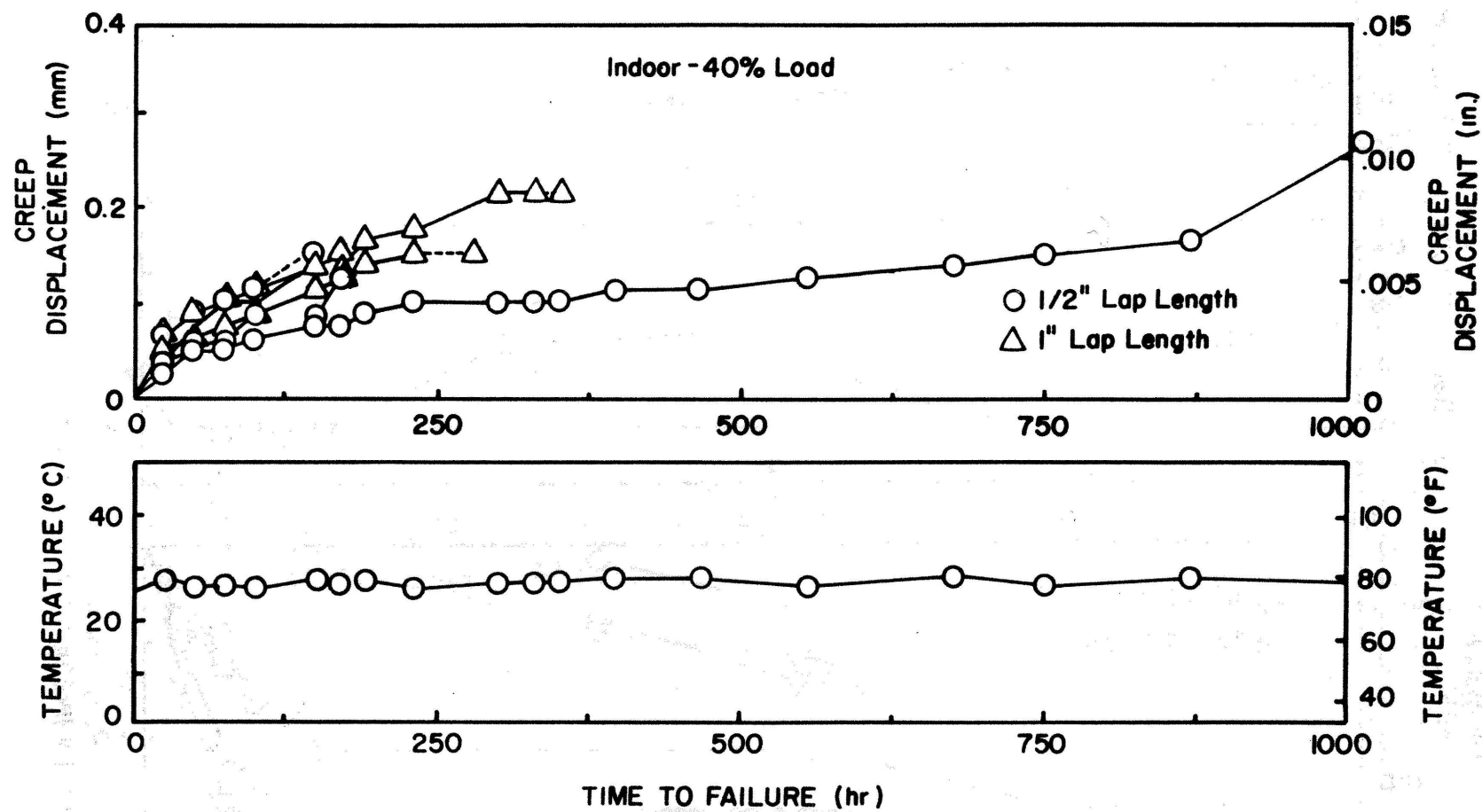


Figure 56: Creep displacements of indoor specimens at 40% stress level



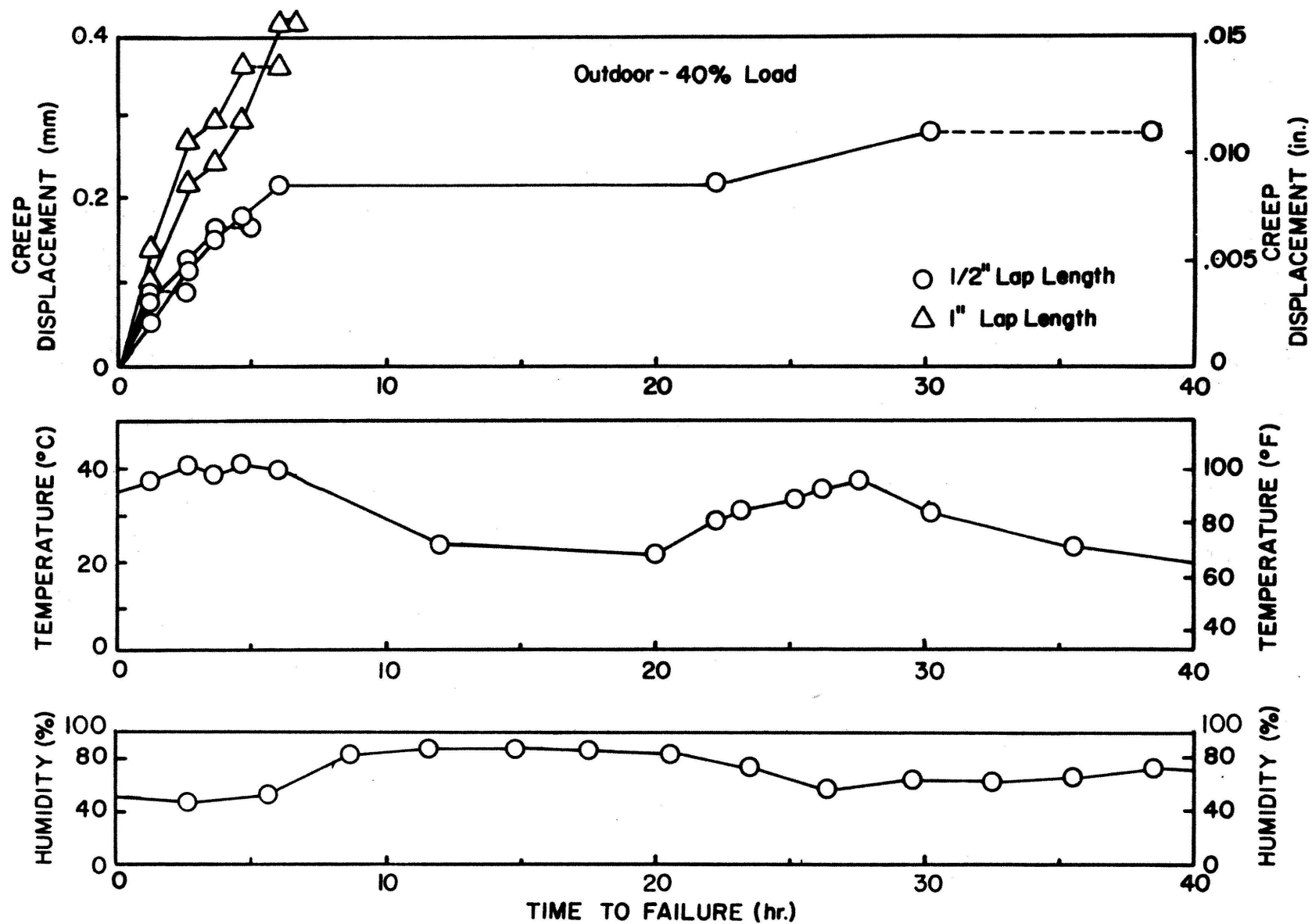


Figure 57: Creep displacements of outdoor specimens at 40% stress level

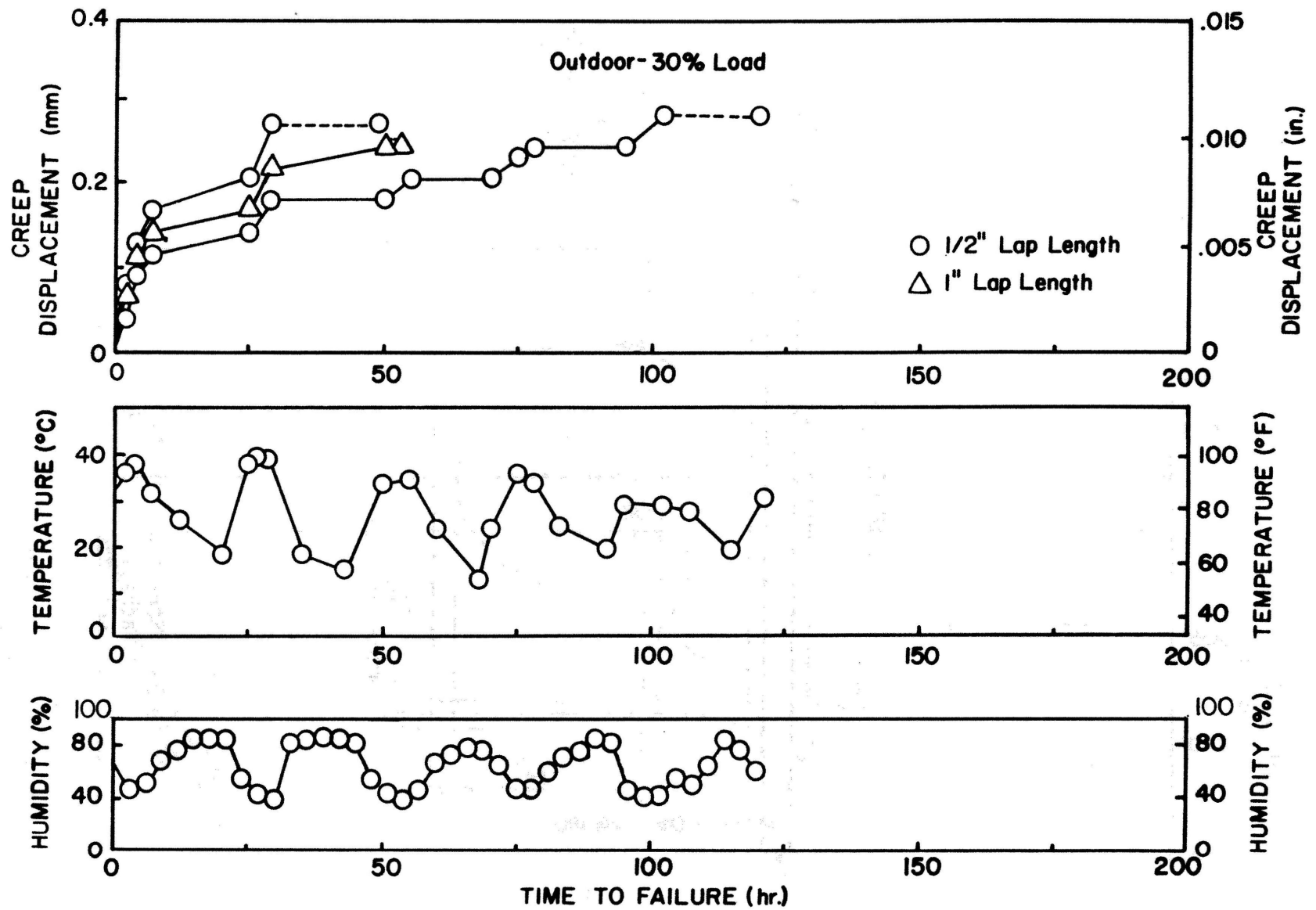


Figure 58: Creep displacements of outdoor specimens at 30% stress level

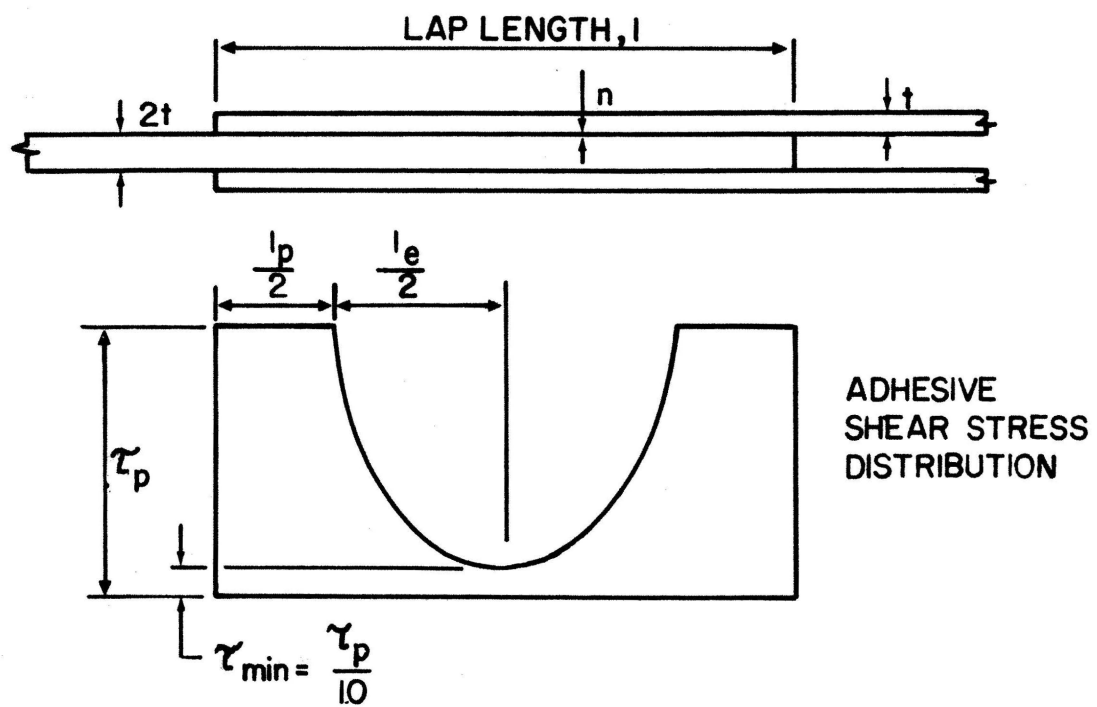


Figure 59: Stress distribution in a double lap adhesive joint. Adapted from Fig. 6, Ref. 41.

## CHAPTER 9: FINDINGS AND CONCLUSIONS

The results of the experimental work performed in this study and an analysis of related data reported in the literature are sufficient to make several important observations about the behavior of composite bonded and bolted structural steel connections. They are summarized in the following by type of loading. Although the conclusions apply, in a strict sense, only to specimens bonded with the acrylic adhesive Versilok 201, one can expect that they would be similar for specimens bonded with other structural adhesives.

### Fatigue Strength:

1. The manner in which cracks initiated and propagated was found to be independent of: (a) the number of bolts in the splice; (b) whether the contact surfaces were bonded or nonbonded; and (c) whether the joint behaved as a friction-type or as a bearing-type connection.
2. The splices with fretting cracks had generally longer fatigue lives than those with bolt hole cracks.
3. The two-bolt tensile splices with bonded contact surfaces had, on average, 1.73 times the fatigue lives of their nonbonded counterparts.
4. Bonding also increased the fatigue lives of the one-bolt tensile splices, but their lives were generally short because the connections were intentionally underdesigned. In this case, the adhesive bond was unable to make up for the deletion of one-half of the bolts in the splice.

5. The bonded six-bolt beam splices had 5.2 and 1.4 times longer lives than their nonbonded counterparts tested at the low and high stress ranges, respectively.
6. The bonded four-bolt beam splices tested at the low stress range had about the same fatigue life as the nonbonded six-bolt splices. In this case, the adhesive bond was able to make up for the deletion of one-third of the bolts. Those tested at the high stress range had relatively shorter fatigue lives because the bond failed during the test.
7. Bonding and end-bolting cover plates increased the fatigue life by a factor of at least 20 over that of conventionally welded cover plates.
8. An extensive evaluation of the previous domestic and foreign data, as well as the results of this study, indicated that nonbonded bolted splices have Category B fatigue strength based on gross area stress range. This conclusion applies to both friction-type and bearing-type joints, provided that the joints meet the AASHTO specification requirements for maximum allowable stress, edge distance, bolt spacing, etc. On the other hand, the fatigue strength of nonbonded bolted splices is reduced to Category C when the load is transmitted by bolts through some but not all of the cross sectional elements of the member.

Static Strength:

9. The bonded and bolted joints slipped into bearing either when the adhesive reached its ultimate shear strength or when yield deformations of the adherend induced adhesive failure.

10. The bolted tensile and beam splices with bonded contact surfaces had up to 2.6 times the slip resistance of their nonbonded counterparts. The increase was greatest when the adhesive reached its ultimate shear strength before the adherend yielded. This usually occurred in joints with underdesigned bolts.
11. Bonding did neither increase the slip load nor the ultimate strength of bolted members above the load corresponding to gross section yielding. This is a result of adhesive failure induced by yielding of an adherend.

Creep Strength:

12. The shear strength of the adhesive decreased substantially with time of loading.
13. The specimens exposed outdoors crept faster than those exposed indoors. The main reason for this was found to be the high ambient temperature during the hot summer days.

Summary:

In summary, bonding in addition to bolting greatly increased the fatigue strength and slip resistance of high-strength bolted connections. It did not, however, increase the ultimate strength.

It is emphasized that the Versilok 201 adhesive had low creep strength at temperatures that were high but still within the service temperature range. The long term behavior and durability of alternate adhesives was not studied. Before steel bridge connections can be bonded and bolted on a regular basis, additional information is needed on the behavior of specific adhesives when exposed to bridge loads and environments for the anticipated service life.

## REFERENCES

1. "Standard Specification for Highway Bridges," American Association of State Highway and Transportation Officials, Washington, D.C. 1977.
2. "Interim Specifications for Bridges," American Association of State Highway and Transportation Officials, Washington, D.C., 1977.
3. Chesson, E., "Exploratory Tests of Structural Steel Joints Assembled with Bolts and Adhesives," Civil Engineering Report, University of Illinois, Urbana, Illinois, 1966.
4. Nara, H., and Gasparini, D., "Fatigue Resistance of Adhesively Bonded Structural Connections," Report No. 45K1-114, Department of Civil Engineering, Case Institute of Technology, Ohio, September 1981.
5. Albrecht, P., Wattar, F., and Sahli, A., "Towards Fatigue-Proofing Cover Plate Ends," Proceedings of W.H. Munse Symposium on Metal Structures, Convention, American Society of Civil Engineering, Philadelphia, Pennsylvania, May 1983.
6. Sahli, A., Albrecht, P., and Albrecht, Ph., "Fatigue Test Data for Bolted Joints; Literature Review," Civil Engineering Report, University of Maryland, College Park, Maryland, July 1983.
7. Albrecht, P., Wattar, F., Sahli, A., and Vannoy, D.W., "End-Bolted Cover Plates," Report No. FHWA/MD-82/01, Department of Civil Engineering, University of Maryland, College Park, Maryland, July 1982.
8. Albrecht, P., Sahli, A., and Vannoy, D.W., "Fatigue Strength of Retrofitted Cover Plate Ends," Report No. FHWA/MD-82/02, Department of Civil Engineering, University of Maryland, College Park, Maryland, January 1983.
9. ASTM D 648-72 (1978), "Standard Test Method for Deflection Temperature of Plastics Under Flexural Load."
10. Fisher, J.W., Frank, K.Y., Hirt, M.A., and McNamee, B.M., "Effects of Weldments on the Fatigue Strength of Steel Beams," NCHRP Report No. 102, Transportation Research Board, National Research Council, Washington, D.C., 1970.
11. Albrecht, P. and Simon, S., "Fatigue Notch Factors for Structural Details," Journal of the Structural Division, American Society of Civil Engineering, Vol. 107, No. ST7, July 1981.

# REFERENCES (continued)

12. Hansen, N.G., "Fatigue Tests of Joints of High Strength Steels," Journal of the Structural Division, American Society of Civil Engineering, Vol. 85, St3, March 1959.
13. Chesson, E., Jr., and Munse, W.H., "Studies of the Behavior of High-Strength Bolts and Bolted Joints," Engineering Experiment Bulletin 469, University of Illinois, Urbana, 1965.
14. Birkemoe, P.C., Meinheit, D.F., and Munse, W.H., "Fatigue of A514 Steel in Bolted Connections," Journal of the Structural Division, American Society of Civil Engineering, Vol. 95, ST10, October 1969.
15. Birkemoe, P.C., and Srīnivasan, R.S., "Fatigue of Bolted High Strength Structural Steel," Journal of the Structural Division, American Society of Civil Engineering, Vol. 97, ST3, March 1971.
16. Frank, K.H., and Yura, J.A., "An Experimental Study of Bolted Shear Connections," Report No. FHWA/RD-81/148, Department of Civil Engineering, University of Texas at Austin, May 1981.
17. Graf, O., "Tests of Bolted Joints," Report 16, Berichte des Deutschen Ausschusses fuer Stahlbau, Stahlbau Verlag Cologne, Germany, 1951 (In German).
18. Steinhardt, O., and Moehler, K., "Tests on Application of High Strength Bolts in Steel Construction" Part II, Report 22, Berichte des Deutschen Ausschusses für Stahlbau, Stahlbau-Verlag, Cologne, Germany, 1959 (In German).
19. Steinhardt, O., and Moelher, K., "Tests on Application of High-Strength Bolts in Steel Construction," Part III, Report 24, Berichte des Deutschen Ausschusses fuer Stahlbau, Stahlbau Verlag, Cologne, Germany, 1962 (In German).
20. Kloeppel, K., and Seeger, T., "Fatigue Tests of St 37 Steel Joints with High Strength Bolts in Single Shear," Der Stahlbau, No. 8, Vol. 33, August 1964, pp. 225-245 (In German).
21. Lieurade, H.P., "Fatigue Study of Bolted Joints Made of High Yield Strength Steels," Report IRSID RE 339, IRSID, Saint-Germain-en-laye, France, February 1976, pp. 439-466 (In French).
22. Yin, W., Wang, S., Fang Q., and Wang, X., "Fatigue Strength of High Strength Bolted Joints." Proceedings, IABSE. Vol. 37, Colloquium Lausanne, 1982.
23. Fisher, J.W., Hausammann, H., and Pense, A.W., "Retrofitting Procedures for Fatigue Damaged Full-Scale Welded Bridge Beams," Fritz Engineering Lab. Report No. 417-3(79), Lehigh University, January 1979.



# REFERENCES (continued)

24. Roberts, R., et al., "Determination of Tolerable Flaw Sizes in Full-Size Welded Bridge Details," Report No. FHWA-RD-77-170, Federal Highway Administration, Washington, D.C., December 1977.
25. Schilling, C.G., Klippstein, K.H., Barsom, J.M., and Blake, G.T., "Fatigue of Welded Steel Bridge Members Under Variable-Amplitude Loading," NCHRP Report No. 188, Transportation Research Board, National Research Council, Washington, D.C., August 1975.
26. Fisher, J.W., Hausamann, H., Sullivan, M.D., and Pense, A.W., "Detection and Repair of Fatigue Damage on Welded Highway Bridges," NCHRP Report No. 206, Transportation Research Board, National Research Council, Washington, D.C., June 1979.
27. Yamada, K., and Albrecht, P., "Fatigue Behavior of Two Flange Details," Journal of the Structural Division, ASCE, Vol. 103, April 1977, pp. 781-791.
28. Yura, J.A., Frank, K.H., and Cayes, L., "Bolted Friction Connections with Weathering Steel," Journal of the Structural Division, American Society of Civil Engineers, Vol. 107, ST 11, November 1981.
29. Lee, J.H., O'Connor, C., and Fisher, J.W., "Effect of Surface Coatings and Exposure on Slip," Journal of the Structural Division, American Society of Civil Engineers, Vol. 95, ST10, October 1969.
30. Fisher, J.W., and Struik, J.A., "Guide to Design Criteria for Bolted and Riveted Joints," John Wiley and Sons, Inc., New York, 1974.
31. Hechtman, R.A., Young, D.R., Chin, A.G., and Savikko, E.R., "Slip of Joints Under Static Loads," ASCE Transactions, Vol. 120, 1955, pp. 1335-1352.
32. Douty, R.T., and McGuire, W.F., "High Strength Bolted Moment Connections," Journal of the Structural Division, American Society of Civil Engineers, Vol. 91, ST2, April 1965.
33. Kulak, G.L., and Fisher, J.W., "A514 Steel Joints Fastened by A490 Bolts," Journal of the Structural Division, American Society of Civil Engineers, Vol. 94, ST10, October 1968.
34. Johnson, L.G., Cannon, J.C., and Spooner, L.A., "High Tensile Preloaded Bolted Joints," British Welding Journal, September 1960.
35. "Local Climatological Data, Monthly Summary," Washington National Airport, Washington, D.C., official publication of the National Oceanic and Atmospheric Administration, June 1982.

REFERENCES (continued)

36. Rioux, R.J., "Epoxies - What They Can and Can't Do," Presented at Northwest Bridge Engineer's Seminar, October 6, 1981.
37. ASTM D 648-72 (1978), "Standard Test Method for Deflection Temperature of Plastics Under Flexural Load."
38. Modern Plastics Encyclopedia, October 1982, Volume 59, Number 10A, McGraw-Hill Inc., New York, N.Y.
39. Quarterly Progress Report No. 11 (January 1 to March 31, 1979), "Fatigue Behavior of Adhesively Bonded Joints." General Dynamics, Fort Worth Division Technical Report FZM-6838, April, 1979.
40. Hart-Smith, L.J., "Advances in the Analysis and Design of Adhesive-Bonded Joints in Composite Aerospace Structures," Douglas Aircraft Co., presented April 24, 1974, Douglas Paper 6224.
41. Hart-Smith, L.J., "Further Developments in the Design and Analysis of Adhesive-Bonded Structural Joints," Douglas Aircraft Co., presented April 16, 1980, Douglas Paper 6922.
42. "Primary Adhesively Bonded Structure Technology," Report No. AFWAL-TR-80-3112, Douglas Aircraft Company, November 1980.
43. Graff, G., "The Glued-Together Airplane," High Technology, September 1983, pp. 67-71.



